T.C.
ERCİYES ÜNİVERSİTESİ
BİLİMSEL ARAŞTIRMA PROJELERİ
KOORDİNASYON BİRİMİ

# SALINIMLI DIŞ MANYETİK ALAN VARLIĞINDA KARMA SPİN (3/2, 2) VE KARMA SPİN (3/2, 5/2) İKİ TABAKALI SİSTEMLERİNİN DİNAMİK MANYETİK ÖZELLİKLERİNİN GLAUBER STOKASİK TİPİ DİNAMİK TEMELLİ ORTALAMA ALAN TEORİSİYLE İNCELENMESİ

**Proje No:** FBA-2016-6324

Proje Türü
Araştırma Projesi

## SONUÇ RAPORU

**Proje Yürütücüsü**
Prof. Dr. Mustafa KESKİN
Fen Fakültesi / Fizik Bölümü

**Araştırmacılar**
Doç. Dr. Mehmet ERTAŞ
Fen Fakültesi / Fizik Bölümü

Yusuf KOÇAK
Fen Bilimleri Enstitüsü Yüksek Lisans Öğrencisi

Ağustos 2017

KAYSERİ

# ÖNSÖZ

Son yıllarda, fiziksel kooperatif sistemlerin dengeli ve dinamik davranışları ve özellikle manyatik özellikleri karma-spin sistemleri kullanılarak incelenmektedir. Dengeli davranışlar veya denge durumundaki manyetik özellikler, dengeli istatistik fizik kapsamında geliştirilen yöntemlerle ayrıntılı olarak incelenmiş ve incelenmeye devam etmektedir. Diğer taraftan, karma-spin sistemlerini kullanarak fiziksel kooperatif sistemlerin dinamik davranışlarının veya dinamik manyetik özelliklerinin incelenmesi üzerine çok az sayıda araştırma yapılmış ve yapılmaktadır. Ayrıca, ilginç ve önemli problemlerden birisi, mekanizması henüz tam bilinmeyen ve dolayısıyla temel fenomenolojisi hâla geliştirilememiş olan, dengesiz veya dinamik faz geçişi (DFG) sıcaklıklarının hesaplanması ve dinamik faz diyagramlarının elde edilmesidir. Yine, son yıllar hem teorik ve hemde deneysel olarak üzerinde çalışılan dinamik manyetik histerisiz özelikler (histerezis alanı, zorlayıcı manyetik alanı ve artık mıknatıslanma), hem teknolojik uygulamaları ve hemde akademik araştırmalar bakımından çok önem arz etmektedir. Bunlara ilaveten, ince film araştırmaları hem teknolojik ve hemde akademik araştırmalar için çok önemli bir konu olduğundan, çalışmalarımızı iki-tabakalı kare örgü üzerinde yaptık.

Bu önemli konuya az da also bir katkıda bulunmak için, karma-spin (3/2, 2) ve karma-spin (3/2, 5/2) Ising bilayer sistemleri Glauber- tipi stokhastik dinamik temelli ortalama-alan teorisi (dinamik ortalama alan teorisi (DOAT) diye de adlandırılır) yöntemiyle incelendi. Her iki karma spin sistemi için DFG sıcaklıkları elde edilerek dinamik faz diyagramları farklı düzlemlerde sunuldu. Bu karma spin sistemlerinin dinamik histerik özellikleri kullanılarak kapsamlıca incelendi. Elde edilen sonuçlar ayrıntılı bir şekilde tartışılarak, benzer teorik ve deneysel çalışmalarla karşılaştırıldı, güzel ve kuantatif uyum gözlendi. Projeden, birisi DOI numarası alınmış basımda olan ve ikiside Hakem aşamasında olan SCI kapsdamında dergilerde üç çalışma üretilmiştir. Ayrıca, uluslararası toplantıda sunulan iki çalışma PROCEEDING olarak yayımlanmıştır. Bir uluslararası sunum yapılmış ve ÖZET olarak yayımlanmıştır. Bunlara ilaveten, karma-spin (3/2, 5/2) sistemiyle ilgili bir veya iki uluslararası sunum yapılması planlanmıştır. Ümit ederiz ki, bu proje ve çıktıları dinamik davranılar üzerine teorik ve deneyeysel araştırma yapanlara ve özellikle DFG, dinamik manyetk histerisiz üzerinde çalışanlara, faydalı olur ve aynı zamanda yeni ve daha kaliteli çalışmalara ışık tutar.

Bu projenin tamamlanmasında ve üretilen makale ve bildirilerde, Erciyes Üniversitesi Bilimsel Araştırma Projeleri Koordinasyon Birimi Proje No: FBA-2016-6324 verdiği maddi desteğin çok önemli rolu olmuştur. Bu destek olmasaydı, bu şekilde çıktılar üretmek mümkün olmayacaktı. Ayrıca, birimde görev yapan idarecilerimizin ve çalışan personellerimizin; çok özverili ve çok iyi niyetli çalışmaları bizlerin işlerini çok kolaylaştırmış ve yukarıda belirtilen olumsuzlukları bir nevi gidermiştir. Bu nedenle, verilen maddı destek için ve ayni zamanda birimde görev yapan bütün idarecilerimize ve personellerimize içteklikle teşekürlerimizi sunarım.

Saygılarımla,
Ağustos, 2017
Mustafa Keskin

# İÇİNDEKİLER

## ÖZET

Zamana bağlı salınımlı dış manyetik alan altında önemli karma spinler arasında olan, karma-spin (3/2, 2) ve karma-spin (3/2, 5/2) Ising sistemlerinin dinamik manyetik özellikleri iki-tabakalı kare örgü kullanılarak incelendi. İlk olarak, sistemlerin dinamik davranışlarını tanımlayan denklemler Glauber tipi stokastik dinamiklere dayanan ortalama alan teorisi, dinamik ortalama-alan yaklaşımı diyede adlandırılır, kullanılarak elde edildi. Ortalama miknatışlanmaların zamanla değişimi ayrıntılı olarak incelenerek sistemlerde meydana gelen fazlar tespit edildi. Dinamik mıknatıslanmaların sıcaklık değişimleri de araştırılarak faz geçişlerinin tabiati (birinci- veya ikinci derece) tanımlandi ve sonuçta, farklı düzlemlerde dinamik faz diagramları elde edilerek sunuldu. Dinamik magnetic histeresiz döngü davranışlar çok kapsamlıca incelendi ve taartışıldı. Ayrıca, zorlayıcı manyetik alan ve kalıcı miknatislanma incelendi ve tartışıldi. En sonunda, elde edilen sonuçlar bazı mevcut teorik ve deneysel sonçlarlar karşılaştırıldı ve güzel ve kuantatif uyum gözlendi.



**Anahtar Kelimeler:** Karma-spin (3/2, 2) ve karma-spin (3/2, 5/2) Ising sistemleri, dinamik histerisiz döngü davranışları, dinamik faz geçişleri, dinamik faz diyagramları, Glauber stokastik -type dinamik temelli ortalama-alan yaklaşımı

**ABSTRACT**

Dynamic magnetic properties of mixed-spins (3/2, 2) and mixed-spins (3/2, 5/2) Ising systems on a two-layer square lattice under an oscillating magnetic field are studied. First, we obtained the dynamic equations that describe the dynamic behaviors by using the mean-field theory based on the Glauber–type stochastic dynamics, also called the dynamic mean-field theory (DMFT). The time variations of the average magnetizations are extensively studied to obtain the phases in the systems. The thermal behavior of the dynamic magnetizations are also investigated in order to characterize the nature (first-or second-order) of the phase transtions and as a result the dynamic phase diagrams are calculated and presented in different planes. Dynamic magnetic hysteresis loops behaviors are also studied and discussed in detail. Moreover, the coercive field and remanent magnetization are also examined and discussed. Finally, the obtained results are compared with some available theoretical and experimental works and observed a quantitatively good agreement.

**Keywords:** Mixed-spins (3/2, 2) and mixed-spins (3/2, 5/2) Ising systems, dynamic hysteresis loop behaviors, dynamic phase transitions, dynamic phase diagrams, mean-field approximation based on Glauber-type stochastic dynamics

# BÖLÜM I

## GİRİŞ

Manyetik ince film malzemeleri, mikroelektronik, manyeto-optik kopyalama (recording), hafıza sistemlerinde kullanılma potansiyellerinin olması, deneysel, uygalamalı ve teorik önemli araştırma konuları içerisine girmiştir ve malzemeler üzerine çok yoğun çalışmalar yapılmaktadır (Bknz. Ref. [1–4] ve içindeki kaynaklar). Deneysel olarak, manyetik tabakalı ince filmlerin yapısal ve manyetik özellikleri üzerine çok sayıda çalışmalar yapılmıştır. Örneğin, Fe/Ni [5], Fe/Ni and Fe/Co [6], Ni/Au [7], and Co/Cu/Ni80Fe20 [8], Ni/ Fex Mn1-x [9], La2/3Ca1/3MnO3/SrTiO3/YBa2Cu3O7-x, [10], FePt/Fe [11], FM/TbFe (FM=Fe, Py-permalloy, FeCo) [12]. Spin Ising sistemlerini kullanarak, manyetik ince filmlerin denge manyetik özellikleri denge istatistiksel fizikte geliştirilen önemli yöntemlerle; örneğin Monte Carlo (MC) hesaplamaları (Bknz. [13–19] ve içindeki kaynaklar), ortalama alan teorisi (OAT) [20-23], etkin alan teorisi (EFT) [24–30], spin-dalgalanma [31], renormalizasyon grup (RG metodu [32-33], seri açılım metodu [34], çift yaklaşımlı kümesel değişim metodu [35] ve Bethe örgüsü üzerinde kesin çözümler (Bknz. [36, 39] ve içindeki kaynaklar), incelenmiş ve halen de incelmelere devam edilmektedir.

İnce filmlerin manyetik denge özellikleri üzerine daha fazla araştırmalar yapıldığı halde, dinamik manyetik özellikleri üzerine çok daha az çalışılmalar yapılmıştır. İlk dikkate değer ilk çalışma, Wu ve arkadaşları [40], iki tabakalı spin-1/2 sisteminin dinamik manyetik özelliklerini dinamik MC hesaplamalarıyla incelemiş ve Jang arkadaşları [41-44] da yine dinamik MC kullanarak manyetik ince Hesenberg filmlerin faz ve histerisiz davranışlarını incelediler, ancak dinamik faz diyagramlarını elde etmediler. Canko ve arkadaşları [45], zamana-bağlı salınımlı manyetik alan varlığında, spin-1/2 Ising sisteminin dinamik manyetik özellikleri iki-tabakalı kare örgü kullanılarak DOAT ile incelediler. Özellikle, DFG sıcaklıklarını elde ettiler ve dinamik faz diyagramlarını sundular. Ertaş ve Keskin [44-45], zamana-bağlı salınımlı manyetik alan varlığında, karma spin (5/2, 2) Ising sistemin dinamik manyetik özellikleri iki-tabakalı kare örgü kullanılarak DOAT incelediler. Ayrıca, ferromagnetik/ferromagnetik, antiferromagnetik/ferromagnetik [46] ve antiferromagnetik/antiferromagnetik [47] etkileşmeleri göz önüne alarak DFG sıcaklıklarını araştırdılar; ilginç ve zengin dinamik faz diyagramlarını buldular. Yakın zamanda, salınımlı dış manyetik alan varlığında spin-1/2 [48] ve karma spin (3/2, 2) [49] iki-tabakalı sistemlerinin yalnız DFG sıcaklıkları ve dinamik faz diyagramları DOAT ile incelenmiştir.

Ancak, histerisiz ve telafi, sıcaklıkları gibi çok önemli manyetik dinamik davranışlar incelenmemiştir.

Projemizde, incelemesini yaptığımız karma-spin (3/2, 2) ve karma-spin (3/2, 5/2) Ising sistemlerinin de yine denge özellikleri daha kapsamlı incelendiği halde dinamik manyetik özellikleri çok daha az incelenmiştir. Dinamik sistemlerin incelenmesinin zor ve karışıklığı ve ayni zamanda daha az yöntemin oluşu, bu sistemlerin de dinamik davranışlarının incelemesine engel olan veya zorlaştıran önemli nedenlerdir. Karma-spin (3/2, 2) sisteminin denge davranışlarının araştırılması üzerine, en iyi bilgilerimiz dâhilinde, Babok and Dely [50] tarafından yapılmıştır ve bunlar sistemdeki denge faz diyagramlarını, Bogoliubov eşitsizliği temelli OAT ile elde etmişler. Faz diyagramlarının üçlü kritik ve yalıtılmış kritik noktalar sergilediğini bulmuşlar. Albayrak [51], Bethe örgüsü üzerinde sistemin kesin denge çözümünü yapmış ve faz diyagramlarını kapsamlıca incelemiş. Miao ve arkadaşları [52], Bogoliubov eşitsizliği temelli OAT ile sistemin geçirdiği faz geçişlerini ve çoklukritik (multicritical) noktaları incelemişlerdir. Deviren ve arkadaşları [53, 54], karma spin (3/2, 2) ferrimagnetic Ising [53] ve birbirini takıp eden tabakalı [54] sistemleri alarak; bu sistemin denge manyetik özelliklerini etkin-alan teorisiyle kapsamlıca incelemişlerdir. Karma spin (3/2, 2) ferrimagnetic Ising sisteminde farklı kristal alan etkileşmeli Hamiltoniyen alarak; bu sistemin denge özelliklerini Abubrig [55] Bogoliubov eşitsizliği temelli OAT kullanarak incelemiştir. Diğer taraftan, ikinci kullanacağımız sistem olan karma spin-3/2 ve spin-5/2 Ising sistemi, aynı zamanda $AFe^{II}\ Fe^{III}\ (C_2O4)_3$ (A= $N(n\text{-}C_3H_7)_4$ ve $Fe(TPrPc)N_3$ manyetik molekül bileşikleri için protatip model oluşturduğundan, üzerinde daha fazla çalışma yapılmıştır. İlk çalışma, Zhang ve arkadaşları [56] taraflarında yapılmış ve bunlar karma spin (3/2, 5/2) ferrimagnetik Ising sistemin iç enerji davranışlarını incelemişlerdir. Albayrak and Yığıt [57, 58], sistemin Bethe örüsü üzerindeki kesin çözümlerini yapmış ve faz diyagramlarını kapsamlıca sunmuşlardır. Rachidi ve arkadaşları [59], sistemin Cayley ağacı örüsü üzerindeki kesin çözümlerini yapmışlardır. Çok tabakalı karma spin (3/2, 5/2) Ising sisteminin de, yüzey etkilerinin manyetik özelliklerin davranışlarına tesirlerin, Ma ve Jiang [60] tarafından incelenmiştir. Sistemin MC hesaplamalarıyla incelemesi, Espriella ve arkadaşları [61, 62] tarafından yapılmıştır. Zhu ve Ling [63], OAT kullanarak her iki karma sistemin; temel faz diyagramlarını da elde ederek farklı düzlemlerde faz diyagramlarını sunmuşlardır. Ayrıca, ferrimanyetik nanoparçacıkların özellikleri, karma spin (3/2, 5/2) ısing sistemi etkin-alan teorisiyle çözülerek, Jiang ve arkadaşları [64] tarafından incelenmiştir. Ve sistem parametrelerinin değerlerine göre bir veya iki telafi noktaları bulunmuştur.

Her iki karma-spin sistemin dinamik manyetik özellikleri yukarıda belirtildiği gibi çok daha az incelenmiştir. Karma-spin (3/2, 2) Ising sisteminin manyetik dinamik davranışı ilk olarak, DOAT kullanılarak, Keskin ve Polat [65] tarafından incelenmiş ve DFG sıcaklıkları ve dinamik faz diyagramları kapsamlıca sunulmuştur. Ayrıca, daha önce belirtildiği gibi ve basit Hamiltoniyenli karma-spin (2, 3/2) iki-tabakalı Ising sisteminin yalnız DFG sıcaklıkları ve dinamik faz diyagramları Temizer ve arkadaşları [49] tarafından incelenmiştir. Ancak, histerisiz ve telafi, gibi çok önemli manyetik dinamik davranışlar incelenmemiştir. Diğer taraftan, karma spin (3/2, 5/2) Ising sisteminin DFG sıcaklıkları, dinamik faz diyagramları ve telafi sıcaklık davranışları DOAT ile Deviren ve Keskin [66] tarafından kapsamlıca incelenmiştir.

Bu literatür özetinden de anlaşılacağı üzere, en iyi bilgilerimiz dahilinde, karma-spin (3/2, 5/2) iki-tabakalı Ising sisteminin dinamik manyetik özellikleri hiç incelenmemiş ve basit Hamiltoniyenli karma-spin (3/2, 2) iki-tabakalı Ising sisteminin yalnız DFG sıcaklıkları ve dinamik faz diyagramları yakın zamanda [49] incelenmiştir. Ancak, bu proje içeriğinde daha fazla etkileşim parametresi içeren Hamiltoniyenli karma-spin (3/2, 2) iki-tabakalı Ising sisteminin incelemesi yapılacak. Ayrıca, önemli manyetik özellikler olan dinamik histerisiz ve telafi sıcaklık davranışları ve manyetik alınganlığın sıcaklığa göre davranışı gibi önemli dinamik manyetik özellikler incelenmediğinden, bunlar bu proje önerisi kapsamında yapılacaktır. Bu nedenle, proje kapsamında bu karma iki-tabakalı Ising sistemlerinin dinamik manyetik özelliklerini çok daha kapsamlı incelenmiş olması; önemli bir literatür boşluğunu doldurmuştur. Ayrıca, bu proje; manyetik tabaka yapılı ince filmlerin ve tabakalı karma spin Ising sistemlerin dinamik manyetik özellikleri üzerinde deneysel ve teorik araştırmalar yapan bilim insanlarına da ışık tutucu/yol gösterici potansiyeli de olacaktır.

Dört bölümden oluşan bu projenin ilk bölümü giriş bölümü olup, Bölüm II de karma-spin (3/2, 2) Ising sisteminin dinamik manyetik özellikleri DOAY ile incelenmiştir. Bölüm III de karma-spin (3/2, 5/2) Ising sisteminin dinamik manyetik özellikleri üzerine salınımlı dış manyetik alan frekansının etkisi kapsamlıca incelenmiştir. Projemiz kapsamında üretilen ve EKLER olarak verilen yayınlarda, içerik ve bulunan sonuçlar çok kapsamlı sunulduğundan, gereksiz tekrarlamaların olmaması için bu SONUÇ RAPORUNDA özet bilgiler verildi.

## BÖLÜM II

## KARMA-SPİN (3/2, 2) ISİNG BİLAYER SİSTEMİNİN DİNAMİK MANYETİK ÖZELLİKLERİNİN İNCELENMESİ

Karma-spin (3/2, 2) Ising bilayer sisteminin dinamik manyetik özellikleri ile ilgili çalışmalar tamamlanmıştır. Sistemin dinamik manyetik özellikleri, salınımlı dış manyetik alan altında Glauber-tipi stokhastik dinamik temelli ortalama-alan yaklaşımı, yani dinamik ortalama-alan yaklaşımı (DOAY), kullanılarak incelendi. Projemiz kapsamında üretilen ve EKLER olarak verilen yayınlarda, içerik ve bulunan sonuçlar çok kapsamlı sunulduğundan, gereksiz tekrarlamaların olmaması için burda özet bilgiler verildi. Bu konuda üretilen çalışmalar:

**a)** Birinci çalışmada farklı kristal alan etkileşim parametreli ($D_A \neq D_B$) karma spin (3/2, 2) Ising bilayer sisteminin dinamik faz diyagramları (DFD), yalnız feromagnetik(FM)/ferromagnetik (FM) etkileşme için, incelendi. $D_A$ ve $D_B$ sırasıyla A ve B alt örgüleri için tanımlanan iki farklı kristal alan etkileşimleridir. Sonuçta, tabakalar arası etkilelme parametresi ($J_3$) ufak olduğunda $D_A$ ve $D_B$, DFD'lara etkisi fazla olduğu, fakat $J_3$ büyük olduğunda etkinin az olduğu gözlendi. Bu çalışma, **Internatinal Conference For Academic Disciplines, Harvard Medical School, Boston, Massachusetts, ABD, 23-27 May 2016,** toplantısında sözlü bildiri olarak sunulmuştur ve PROOCEEDING olarak Conference of the International Journal of Arts &Sciences dergisinde basıldı. **(Bknz. EK-1 ve 2).**

**b)** Busunum ve kısa PROCEEDİNG çalışmada ilginç sonuçlar elde edilince, bu çalışma daha da kapsamlı yapılmış ve çalışma FM/AFM (AFM, antiferromagnetic) ve AFM/AFM etkileşmeleri içinde kapsamlıca incelenmiş ve DFD'ları elde edilmiştir. Sonuçta, zengin ve farklı topolojide faz diyagramları elde edildi. Özellikle, etkileşim parametrelerine bağlı olarak, sistemde üçlükritik nokta dışında, dinamik çift kritik son nokta, dinamik sıfır kritik son nokta, dinamik çoklu kritik nokta, dinamik üçlü nokta gibi özel kritik noktalar da gözlendi. Aynı zamanda, $D_A$, $D_B$ ve $J_3$, etkileşme parametrelerinin DFD'larına etkisi de incelendi ve sonuçta $D_A$, $D_B$ ve $J_3$, FM/FM, AFM/FM etkileşmeleri için elde edilen DFD'larına etkilerinin çok fazla olduğu, fakat AFM/AFM etkileşmesi için elde edilen faz diyagramlarına etkileri daha az oldupu tespit edildi. Bu çalışma, yayımlanması için SCI kapsamında olan **Journal of Superconductivity and Novel Magnetism** dergisine sunulmuş olup bu anda Hakem incelemesi aşamasındadır (**Bknz. EK-3**).

**c)** Dinamik manyetik histerisiz (DMH) davranışları üzerine olan ilk çalışmamız; Tek kristal alan etkileşim (D) Hamiltoniyenli karma-spin (3/2, 2) Isimg bilayer sisteminde oluşan DMH davranışlarının incelenmesi üzerine olmuştur. Bu çalışmada sistemin dinamik histerezis döngüsü (loop) üzerine, sıcaklığın ve salınımlı dış manyetik alan frekansının etkisi, detaylıca incelendi. Sistemin yalnızca tekli döngü histerisis davranış gösterdiği gözlemlendi. Ayrıca sistemin zorlayıcı alanı ve artık mıknatıslanmasının sıcaklığa bağlı davranışı da incelenmiştir. Bu çalışma "*Dynamic Magnetic Hysteresis Behavıor in a Mixed Spin (3/2, 2) Bılayer System Under A Time-Dependent Oscillating Magnetic Field"* başlığı ile **ISERD 125th International Conference on Science and Innovative Engineering (ICSIE), 23 Ocak - 24 Ocak 2017, Mekke, SUUDI ARABISTAN,** uluslararası toplantısında DAVETİYELİ bildiri olarak sunulmuştur (**Bknz. EK-4**). Çalışma aynı zamanda **Proceedings of 65th ISERD International Conference, Mecca, Saudi Arabia, 23rd-24th January 2017, ISBN: 978-93-86291-92-9** proceding olarak yayınlanmıştır (**Bknz. EK-5**).

**d)** DMH davranışları üzerine yaptığımız ikinci çalışmada, alt örgüler için farklı kristal alan etkileşim parametreli ($D_A \neq D_B$) seçildi. Böylece, karma-spin (3/2, 2) Ising bilayer sisteminin dinamik histerisis özellikleri salınımlı dış manyetik alan altında DOAY ile incelendi. Çalışmada, özellikle DA, $D_B$ 'nin DMH davranışları üzerine etkisinin yanısıra sıcaklığın, salınımlı dış manyetik alan frekansının (w) ve tabakalar arası bilineer etkileşim parametresinin ($J_3$) dinamik histerezis döngüleri üzerine etkileri kapsamlıca incelenmiştir. Sistemin tekli ve üçlü histerisis davranışlar gösterdiği gözlemlendi. Ayrıca, zorlayıcı manyetik alan ve kalıcı miknatislanma davranışları üzerine w ve $J_3$ etkileri araştırıldı. Bu çalışma, SCI kapsamıda olan **Journal of Superconductivity and Novel Magnetism** dergisinde basım (DOI 10.1007/s10948-017-4145-y) aşamasındadır (**Bknz. EK-6**). Çalışma aynı zamanda sözlü bildiri olarak **Sixth Bozok Science Workshop: Studies from Nuclei to Nanomaterials with Applications 23-25 August 2017, Yozgat, Turkey**, toplantısında sözlü bildiri olarak sunulmuştur (**Bknz. EK-7**).

Bu çalışmalarda elde edilen sonuçlar literatürdeki mevcut diğer dinamik sonuçlarla karşılaştırıldı ve güzel, kuantatif, uyum gözlendi.

# BÖLÜM III

## KARMA-SPİN (3/2, 5/2) ISİNG BİLAYER SİSTEMİNİN DİNAMİK MANYETİK ÖZELLİKLERİ ÜZERİNE SALININLI DIŞ MANYETİK ALAN FREKANSININ ETKİSİ

Karma-spin (3/2, 5/2) ısing bilayer sisteminin dinamik manyetik özellikleri üzerine salınınlı dış manyetik alan frekansının etkisi kapsamlıca incelenmiştir. Sistemin ortalama alana dinamik denklemeleri DOAY kullanılarak elde edilmiş ve dinamik düzen parametrelerinin ($M_1^A$, $M_1^B$, $M_2^A$ ve $M_2^B$) sıcaklığa göre davranışı kapsamlıca incelenerek DFG noktaları hesaplandı ve dinamik faz diyagrmları üç farklı düzlemde (h, T), (d, T) ve (w/π, T) düzlemlerinde sunularak dış manyetik alan frekansının etkisi incelenmiştir. Manyetik alan frakansonın küçük değerlerinde sistemin daha basit faz diyagramları sergilediği gözlemlenirken, frekansın büyük değerlerinde sistemin daha karmaşık/zengin dinamik faz diyagramları sergilediği gözlemlenmiştir. Etkileşim parametrelerine bağlı olarak, sistemin üçlükritik nokta dışında, dinamik üçlü nokta ve dörtlü nokta gibi özel noktalar sergilediği gözlenmiştir. Son olarak sistemin dinamik histerisiz alanı üzerine salınımlı dış manyetik alan frekansının etkisi incelenmiş ve sistemin tekli ve üçlü histerisiz davranış sergilediği gözlenmiştir. Çalışmadan elde edilen sonuçlar literatürdeki mevcut diğer dinamik sonuçlarla karşılaştırıldı ve güzel, kuantatif, uyum gözlendi. Çalışma yayımlanması için **Journal of Magnetism and Magnetic Materials** dergisine sunulmuş olup bu anda Hakem inceleme aşamasındadır (**Bknz. EK-8**).

,

# BÖLÜM IV

# SONUÇ VE ÖNERİLER

**Bulunan sonuçlar:**

Karma spin (3/2, 2) Ising bilayer sisteminin dinamik histerisis özelliklerinin Glauber-tipi stokhastik dinamik temelli ortalama-alan yaklaşımı, yani dinamik ortalama-alan yaklaşımı (DOAY) incelenmesi ile elde edilen sonuçlar: Etkileşim parametrelerine bağlı olarak sistemin tekli ve üçlü dinamik histerisiz davranış sergilediği gözlendi. Histerisiz alan üzerine sıcaklığın etkisi incelendiğinde, sıcaklık artırıldığında dinamik histerisiz alanının belirli bir krtitik sıcaklık değerine kadar arttığı ve daha sonra azaldığı gözleniştir. Kritik sıcaklığın çok büyük değerleri için histeris alanın yok olduğu gözlenmiştir. Salınımlı dış manyetik alan frekansının histerisiz alanı üzerine etkisi incelendiğinde frekansın artmasıyla birlikte histerisisz alanın arttığı ve daha sonra azldığı görülmüştür. Tabakalar arası bilineer etkileşim parametresi $J_3$'ün negatif değerlerden başlayarak artması ile birlikte histerisiz alanın arttığı ve belirli yüksek pozitif $J_3$ değerinden itibaren histerisiz alanın azaldığı ve en sonundada yok olduğu gözlenmiştir. Son olarak kristal alan etkileşim parametrelerinin histerisz alan üzerine etkisi incelendi. A alt örgüsünün kristal alan etkileşim parametresinin ($d_A$) etkisi incelendiğinde, $d_A$'nın artmasıyla birlikte histerisiz alanın arttığı gözlenmiştir. Ayrıca, $d_A$'nın küçük negatif değerlerinde sistemin üçlü histerisiz davranış sergilediği görülmüştür. B alt örgüsünün kristal alan etkileşim parametresinin ($d_B$) etkisi incelendiğinde, sistemin daima tekli histerisiz davranış gösterdiği bulunmuştur.

Farklı kristal alan etkileşim parametreli ($d_A \neq d_B$) karma spin (3/2, 2) Ising bilayer sisteminin dinamik dinamik faz diyagramlarının DOAY ile incelenmesi sonucu elde edilen sonuçlar: Elde edilen dinamik faz diyagramları indirgenmiş sıcaklık ve salınımlı dış manyetik alan genliği düzleminde sunulmuştur. Sistemde paramanyetik (p), ferromanyetik (f), antiferromanyetik (af), yüzey (sf), telafi (c) ve karma (m) temel fazlarının yanı sıra, f + p, m+ p, f + c, f + sf, c + p, c + af, af + p karma fazı elde edilmiştir. Fazlar arası dinamik faz sınırları birinci-derece ve ikinci-derece faz geçiş çizgilerinden oluşmaktadır. Temel fazlar arası dinamik faz sınırları genellikle ikinci-derece faz geçiş çizgileri olduğu halde, karma fazlar ise çoğunlukla birinci-derece ve az sayıda ikinci-derece faz geçiş çizgileri ile ayrılmaktadır. Etkileşim parametrelerine bağlı olarak, sistemde üçlükritik nokta dışında, dinamik çift kritik son nokta, dinamik sıfır kritik son nokta, dinamik çoklu kritik nokta gibi özel kritik noktalar da gözlenmiştir. Dinamik faz diyagramları üzerine kristal alan etkileşme

parametrelerinin etkisinin iki tabaka arası etkileşme parametresi olan $J_3$ bilineer etkileşim parametresinin küçük değerleri için büyük olduğu, $J_3$ bilineer etkileşim parametresinin büyük değerleri için küçük olduğu gözlenmiştir.

Karma spin (3/2, 5/2) Ising bilayer sisteminin dinamik manyetik özelliklerinin DOAY ile incelenmesi sonucu elde edilen sonuçlar: Elde edilen dinamik faz diyagramları üç farklı düzlemde (h, T), (d, T) ve (w/π, T) düzlemlerinde sunularak dış manyetik alan frekansının etkisi incelenmiştir. Manyetik alan frakansının küçük değerlerinde sistemin daha basit faz diyagramları sergilediği gözlemlenirken, frekansın büyük değerlerinde sistemin daha karmaşık/zengin dinamik faz diyagramları sergilediği gözlemlendi. Etkileşim parametrelerine bağlı olarak, sistemin üçlükritik nokta dışında, dinamik üçlü nokta ve dörtlü nokta gibi özel noktalar sergilediği gözlendi. Son olarak sistemin dinamik histerisiz alanı üzerine salınımlı dış manyetik alan frekansının etkisi incelendi ve sistemin tekli ve üçlü histerisiz davranış sergilediği gözlendi.

**Öneriler:**

**1-** Glauber-tipi stokastik dinamik kullanılarak değişik ve özellikle de daha karmaşık fiziksel sistemlerin dinamik davranışları incelenebilir ve dinamik faz diyagramları elde edilebilir.

**2-** Glauber geçiş oranları temelli etkin alan teorisi, dinameik etkin alan teorisi (DEAT) Dinamik etkin alan teorisinde (DEAT) spinler arası korelasyonlar göz önüne alındığından dolayı karma spin sistemlerinin dinamik faz geçiş sıcaklıkları, dinamik histerisis davranışları, dinamik faz diyagramları gibi dinamik özellikleri, DEAT ile incelenmesi, sistemlerin dinamik özelliklerininin incelenmesi konusuna önemli katkılar sağlayacaktır.

## KAYNAKLAR


[1] R.F. Bunshah (Ed.), Handbook of Deposition Technologies for Films and Coatings, 2nd ed., Noyes Publications, Westwood, NJ, 1994.

[2] J.E. Mahan, Physical Vapor Deposition of Thin Films, Wiley, New York, 2000.

[3] M. Ohring, Materials Science of Thin Films: Deposition and Structure, 2nd ed., Academic, San Diego, CA, 2002.

[4] D.A. Glocker, C. Morgan, S.I. Shah (Eds.), Handbook of Thin Film Process Technology, 2nd ed.,Taylor and Francis, London, 2010.

[5] A.D. Edelstein, C. Kim, S.B. Quadri, K.H. Kim, V. Browning, H.Y. Yu, B. Maruyuma, K. Everett, Solid State Commun. 76 (1990) 1379;

N.M. Jennet, D.J. Dingley, J. Magn. Magn. Mater. 93 (1991) 472;

E. Colombo, O. Donzelli, G.B. Fraatucello, F. Ronconi, J. Magn. Magn. Mater. 107 (1992) 1857.

[6] R. Krishnan, H.O. Gupta, H. Lassri, C. Sella, J. Kaaboutchi, J. Appl. Phys. 70 (1991) 6421.

[7] G. Bayreuther, F. Bensch, V. Kottler, J. Appl. Phys. 79 (1996) 4509.

[8] K.W. Chou, A. Puzic, H. Stoll, G. Schütz, B.V. Waeyenberge, T. Tyliszczak, K. Rott, G. Reiss, H. Brückl, I. Neudecker, D. Weiss, C.H. Back, J. Appl. Phys. 99 (2006) 08F305.

[9] M. Stampe, P. Stoll, T. Homberg, K. Lenz, W. Kuch, Phys. Rev. B 81 (2010) 104420.

[10] G. Yashwant, C.L. Prajapat, G. Ravikumar, S.Soltan, G. Christiani, H.U. Habermeier, J. Magn. Magn. Mater. 324 (2012) 1406.

[11] L. S. Huang, F. F. Hu, J. S. Chen, J. Magn. Magn. Mater. 324 (2012) 1242.

[12] J. Li, J. Magn. Magn. Mater. 324 (2012) 1512.

[13]Y. Laosiritaworn, J. Poulter, J.B. Staunton, Phys. Rev. B 70 (2004)104413.

[14] P.Cossio, J.Mazo-Zuluaga, J. Restrepo, Physica B 384 (2006) 227.

[15] A. Zaim, Y. El Amraoui, M.Kerouad, L. Bihc, Ferroelectrics 372 (2008) 3.

[16] Y.L.Chou, M.Pleimling, Phys. Rev. B 84 (2011) 134422.

[17] J. Candia, E.V.Albano, J. Stat. Mech. 2012 (2012) P08006.

[18] A.V. Albano, K.Binder, Phys. Rev. E 85 (2012) 061601.

[19] A. Feraoun, A. Zaim, M. Kerouad, J. Magn. Mag. Mater. 377 (2015) 126.

[20] D.L. Mills, Phys. Rev. B 3 (1971) 3887.

[21] T.C.Lubensky, M. H. Rubin, Phys. Rev. B12 (1975 ) 3885.

[22] X.Q. Hong, Phys. Rev.B41(1990)9621.

[23] F.Aguilera-Granja, J.L. Moran-Lo´pez, Solid State Commun.74 (1990) 155.

[24] T.Kaneyoshi,PhysicaA293 (2001)200.

[25] B. Deviren, O. Canko, M. Keskin, J. Magn. Magn. Mater. 320 (2008) 2291.

[26] B. Deviren, S. Akbudak, M. Keskin, Solid State Commun. 151 (2011) 193.

[27] T.Kaneyoshi, Solid State Commun. 152 (2012) 1686.

[28] T.Kaneyoshi, Physica B 407 (2012 ) 4358.

[29] Ü. Akıncı, J. Magn. Magn. Mater. 329 (2012) 178.

[30] T.Kaneyoshi, Phase Transit. 85 (2012) 264.

[31] K.H. Benneman, Magnetic Properties of Low-Dimensional Systems, Springer- Verlag, NewYork, 1986.

[32] K. Ohno, Y.Okabe, Phys. Rev. B39 (1989) 9764.

[33] Q. Jiang, Z.Y.Li, J. Magn. Magn. Mater. 80 (1989) 78.

[34] J. Oitmaa, R.R.P.Singh, Phys. Rev. B 85 (2012) 014428.

[35] T.Balcerzak, I. Łuźniak, Physica A 388 (2009)357.

[36] O. Canko and E. Albayrak, Phys. Rev. E 75 (2007) 01116.

[37] E. Albayrak, S.Akkaya, T.Cengiz, J. Magn. Magn. Mater.321 (2009) 3726.

[38] E. Albayrak, A.Yiğit, Phys. Status Solidi B 246 (2009) 2172.

[39] E. Albayrak, A. Yığıt, T. Cengiz, Physica A 389 (2010) 2522.

[40] M.Y. Wu, A.J. Ye, Z.B. Li, W.G. Zeng, Acta Phys. Sin. 49 (2000) 1168.

[41] H. Jang, M.J. Grimson, Phys. Rev. E 63 (2001) 066119.

[42] H. Jang, M.J. Grimson, C.K. Hall, Phys. Rev. B 67 (2003) 094411.

[43] H. Jang, M.J. Grimson, C.K. Hall, Phys. Rev. E 68 (2003) 046115.

[44] H. Jang, M.J. Grimson, T.B. Woolf, Phys. Rev. E 70 (2004) 047101.

[45] O. Canko, E. Kantar, M. Keskin, Physica A 388 (2009) 28.

[46] M. Ertaş, M.Keskin, Phys. Lett. A 376 (2012) 2455.

[47] M. Ertaş, M. Keskin, Chinese Physics B 22 (2013) 120507.

[48] M. Ertaş, E. Kantar, M. Keskin, J.Magn. Magn. Mater. 358-359 (2014) 56.

[49] Ü. Temizer, M. Tülek, S. Yarar, Physica A 415 (2014) 156.

[50] A. Babok, J. Dely, J. Magn. Magn. Mater. 310 (2007) 1419.

[51] E. Albayrak, Physica B 391 (2007) 47.

[52] H. Miao, G. Wei, J. Geng, J. Magn. Magn. Mater. 321 (2009) 4139.

[53] B. Deviren, E. Kantar, M. Keskin, J. Korean Phys. Soc. 56 (2010) 1738.

[54] B. Deviren, Y. Polat, M. Keskin, Chin. Phys. B 20 (2011) 060507.

[55] F. Abubrig, World Journal of Condensed Matter Physics 3 (2013) 111.

[56] Q. Zhang, G. Wei, Y. Gu, phys. stat. sol. (b) 242 (2005) 924.

[57] E. Albayrak, A. Yığıt, Phys. Lett. A 353 (2006) 121.

[58] A. Albayrak, A. Yığıt, phys. stat. sol. 244 (2007) 748.

[59] A.Rachidi, A. Yessoufou, S. H. Amoussa, F. Hontinfinde, Cent. Eur. J. Phys. 7 (2009) 555.

[60] B. Ma, W. Jiang, IEEE Transactions on Magnetism 47 (2011) 3118.

[61] N. D. Espriella, G. M. Buendia, J. Phys.: Condens. Matter 23 (2011) 176003.

[62] N. D. Espriella Valez, C. O. Lopez, F. T. Hoyos, Revista Mexicana de Fisica 59 (2013) 95.

[63] W. Zhu, M. Ling, Commun. Theor. Phys. (Bejing China) 51 (2009) 756.

[64] W. Jiang, H. Guan, Z. Wang, A. Guo, Physica B 407 (2012) 378.

[65] M. Keskin, Y. Polat, J. Mgn. Magn. Mater. 321 (2009) 3905.

[66] B. Deviren, M. Keskin, J. Stat. Phys. 140 (2010) 934.

## EKLER

### A- Projeden SCI Kapsamında Yapılan Çalışmalar

**1-** Keskin, M. and Ertaş, M., *Dynamic Magnetic Hysteresis Behaviors in a Mixed Spin (3/2, 2) Bilayer System with Different Crystal-Field Interactions*, Journal of Superconductivity and Novel Magnetism, DOI 10.1007/s10948-017-4145-y, baskıda

**2-** Keskin, M. and Koçak, Y., *Influence of Crystal-Field and Interlayer Coupling Interactions on Dynamic Magnetic Critical Properties of a Mixed Spins (3/2, 2) Bilayer System*, Journal of Superconductivity and Novel Magnetism, incelemede.

**3-** Keskin, M. and Ertaş, M., *Dynamic magnetic properties of the Ising bilayer system consisting of spin-3/2 and spin-5/2 atoms with a crystal-field interaction in an oscillating field*, Journal of Magnetism and Magnetic Materials, incelemede.

### B- PROCEEDİNG olarak Yayımlanan Çalışmalar

**1-** Ertaş, M., Koçak, Y. and Keskin, M., *The crystal field effects on the dynamic phase diagrams ın the ferromagnetic mixed spin (3/2, 2) bilayer system: mean-field theory and Glauber-type stochastic dynamic approaches*, Conference of the International Journal of Arts & Sciences, CD-ROM. ISSN: 1943-6114 :: 09(03):145–152 (2016).

**2-** Ertaş, M. and Keskin, M., *Dynamic Magnetic Hysteresis Behavior in a Mixed Spin (3/2, 2) Bilayer System Under a Time-Dependent Oscilating Magnetic Field*, Proceedings of 65th ISERD International Conference, Mecca, Saudi Arabia, 23rd-24th January 2017, ISBN: 978-93-86291-92-9.

### C- Uluslararsı Sunulan Bildiriler

**1-** Ertaş, M., Koçak, Y. and Keskin, M. "*The crystal field effects on the dynamic phase diagrams ın the ferromagnetic mixed spin (3/2, 2) bilayer system: mean-field theory and Glauber-type stochastic dynamic approaches*" Internatinal Conference for Academic Disciplines, Harvard Medical School, Boston, Massachusetts, ABD, 23-27 May 2016, **SÖZLÜ BİLDİRİ**.

**2-** Ertaş, M. and Keskin, M., *Dynamıc Magnetic Hysteresis Behavior in a Mixed Spin (3/2, 2) Bilayer System Under a Time-Dependent Oscilating Magnetic Field*, ISERD 125th International Conference on Science and Innovative Engineering (ICSIE), 23 Ocak - 24 Ocak 2017, Mekke, SUUDI ARABISTAN, **SÖZLÜ BİLDİRİ.**

**3-** Kekin, M. and Ertaş, M., *Dynamic Magnetic Hysteresis Behaviors in a Mixed Spin (3/2, 2) Bilayer System with Different Crystal-Field Interactions*, Bozok Science Workshop 2017, Yozgat, August 23-25, 2017, **SÖZLÜ BİLDİRİ**.

EK-1



INTERNATIONAL JOURNAL OF ARTS AND SCIENCES

55 Farm Drive
Cumberland, Rhode Island 02864-3565
USA

H6V909

March 13, 2016

Professor Mustafa Keskin
Erciyes University
Depatment of Physics
Kayseri 38039
Turkey

Dear Prof. Dr. Mustafa Keskin,

**RESEARCH TITLE**
*The Crystal Field Effects On The Dynamic Phase Diagrams In The Ferromagnetic Mixed Spin (3/2, 2) Bilayer System: Mean-Field Theory And Glauber-Type Stochastic Dynamic Approaches*

**AUTHOR/S**: Mehmet Ertaş, Yusuf Koçak, and Mustafa Keskin
**RESEARCH ID**: H6V909
**REGISTRATION FEE**: $375 (if one registers for the full conference); $575 (if two co-authors register)
**REGISTRATION DATE**: 30 March 2016

I am pleased to inform you that your submission was subjected to a double-blind review process, and the reviewers accepted the above for oral presentation at the International Journal of Arts & Sciences' (IJAS) *International Conference for Physical, Life and Health Sciences* which will be held at Harvard Medical School, 77 Avenue Louis Pasteur, Boston, Massachusetts. The conference will run from 23 to 27 May 2016.

The conference follows the multidisciplinary TED format at http://www.ted.com. The comprehensive program for our last conference on the Harvard campus will give you an idea of what to expect: https://ijas2015boston.sched.org/.

In order for IJAS to remain in compliance with the American immigration laws, it is imperative that you enter the USA in an appropriate non-immigration status. For example, if you're a citizen of Australia, Canada or the EU, you may not need a visa to enter for the conference. If you require a visa to enter the United States, please present this letter at an American Embassy or Consulate with your non-immigrant visa application and passport.

For your submission to appear in one of our refereed ISSN-numbered publications, please format your work in line with this template http://www.internationaljournal.org/template.html. There is no limit on the number of pages. Email your properly formatted abstract/paper only to ManuscriptSubmission@gmail.com. Please make sure that it is in Microsoft Word and that the above "Research ID" is included in all your future emails' Subject line.

The registration fee does not include food and lodging. To get through security at Harvard you need to pay your registration in advance and show your receipt to the security.

As a professor at Central Connecticut State University, I witness firsthand the benefits of international education emanating from study abroad programs. Our conference will highlight these benefits while offering you a forum to share your specialized research with international professors.

We look forward to your presentation at Harvard.

Sincerely,

**Professor J.L. Bonnici, PhD, JD**
IJAS Conferences Coordinator

# 25 May 2016
# Room 217 (Conference Center at Harvard Medical School)



**B = Business and Economics;** **E = Teaching and Education;** **S = Technology and Science** **C = Social Sciences and Humanities**

| | | | |
|---|---|---|---|
| 10:15am – 10:30am | S | EVALUATION OF TOPIARY APPLICATIONS AND PROBLEMS: A CASE STUDY OF KASTAMONU | Mehmet Cetin, Hakan Sevik |
| 10:30am – 10:45am | S | POTENTIAL CONCENTRATIONS OF SELECTED TRACE METALS FROM ROAD SALT CORROSION | Peter R. Pascucci |
| 10:45am – 11:00am | S | THE CRYSTAL FIELD EFFECTS ON THE DYNAMIC PHASE DIAGRAMS IN THE FERROMAGNETIC MIXED SPIN (3/2, 2) BILAYER SYSTEM... | Mehmet Ertaş, Mustafa Keskin, Yusuf Koçak |
| 11:00am – 11:15am | S | INDOOR QUALITY ANALYSIS OF CO2 FOR KASTAMONU UNIVERSITY | Mehmet Cetin, Hakan Sevik |
| 11:15am – 11:30am | S | INVESTIGATION OF MDMO-PPV CONDUCTING POLYMER BASED ORGANIC FIELD EFFECT TRANSISTOR CHARACTERISTICS ... | Zeynep Kara, Serhat Tunc |
| 11:30am – 11:45am | S | ENVIRONMENTAL EFFECTS OF ROAD CONSTRUCTION IN FOREST AREAS IN TURKEY | Burak Aricak |
| 11:45am – 12:00pm | S | FASHION AND THE ENVIRONMENT | Ashish Hooda |
| 12:00pm – 12:15pm | S | SEASONAL, EQUINOX AND SOLSTICE VARIATIONS OF THE IONOSPHERE OVER TURKEY | Feza Arikan, Ali Cinar, Tamara Gulyaeva, Secil Karatay |
| 1:00pm – 1:15pm | S | AN INTERPRETER PROGRAM WRITTEN IN JAVA FOR A PROGRAMMING LANGUAGE | Octavian Nicolio |
| 1:30pm – 1:45pm | S | METHODS TO REDUCE THE FRICTION OF TURBULENT FLOW | Chaim Elata |
| 1:45pm – 2:00pm | S | A COMPARATIVE RESEARCH ON PERCEPTIONS OF FUTURE SUSTAINABLE TRANSPORT INTERVENTIONS ... | Can Bıyık, Michael Burrow, Miles Tight |
| 2:00pm – 2:15pm | S | DETERMINANTS OF OBSTETRIC FISTULA IN ETHIOPIA | Asrat Atsedeweyn Andargie, Abebe Debu |
| 2:10pm – 2:25pm | S | STUDY OF THE DIFFERENT REGIMES FLOW IN PERIODIC DESIGNS CHANNELS | Djehiche Abdelkader, Boutassouna Kheira, et al. |
| 2:20pm – 2:35pm | S | EFFECT OF HORIZONTAL DRAIN LENGTH ON THE SEEPAGE FLOW IN A HOMOGENEOUS EARTH DAM | Djehiche Abdelkader, Gafsi Mostefa, Amieur Rekia |
| 2:30pm – 2:45pm | S | INTERNET USERS' EXPERIENCES OF CYBERHATE | Serkan Celik |
| 2:40pm – 2:55pm | S | NIGERIA COLLEGES OF EDUCATION GAMES: A PANACEA FOR STUDENTS' SOCIALIZATION | Adeyinka Theophilus Olusegun |
| 2:50pm – 3:05pm | S | EFFICACY OF SOME PLANT EXTRACT AGAINST AMERICAN BOLL WORM INCLUDING THE EFFECT ON PERITROPHIC MEMBRANE | Deepali Lall, Sudha Summerwar |
| 3:00pm – 3:15pm | C | WIG OR NO WIG: WHEN EARLY AMERICAN DIPLOMATS ENCOUNTERED EUROPEAN COURT PROTOCOL | Lukrecija Maljkovic Atanasovska |
| 3:15pm – 3:30pm | C | ABU AL FAWARES' TIMELESS ARGUMENT | Mohammed Saleh Alghamdi |
| 3:30pm – 3:45pm | C | LEVERAGES OF POLITICAL PRESSURE IN MEDIA: CASE OF POST-SOVIET GEORGIA | Rusudan Vashakidze |
| 3:45pm – 4:00pm | C | LABOR, ALIENATION AND AESTHETICS: PERSPECTIVES FROM CHINESE FEMALE WORKER POETS | Yun Li |
| 4:00pm – 4:15pm | C | SUFFERING AND SMILING: EBOLA SCOURGE, THE GENERAL ELECTIONS AND COMEDIC SOCIAL MEDIA RESPONSES IN NIGERIA | Izuu Nwankwo E. |
| 4:15pm – 4:30pm | C | RELIGIOUS VIOLENCE PEACE AND SECURITY IN NIGERIA | Patricia Anwuluorah |
| 4:30pm – 4:45pm | C | ALANG: FROM GLORIOUS PAST TO GLOOMY PRESENT | Alpa Mehta |
| 4:45pm – 5:00pm | B | PRODUCT QUALITY AND CUSTOMER SATISFACTION OF CONSUMER GOODS IN NIGERIA | Hindu J Amin, Pauline E Onyeukwu, Aminu Ahmed |

INTERNATIONAL JOURNAL OF ARTS AND SCIENCES

# *Certificate of Excellence*

## MUSTAFA KESKIN

*Recognized for Outstanding Research and Presentation at the*

INTERNATIONAL CONFERENCE FOR ACADEMIC DISCIPLINES

*Joseph B. Martin Conference Center*
Harvard Medical School, Boston, Massachusetts

*23 - 27 May 2016*

H6V 909

The research title is posted online at https://ijas2016harvard.sched.org

*Conference of the International Journal of Arts & Sciences,*
CD-ROM. ISSN: 1943-6114 :: 09(03):145–152 (2016)

# THE CRYSTAL-FIELD EFFECTS ON THE DYNAMIC PHASE DIAGRAMS IN FERROMAGNETIC MIXED SPIN (3/2, 2) BILAYER SYSTEM: THE MEAN-FIELD THEORY AND GLAUBER-TYPE STOCHASTIC DYNAMICS

**Mehmet Ertaş, Yusuf Koçak and Mustafa Keskin**

*Erciyes University, Turkey*

We study the crystal field effects on the dynamic phase diagrams in the ferromagnetic mixed spin (3/2, 2) bilayer system within the Glauber-type stochastic dynamics based on the mean-field theory. Dynamic phase diagrams are presented in the reduced temperature (T) and magnetic field amplitude (h) plane. We find that when the coupling constant ($J_3$) is small, the effects of crystal–field interactions parameters ($D_A$ and $D_B$) on the behavior of the dynamic phase diagrams are very much. If $J_3$ is large, the influences of $D_A$ and $D_B$ are small.

**Keywords:** Mixed spin (3/2, 2) bilayer system, Dynamic phase diagrams, Glauber-type stochastic dynamics, Mean-field theory.

## Introduction

Magnetic properties of various magnetic multilayers, layered structure and thin films have been attracted significant attention, because of their great potential for technological application as well as for academic research. Magnetic materials have been usually modeled by means of the mixed Ising systems and these systems also give very rich phase diagrams. A mixed spin-3/2 and spin-2 Ising system is the one of the well-known mixed spin which correspond to the Prussian blue of the type $Fe^{II}_{1.5}[Cr^{III}(CN)_6]. nH_2O$ [1-2]. Miao, et al. [3] studied the phase diagram of the mixed spin (3/2, 2) Ising ferromagnetic model with different crystal fields by the use of the mean-field theory (MFT) based on the Bogoliubov inequality for the Gibbs free energy. Bayram et al. [4] investigate the magnetic properties of a mixed spin (3/2, 2) Ising ferrimagnetic system within the effective-field theory (EFT) in the presence of external magnetic field on a honeycomb and square lattices. Abugrig [5] studied magnetic properties of the mixed spin (3/2, 2) Ising ferrimagnetic system in an applied longitudinal magnetic field within the MFT based on the Bogoliubov inequality for the Gibbs free energy. It has also gives very rich equilibrium [2] and nonequilibrium phase diagrams [3]. Deviren et al. [6] studied phase diagrams in the mixed spin3/2 and spin-2 Ising system with two alternative layers by using the EFT. Recently, Jabar et al [7] investigate the magnetic properties of the mixed spin (3/2, 2) system using Monnte Carlo (MC) calculations. On the other hand, Keskin and Polat [8] studied the phase diagrams of the nonequilibrium mixed spin-3/2 and spin-2 Ising ferrimagnetic system on square lattice under a time-dependent external magnetic field are presented by using the Glauber-type stochastic dynamics based on the MFT, also called the dynamic mean-field theory (DMFT). Recently, dynamic phase diagrams of the mixed spin (3/2, 2) Ising bilayer system studied by Temizer

et al. [9] and they presented dynamic phase diagrams in four different planes. They took the crystal-field interaction for A and B sublatices as same (D); hence the influence of the crystal-field interactions was not studied in which it is important to study their effects in detail. In this talk, we took the crystal-field interaction for sites on A lattice as $D_A$ and for sites on B lattice as $D_B$. We investigate the effects of $D_A$ and $D_B$ on the behavior of dynamic phase diagrams in the ferromagnetic mixed spin (3/2, 2) bilayer system within the DMFT.

We consider a mixed spin-3/2 and Spin-2 Ising system with a two-layers, namely $L_1$ and $L_2$, on a square lattices, seen in Fig. 1. Each layer of the system is also a two-sublattice system (A and B) with spin variables $\sigma_i^A$ , $\sigma_i^B = \pm 3/2, \pm 1/2$ occupy $L_1$ layer and $S_j^A$ , $S_j^B = \pm 2, \pm 1, 0$ $L_2$ layer. Therefore, the system can be described with four sublattice magnetizations or four simple magnetizations that are introduced as follows: $m_1^A \equiv \langle \sigma_i \rangle$, $m_1^B \equiv \langle \sigma_j \rangle$, $m_2^A \equiv \langle S_{i'} \rangle$, $m_2^B \equiv \langle S_{j'} \rangle$, where $\langle ... \rangle$ is the thermal expectation value. Each layer has N sites and interacts with its nearest-neighbor (NN) and the corresponding adjacent spins in the other layer whose sites are labeled by i, i′, j and j′, as seen in Fig. 1.

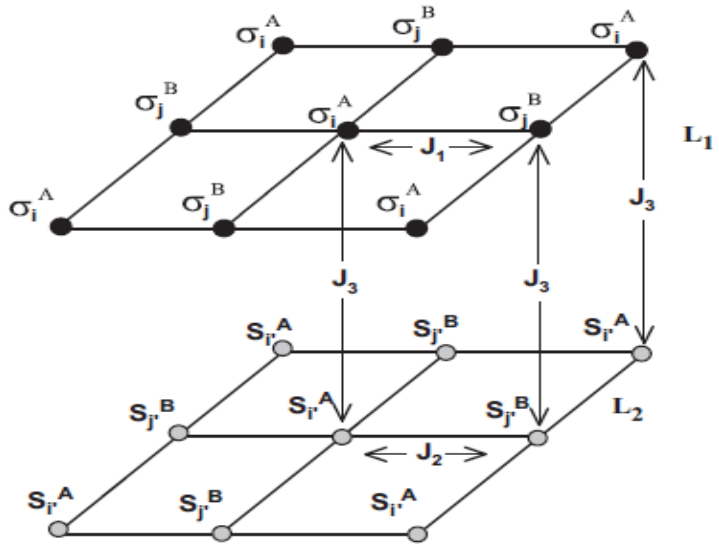


**Figure 1.** Schematic representation of a two-layer square lattice: $L_1$ and $L_2$ refer to the upper and lower layers containing the spins labeled as $\sigma_i^A$, $\sigma_j^B$ and $S_{i'}^A$, $S_{j'}^B$

The Ising Hamiltonian of such a bilayer square lattice system can be written as

$$\mathcal{H} = -J_1 \sum_{<ij>} \sigma_i^A \sigma_j^B - J_2 \sum_{<i'j'>} S_{i'}^A S_{j'}^B - J_3 \left( \sum_{<ii'>} \sigma_i^A S_{i'}^A + \sum_{<jj'>} \sigma_j^B S_{j'}^B \right) - D_A \left( \sum_{<i>} \left(\sigma_i^A\right)^2 + \sum_{<i'>} \left(S_{i'}^A\right)^2 \right)$$
$$- D_B \left( \sum_{<j>} \left(\sigma_j^B\right)^2 + \sum_{<j'>} \left(S_{j'}^B\right)^2 \right) - H \left( \sum_{<i>} \sigma_i^A + \sum_{<j>} \sigma_j^B + \sum_{<i'>} S_{i'}^A + \sum_{<j'>} S_{j'}^B \right), \quad (1)$$

where <ij> and <i′j′> indicate a summation over all pairs of nearest-neighboring sites of each layer. $J_1$ and $J_2$ are exchange constants for the first and second layer, respectively, which are also called intralayer coupling constants, and $J_3$ is the interlayer coupling constant over all the adjacent neighboring sites of layers, as seen in Fig. 1. H is an oscillating external magnetic field which is given $H = H_0 \cos(wt)$, where $H_0$ and $w = 2\pi\nu$ are the amplitude and the angular frequency of the oscillating field, respectively. $D_A$ and $D_B$ are the crystal fields for sites on A lattice and for sites on B lattice, respectively. The system is in contact with an isothermal heat bath at absolute temperature $T_{abs}$.

To obtain the set of mean-field dynamic equations for magnetizations we apply the Glauber-type stochastic dynamics. Thus, the system evolves according to a Glauber-type stochastic process at a rate of $1/\tau$ transitions per unit time. We define $P(\sigma_1,\sigma_2,...,\sigma_N, S_1, S_2,..., S_N; t)$ as the probability that the system has σ- and S- spin configurations in each layer $\sigma_1,\sigma_2,...,\sigma_N, S_1, S_2,..., S_N$, at time t. If we let $W_i(\sigma_i^A \to \sigma_i^{A'})$ be the probability per unit time that the *i*th spin changes from the values $\sigma_i^A$ to $\sigma_i^{A'}$, while the others, i.e., $(S_1,S_2,...,S_N)$ and spins on sublattice B, remain momentarily fixed, then we may write the master equation that describes the interaction between the spins and the heat bath as

$$\frac{d}{dt}P_1^A(\sigma_1^A,\sigma_2^A,...,\sigma_N^A;t) = -\sum_i\left(\sum_{\sigma_i^A\neq\sigma_i^{A'}} W_i^A(\sigma_i^A\to\sigma_i^{A'})\right)P_1^A(\sigma_1^A,\sigma_2^A,...,\sigma_i^A,...,\sigma_N^A;t)$$
$$+\sum_i\left(\sum_{\sigma_i^A\neq\sigma_i^{A'}} W_i^A(\sigma_i^{A'}\to\sigma_i^A)P_1^A(\sigma_1^A,\sigma_2^A,...,\sigma_i^{A'},...,\sigma_N^A;t)\right), \qquad (3)$$

where $W_i^A(\sigma_i^A \to \sigma_i^{A'})$ is the probability per unit time that *i*th spin changes from the values $\sigma_i^A$ to $\sigma_i^{A'}$. In this sense the Glauber model is stochastic. Since the system is in contact with a heat bath at absolute temperature $T_A$, each spin can change from the value $\sigma_i^A$ to $\sigma_i^{A'}$ with the probability per unit time

$$W_i^A(\sigma_i^A\to\sigma_i^{A'}) = \frac{1}{\tau}\frac{\exp(-\beta\Delta E(\sigma_i^A\to\sigma_i^{A'}))}{\sum_{\sigma_i^{A'}}\exp(-\beta\Delta E(\sigma_i^A\to\sigma_i^{A'}))}, \qquad (4)$$

where $\beta = 1/k_BT_A$, $k_B$ being the Boltzmann factor, $\sum_{\sigma_i^{A'}}$ is the sum over the five possible values of $\sigma_i^{A'} = \pm2, \pm1, 0$ and

$$\Delta E_i^A(\sigma_i^A\to\sigma_i^{A'}) = -(\sigma_i^{A'}-\sigma_i^A)(J_1\sum_{j'}\sigma_j^B + J_3\sum_i S_{i'}^A + H) - \left(\left(\sigma_i^{A'}\right)^2 - \left(\sigma_i^A\right)^2\right)D_A, \qquad (5)$$

gives the change in the energy of the system when the $\sigma_i$-spin changes. The probabilities satisfy the detailed balance condition. Using Eqs. (1)-(4), we obtain the dynamic equations for $m_1^A$

$$\Omega\frac{d}{d\xi}m_1^A = -m_1^A$$
$$+\frac{3\exp\left(\frac{4d_A}{T}\right)\sinh\left[\frac{3}{2T}\left(zm_1^B+\frac{J_3}{J_1}m_2^A+h\cos\xi\right)\right]+\exp\left(-\frac{d_A}{T}\right)\sinh\left[\frac{1}{2T}\left(zm_1^B+\frac{J_3}{J_1}m_2^A+h\cos\xi\right)\right]}{2\exp\left(\frac{d_A}{T}\right)\cosh\left[-\frac{3}{2T}\left(zm_1^B+\frac{J_3}{J_1}m_2^A+h\cos\xi\right)\right]+2\exp\left(-\frac{d_A}{T}\right)\cosh\left[\frac{1}{2T}\left(zm_1^B+\frac{J_3}{J_1}m_2^A+h\cos\xi\right)\right]}, \qquad (6)$$

where $m_1^A \equiv \langle\sigma_i^A\rangle$, $m_1^B \equiv \langle\sigma_j^B\rangle$, $m_2^A \equiv \langle S_{i'}^A\rangle$, $m_2^B \equiv \langle S_{j'}^B\rangle$, $\xi = wt$, $T = (\beta J_1)^{-1}$, $h = H_0/J_1$, $d_A = D_A/J_1$ and $\Omega = \tau w$. We fixed $z = 4$ and $w = 2\pi\nu$.

The other mean–field dynamical equations for $m_1^A$, $m_1^B$, $m_2^A$ and $m_2^B$ can be similarly calculated as

$$\Omega\frac{d}{d\xi}m_1^B=-m_1^B + \frac{3\exp\left(\frac{d_B}{T}\right)\sinh\left[\frac{3}{2T}\left(zm_1^A+\frac{J_3}{J_1}m_2^B+h\cos\xi\right)\right]+\exp\left(-\frac{d_B}{T}\right)\sinh\left[\frac{1}{2T}\left(zm_1^A+\frac{J_3}{J_1}m_2^B+h\cos\xi\right)\right]}{2\exp\left(\frac{d_B}{T}\right)\cosh\left[-\frac{3}{2T}\left(zm_1^A+\frac{J_3}{J_1}m_2^B+h\cos\xi\right)\right]+2\exp\left(-\frac{d_B}{T}\right)\cosh\left[\frac{1}{2T}\left(zm_1^A+\frac{J_3}{J_1}m_2^B+h\cos\xi\right)\right]}, \tag{7}$$

$$\Omega\frac{d}{d\xi}m_2^A=-m_2^A + \frac{2e\exp\left(\frac{4d_A}{T}\right)\sinh\left[\frac{2}{T}\left(\frac{J_2}{J_1}zm_2^B+\frac{J_3}{J_1}m_1^A+h\cos\xi\right)\right]+\exp\left(\frac{d_A}{T}\right)\sinh\left[\frac{1}{T}\left(\frac{J_2}{J_1}zm_2^B+\frac{J_3}{J_1}m_1^A+h\cos\xi\right)\right]}{e\exp\left(\frac{4d_A}{T}\right)\cosh\left[\frac{2}{T}\left(\frac{J_2}{J_1}zm_2^B+\frac{J_3}{J_1}m_1^A+h\cos\xi\right)\right]+\exp\left(\frac{d_A}{T}\right)\cosh\left[\frac{1}{T}\left(\frac{J_2}{J_1}zm_2^B+\frac{J_3}{J_1}m_1^A+h\cos\xi\right)\right]+1/2}, \tag{8}$$

$$\Omega\frac{d}{d\xi}m_2^B=-m_2^B + \frac{2e\exp\left(\frac{4d_B}{T}\right)\sinh\left[\frac{2}{T}\left(\frac{J_2}{J_1}zm_2^A+\frac{J_3}{J_1}m_1^B+h\cos\xi\right)\right]+\exp\left(\frac{d_B}{T}\right)\sinh\left[\frac{1}{T}\left(\frac{J_2}{J_1}zm_2^A+\frac{J_3}{J_1}m_1^B+h\cos\xi\right)\right]}{e\exp\left(\frac{4d_B}{T}\right)\cosh\left[\frac{2}{T}\left(\frac{J_2}{J_1}zm_2^A+\frac{J_3}{J_1}m_1^B+h\cos\xi\right)\right]+\exp\left(\frac{d_B}{T}\right)\cosh\left[\frac{1}{T}\left(\frac{J_2}{J_1}zm_2^A+\frac{J_3}{J_1}m_1^B+h\cos\xi\right)\right]+1/2}, \tag{9}$$

Therefore, a set of mean-field dynamical equations are obtained.

**Numerical Results and Discussion**

In order to present the dynamic phase diagram, first we should find the phases in the system and then obtain the dynamic phase transition (DPT) temperatures as well as to characterize the nature (continuous or discontinuous) of the dynamic phase transitions.

The phases in the system can be found by solving Eqs. (6) – (8) numerically by Adams-Moulton predictor-corrector method for a given set of parameters and initial values. Since our aim is to study the ferromagnetic (FM) mixed spin (3/2, 2) bilayer system, we take $J_1> 0$ and $J_2>0$that usually called the ferromagnetic/ferromagnetic (FM/FM) interaction. Since the solution of these kind of dynamic equations are given [9-12] in detail, we will not discuss the solutions and present any figures here. From the investigations of the numerical solution, we observe that the dynamic phase diagrams contain the paramagnetic (p), ferromagnetic (f), compensated (c) and fundamental phases and the f+p and c+p mixed phases which depending on the system parameters. To investigate the crystal-filed effect on the phase diagram one has to determine the DPT points as well as to characterize the nature of the dynamic phase transitions by examining the temperature dependence of the average magnetizations in a period or the dynamic magnetizations as a function of the reduced temperature. The dynamic magnetizations ($M_{1,2}^{A,B}$), are defined as

$$M_{1,2}^{A,B}=\frac{1}{2\pi}\int_0^{2\pi}m_{1,2}^{A,B}(\xi)d\xi, \tag{10}$$

We solve Eq. (10) by combining the numerical methods of the Adams-Moulton predictor corrector with Romberg integration to obtain the DPT points as well as to characterize the nature of the dynamic boundaries. Since these kind of investigations are given [9-12] in detail, we will not discuss the

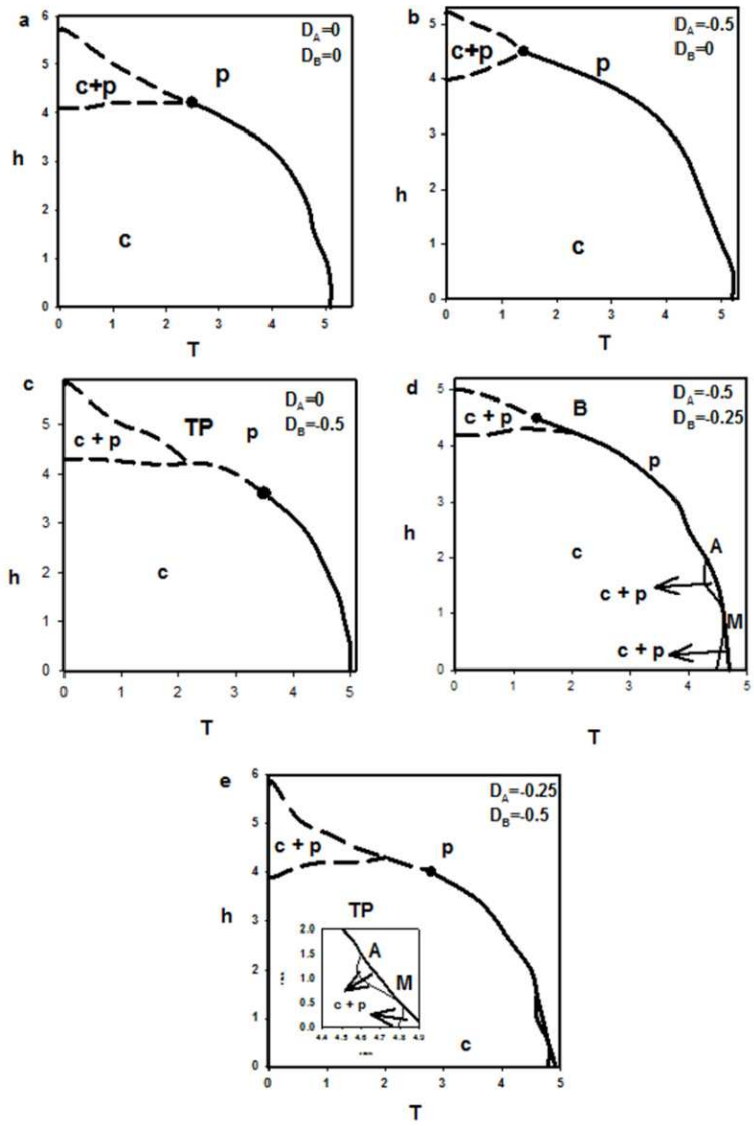


**Figure 2.** The dynamic phase diagrams in (T, h) plane for $J_1$=1.0, $J_2$=0.1 and $J_3$=-0.25. The paramagnetic (p), compensated (c) and the c+p mixed phases are found. Dashed and solid lines represent the first- and second-order phase transitions, respectively. The special points are the dynamic tricritical point with filled circle, the dynamic critical end (B), dynamic multicritical (A), dynamic tetracritical (M) and dynamic triple (TP) points. a) $D_A$= 0.0 and $D_B$= 0.0, b) $D_A$=-0.5, $D_B$= 0.0; c) $D_A$= 0.0, $D_B$= -0.5; d) $D_A$=- 0.5, $D_B$=- 0.25 and e) $D_A$= -0.25 and $D_B$=- 0.5.

solutions and present any figures here. From this detail investigation we find that system either undergoes a first-order or a second- phase transitions depending on the system parameters. We presented the dynamic phase diagrams for two cases; one $J_3$< 0 that the interaction between the layers is repulsive (Fig. 1) and the other $J_3$>0 in which the attractive interaction occurs between layers (Fig. 2). We should remind that in Eq. (1), $J_3$ is taken as a negative, i.e., $J_3$<0. We should remind that in Eq. (1), $J_3$ is taken as a negative, namely $J_3$<0. In these figures, the solid and dashed lines represent the second- and first-order phase transition lines, respectively, and the dynamic tricritical points is denoted by a filled circle. B, A, M and TP represent the dynamic critical end, dynamic multicritical , dynamic tetracritical and dynamic triple points, respectively. From these phase diagrams in Fig. 1, the effect of crystal-field interactions can be seen as follows: (1) If only $D_A$ is exist or dominant very much, the dynamic tricritical points occurs at

low values of T and high values of h, compare Fig. 1 (a) with Fig. 1 (b). (2) If only $D_B$ exists or dominant very much, the dynamic tricritical points occurs at high values of T and low values of h as well as the system exhibits the TP point, compare Fig. 1 (a) with Fig. 1 (c). (3) If both $D_A$ and $D_B$ exist, the system exhibits the A and M points beside the dynamic tricritical point and the two different c+p mixed phase at the high values of T and low values h, compare Fig. 1 (a) with Fig. 1 (d) and (e). (4) If $D_A < D_B$, the B critical point occurs and the dynamic tricritical point appears at low values of T and high values of h. On the other hand for $D_A > D_B$, the TP special point occurs and the dynamic tricritical points appears at high values of T and low values of h. These fact also seen by comparing Fig. 1 (a), Fig. 1 (d) and (e) together.

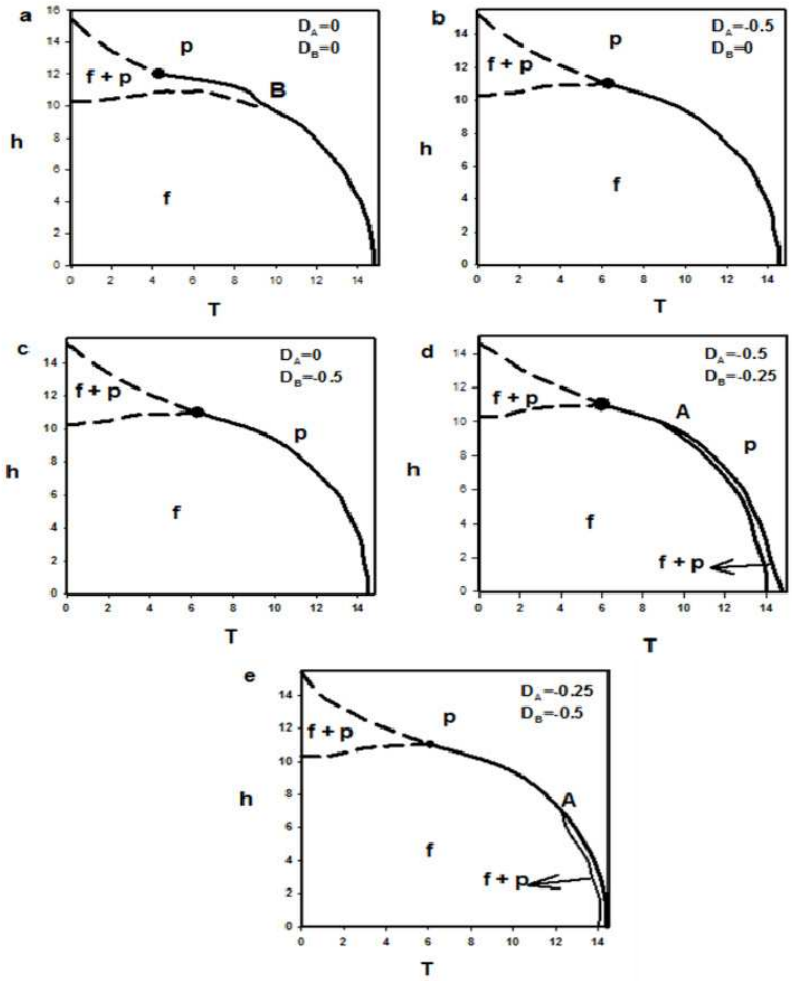


**Figure 3.** Same as Fig. 2, but for $J_1$=1.0, $J_2$=0.1 and $J_3$=5 that the interaction between layers is attractive. The f represents the ferromagnetic phase. a) $D_A$= 0.0 and $D_B$= 0.0, b) $D_A$=-0.5 $D_B$= 0.0; c) $D_A$= 0.0, $D_B$= -0.5; d) $D_A$=- 0.5, $D_B$=- 0.25 and e) $D_A$= -0.25 and $D_B$=- 0.5.

Fig. 3 is obtained for $J_1$=1.0, $J_2$=0.1 and $J_3$=5 to also see the effect of the crystal-field interactions when the coupling constant is large. First of all, since $J_3$>0, the c phase in Fig. 1 becomes the ferromagnetic (f) phase and the effect of $D_A$ and $D_B$ are not much. Nevertheless the following important influences are observed from Fig. 2. (1) When $D_A = D_B = 0$, B critical point appears. (2) Existence of only $D_A$ or only $D_B$ give the similar behavior of the dynamic phase diagrams, compare Fig. 2 (b) with Fig. 2(c). (3) If both $D_A$ and $D_B$ exist, the system exhibits the A point beside the dynamic tricritical point and the f+p mixed phase at the high values of T and low values h, seen in Fig. 2(d) and Fig. 2 (e). (4) For $D_A > D_B$, A critical point appears at high values of T and low values of h.

In conclusion, we study the effects of crystal field interaction parameters on the dynamic phase diagrams in the ferromagnetic mixed system consisting of spin-3/2 and spin-2 on a two-layer square lattice within the Glauber-type stochastic dynamics based on the mean-field theory. In particular, we took the crystal-field interactions for sites on A lattice as $D_A$ and for sites on B lattice as $D_B$ and investigate the effects of $D_A$ and $D_B$ on the behavior of dynamic phase diagrams in detail. Dynamic phase diagrams are presented in (T, h) plane. We find that if the coupling constant ($J_3$) is small, crystal–field interactions parameters ($D_A$ and $D_B$) influence on the behavior of the dynamic phase diagrams very much. If $J_3$ is large, the influences of $D_A$ and $D_B$ are small. We should also mention that more detailed exposition, as well as some new results will appear in future communications.

## Acknowledgments

This work was supported by Erciyes University Research Fund, Grant No: FBA- 2016-6324.

## References

1. K. Hashimoto, S. Ohkoshi, Philos. Trans. R. Soc. London A 357 (1999) 2977.
2. A. Bobak, J. Dely, J. Magn. Magn. Mater. 310 (2007) 1419.
3. H. Miao, G. Wei, J. Geng, J. Magn. Magn. Mater. 321 (2009) 4139.
4. B. Deviren, E. Kantar, M. Keskin, Journal of the Korean Physical Society 56 (2010) 1738.
5. F. Abugrig, World Journal of Condensed Matter Physics 3 (2013) 111.
6. B. Deviren, Y. Polat, M. Keskin, Chin. Phys. B 20 (2011) 060507.
7. A. Jabar, A. Belhaj, H. Labrim, L. Bahmad, N. Hassanain, J Supercond Nov Magn 28 (2015) 2721.
8. M. Keskin, Y. Polat, J. Magn. Magn. Mater. 321 (2009) 3905.
9. Ü. Temizer, M. Tülek, S. Yarar, Physica A 415 (2014) 156.
10. M. Keskin, O. Canko, E. Kantar, International Journal of Modern Physics C, 17 (2006) 1239.
11. M. Ertaş, M. Keskin, Phys. Lett. A 376 (2012) 2455.
12. M. Ertaş, E. Kantar, M. Keskin, J. Magn. Magn. Mater. 358-359 (2014) 56.

EK-3

Journal of Superconductivity and Novel Magnetism

# Influence of Crystal-Field and Interlayer Coupling Interactions on Dynamic Magnetic Critical Properties of a Mixed Spins (3/2, 2) Bilayer System

--Manuscript Draft--

| | |
|---|---|
| Manuscript Number: | |
| Full Title: | Influence of Crystal-Field and Interlayer Coupling Interactions on Dynamic Magnetic Critical Properties of a Mixed Spins (3/2, 2) Bilayer System |
| Article Type: | Original Research |
| Keywords: | Spins (3/2, 2) bilayer system; dynamic phase diagrams; Glauber-type stochastic dynamics, mean-field theory |
| Corresponding Author: | Mustafa Keskin<br>Erciyes Universitesi<br>KAYSERİ, talas TURKEY |
| Corresponding Author Secondary Information: | |
| Corresponding Author's Institution: | Erciyes Universitesi |
| Corresponding Author's Secondary Institution: | |
| First Author: | Mustafa Keskin |
| First Author Secondary Information: | |
| Order of Authors: | Mustafa Keskin |
| | Yusuf Koçak |
| Order of Authors Secondary Information: | |
| Funding Information: | |

# Influence of Crystal-Field and Interlayer Coupling Interactions on Dynamic Magnetic Critical Properties of a Mixed Spins (3/2, 2) Bilayer System

**Mustafa Keskin[1]*, Yusuf Koçak[1],**

**Abstract** Influences of crystal-fields ($D_A$ and $D_B$) and interlayer coupling interactions ($J_3$) on dynamic magnetic critical behaviors of a mixed spins (3/2, 2) bilayer system under an oscillating magnetic field are investigated by the Glauber-type stochastic dynamics based on the mean-field theory. Dynamic phase diagrams are constructed in the reduced temperature and magnetic field amplitude plane for the ferromagnetic/ferromagnetic (FM/FM), antiferromagnetic/ferromagnetic (AFM/FM) and AFM/AFM interactions and examined in detail. We find that the $D_A$, $D_B$ mostly influence the critical behavior of the dynamic phase diagrams and the $J_3$ affects the phases that will be occurred in the system.

**Keywords:** Spins (3/2, 2) bilayer system; dynamic phase diagrams; Glauber-type stochastic dynamics, mean-field theory

## 1 Introduction

Magnetic properties of thin magnetic films with magnetic–layered structures have been the subject of intense experimental and theoretical researches due to their great potential for technological application, such as electronic semiconductor devices, optical coatings, computer memory, protection of substrate materials against corrosion, oxidation and wear [1]. Many works have been experimentally investigated on the magnetic properties of the bilayers and multilayers thin films, such as Co/Pt, Pt/Co/Pt, Pt/Co/AlOx, Gd-Co/Ti, W/$B_4C$, CoSiB/CSiB, Cd/Pd, Ni-Zr, Ni/Ti, Fe/Ni, Fe/Co, Ni/Au, Co/Cu/Ni80Fe20, La2/3Ca1/3MnO3/SrTiO3 /YBa2Cu3O7-x, FePt/Fe, and Fe/TbFe etc.) (see [2-17] and references therein). Theoretically, the spin-1/2 (see [18-30] and references therein), spin-1 (see [31-35] and references therein) and also mixed Ising systems, namely spin (2, 5/2) [36, 37], spin (1, 3/2) [38], spin (3/2, 2) [39] and spin (3/2, 5/2) [40], have been used to study magnetic behaviors of the bilayers and multilayers thin films within the methods of the equilibrium statistical physics. Moreover, the bilayer spin-1 [41], spin-3/2 [42], spin [43] as well as mixed spin [44, 45] systems on the Bethe lattices have been also investigated to observe some magnetic properties thin films. Recently, dynamic magnetic properties thin films have been examined by using the spin-1/2 [46-49], spin-1 [50-52], spin (2, 5/2) [53, 54], spin (3/2, 2) [55-57] bilayer systems.

*Corresponding author. E. Mail: keskin@erciyes.edu.tr

[1] *Physics Department, Erciyes University, 38039 Kayseri-Turkey*

In spite of these studies, the dynamic magnetic critical properties of bilayer systems have not been investigated in detail. Especially, the crystal-field interaction, in which one of the important interaction parameter, either taken as zero or taken as same (D) for A and B sublatices in all these studies, except ref. 56. In ref. 56, the crystal-field interaction for sites on A lattice as $D_A$ and for sites on B lattice as $D_B$ were taken and only the dynamic phase diagrams (DPDs) in the ferromagnetic mixed spins (3/2, 2) bilayer system was investigated. In this paper, influences of crystal-fields ($D_A$ and $D_B$) and interlayer coupling interactions ($J_3$) on dynamic magnetic behaviors of a spin (3/2, 2) bilayer system under a time-dependent magnetic field are investigated by the Glauber-type stochastic dynamics (GTSD) based on the mean-field theory (MFT) in detail. For this aim, the DPDs are presented in the reduced temperature (T) and magnetic field amplitude (h) plane for the ferromagnetic/ferromagnetic (FM/FM), antiferromagnetic /ferromagnetic (AFM/FM) and AFM/AFM interactions. The effect of the $D_A$, $D_B$ as well as $J_3$ which is related to the thickness, on the critical behaviors of the system are extensively studied and discussed.

# 2 Model and Formulation

We take into account a mixed spins (3/2, 2) system with a two-layers ($L_1$ and $L_2$) on a square lattices, seen in Fig. 1. Each layer of the system contains two sublattices (A and B) with spin variables $\sigma_i^A$ , $\sigma_i^B = \pm 3/2, \pm 1/2$ occupy $L_1$ layer and $S_j^A$ , $S_j^B = \pm 2, \pm 1, 0$ $L_2$ layer. Thus, the system can be portrayed with four sublattice magnetizations that are introduced as follows: $m_1^A \equiv \left\langle \sigma_i^A \right\rangle$, $m_1^B \equiv \left\langle \sigma_j^B \right\rangle$, $m_2^A \equiv \left\langle S_{i'}^A \right\rangle$, $m_2^B \equiv \left\langle S_{j'}^B \right\rangle$, $\langle ... \rangle$ denotes the thermal expectation value. Each layer has N sites and interacts with its nearest-neighbor (NN) and the corresponding adjacent spins in the other layer whose sites are labeled by i, i′, j and j′, as illustrated in Fig. 1.

The Hamiltonian of the system can be given by

$$\begin{aligned}\mathcal{H} = &-J_1 \sum_{<ij>} \sigma_i^A \sigma_j^B - J_2 \sum_{<i'j'>} S_{i'}^A S_{j'}^B - J_3 \left( \sum_{<ii'>} \sigma_i^A S_{i'}^A + \sum_{<jj'>} \sigma_j^B S_{j'}^B \right) - D_A \left( \sum_{<i>} \left(\sigma_i^A\right)^2 + \sum_{<i'>} \left(S_{i'}^A\right)^2 \right) \\ &- D_B \left( \sum_{<j>} \left(\sigma_j^B\right)^2 + \sum_{<j'>} \left(S_{j'}^B\right)^2 \right) - H \left( \sum_{<i>} \sigma_i^A + \sum_{<j>} \sigma_j^B + \sum_{<i'>} S_{i'}^A + \sum_{<j'>} S_{j'}^B \right),\end{aligned} \tag{1}$$

where <ij> and <i′j′> represent a summation over all pairs of the NN sites of each layer. $J_1$ and $J_2$ are exchange interactions for the $L_1$ and $L_2$ layers, respectively, also called intralayer coupling constants, and $J_3$ is the interlayer coupling constant over all the adjacent neighboring sites of layers, as illustrated in Fig. 1. H is an external field that is $H = H_0 \cos(wt)$, $H_0$ and $w = 2\pi\nu$ are the amplitude and the angular frequency, respectively. $D_A$ and $D_B$ represent the crystal fields for sites on A and B lattices, respectively. The system is in contact with an isothermal heat reservoir at absolute temperature $T_A$.

The set of mean-field dynamic equations for sublattice magnetizations are found by using the GTSD; hence the system evolves according to the GTSD process at a rate of $1/\tau$ transitions per unit time. We identify $P(\sigma_1, \sigma_2, ..., \sigma_N, S_1, S_2, ..., S_N; t)$ as the probability that the system has σ- and S- spin configurations in each layer $\sigma_1, \sigma_2, ..., \sigma_N, S_1, S_2, ..., S_N$, at time t. Let $W_i(\sigma_i^A \to \sigma_i^{A'})$ be the probability per unit time that the *i*th spin changes from the values $\sigma_i^A$ to $\sigma_i^{A'}$, while the others, i.e., $(S_1, S_2, ..., S_N)$ and spins on sublattice B, remain momentarily fixed, then the master equation can be written in which describes the interaction between the spins and the heat reservoir as

$$\frac{d}{dt}P_1^A(\sigma_1^A,\sigma_2^A,...,\sigma_N^A;t) = -\sum_i\left(\sum_{\sigma_i^A\neq\sigma_i^{A'}} W_i^A(\sigma_i^A\to\sigma_i^{A'})\right)P_1^A(\sigma_1^A,\sigma_2^A,...,\sigma_i^A,...,\sigma_N^A;t)$$
$$+\sum_i\left(\sum_{\sigma_i^A\neq\sigma_i^{A'}} W_i^A(\sigma_i^{A'}\to\sigma_i^A)P_1^A(\sigma_1^A,\sigma_2^A,...,\sigma_i^{A'},...,\sigma_N^A;t)\right), \qquad (2)$$

where $W_i^A(\sigma_i^A\to\sigma_i^{A'})$ is the probability per unit time that *i*th spin changes from the values $\sigma_i^A$ to $\sigma_i^{A'}$. Each spin can change from the value $\sigma_i^A$ to $\sigma_i^{A'}$ with the probability per unit timedue to the reason that the system is in contact with a heat bath at absolute temperature $T_A$,

$$W_i^A(\sigma_i^A\to\sigma_i^{A'}) = \frac{1}{\tau}\frac{\exp(-\beta\Delta E(\sigma_i^A\to\sigma_i^{A'}))}{\sum_{\sigma_i^{A'}}\exp(-\beta\Delta E(\sigma_i^A\to\sigma_i^{A'}))}, \qquad (3)$$

where $\beta = 1/k_BT_A$, $k_B$ being the Boltzmann factor, $\sum_{\sigma_i^{A'}}$ is the sum over the five possible values of $\sigma_i^{A'} = \pm2, \pm1, 0$ and

$$\Delta E_i^A(\sigma_i^A\to\sigma_i^{A'}) = -(\sigma_i^{A'}-\sigma_i^A)(J_1\sum_{j'}\sigma_j^B + J_3\sum_i S_{i'}^A + H) - \left(\left(\sigma_i^{A'}\right)^2 - \left(\sigma_i^A\right)^2\right)D_A, \qquad (4)$$

is the change in the energy of the system when the $\sigma_i$-spin changes. The probabilities satisfy the detailed balance condition. Utilizing Eqs. (1)-(4), we calculate the dynamic equation for $m_1^A$ as

$$\Omega\frac{d}{d\xi}m_1^A = -m_1^A$$
$$+\frac{3\exp\left(\frac{4d_A}{T}\right)\sinh\left[\frac{3}{2T}\left(zm_1^B+\frac{J_3}{J_1}m_2^A+h\cos\xi\right)\right]+\exp\left(-\frac{d_A}{T}\right)\sinh\left[\frac{1}{2T}\left(zm_1^B+\frac{J_3}{J_1}m_2^A+h\cos\xi\right)\right]}{2\exp\left(\frac{d_A}{T}\right)\cosh\left[-\frac{3}{2T}\left(zm_1^B+\frac{J_3}{J_1}m_2^A+h\cos\xi\right)\right]+2\exp\left(-\frac{d_A}{T}\right)\cosh\left[\frac{1}{2T}\left(zm_1^B+\frac{J_3}{J_1}m_2^A+h\cos\xi\right)\right]}, \qquad (5)$$

where $\xi = wt$, $T = (\beta J_1)^{-1}$, $h = H_0/J_1$, $d_A = D_A/J_1$ and $\Omega = \tau w.\ z = 4$ and $w = 2\pi\nu$ are taken. The dynamical equations for $m_1^B$, $m_2^A$ and $m_2^B$ can be similarly obtained as

$$\Omega\frac{d}{d\xi}m_1^B = -m_1^B$$
$$+\frac{3\exp\left(\frac{d_B}{T}\right)\sinh\left[\frac{3}{2T}\left(zm_1^A+\frac{J_3}{J_1}m_2^B+h\cos\xi\right)\right]+\exp\left(-\frac{d_B}{T}\right)\sinh\left[\frac{1}{2T}\left(zm_1^A+\frac{J_3}{J_1}m_2^B+h\cos\xi\right)\right]}{2\exp\left(\frac{d_B}{T}\right)\cosh\left[-\frac{3}{2T}\left(zm_1^A+\frac{J_3}{J_1}m_2^B+h\cos\xi\right)\right]+2\exp\left(-\frac{d_B}{T}\right)\cosh\left[\frac{1}{2T}\left(zm_1^A+\frac{J_3}{J_1}m_2^B+h\cos\xi\right)\right]}, \qquad (6)$$

$$\Omega\frac{d}{d\xi}m_2^A=-m_2^A + \frac{2e\exp\left(\frac{4d_A}{T}\right)\sinh\left[\frac{2}{T}\left(\frac{J_2}{J_1}zm_2^B+\frac{J_3}{J_1}m_1^A+h\cos\xi\right)\right]+\exp\left(\frac{d_A}{T}\right)\sinh\left[\frac{1}{T}\left(\frac{J_2}{J_1}zm_2^B+\frac{J_3}{J_1}m_1^A+h\cos\xi\right)\right]}{e\exp\left(\frac{4d_A}{T}\right)\cosh\left[\frac{2}{T}\left(\frac{J_2}{J_1}zm_2^B+\frac{J_3}{J_1}m_1^A+h\cos\xi\right)\right]+\exp\left(\frac{d_A}{T}\right)\cosh\left[\frac{1}{T}\left(\frac{J_2}{J_1}zm_2^B+\frac{J_3}{J_1}m_1^A+h\cos\xi\right)\right]+1/2}, \quad (7)$$

$$\Omega\frac{d}{d\xi}m_2^B=-m_2^B + \frac{2e\exp\left(\frac{4d_B}{T}\right)\sinh\left[\frac{2}{T}\left(\frac{J_2}{J_1}zm_2^A+\frac{J_3}{J_1}m_1^B+h\cos\xi\right)\right]+\exp\left(\frac{d_B}{T}\right)\sinh\left[\frac{1}{T}\left(\frac{J_2}{J_1}zm_2^A+\frac{J_3}{J_1}m_1^B+h\cos\xi\right)\right]}{e\exp\left(\frac{4d_B}{T}\right)\cosh\left[\frac{2}{T}\left(\frac{J_2}{J_1}zm_2^A+\frac{J_3}{J_1}m_1^B+h\cos\xi\right)\right]+\exp\left(\frac{d_B}{T}\right)\cosh\left[\frac{1}{T}\left(\frac{J_2}{J_1}zm_2^A+\frac{J_3}{J_1}m_1^B+h\cos\xi\right)\right]+1/2}, \quad (8)$$

where $d_B = D_B/J_1$. The solutions and discussions of these the mean-field dynamical equations will be given and discussed in Section 3. In numerical calculations, we fixed $J_1$=I1I, hence $d_A$=$D_A$ and $d_B$=$D_B$.

# 3 Numerical Results and Discussion

Eqs. (5)-(8) were solved by Adams-Moulton predictor-corrector method to find phases in the system for the FM/FM ($J_1$> 0 and $J_2$>0) , AFM/FM ($J_1$< 0 and $J_2$>0) and AFM/AFM ($J_1$< 0 and $J_2$<0) interactions for the given system parameters and initial values. Since the solution of these kind of dynamic equations were presented [46, 50, 53-55] in detail, the solutions are not discussed and figures are not given. From these investigations we find that system comprises, depending on system parameters, the paramagnetic (p), $m_1^A = m_1^B = m_2^A = m_2^B = 0$, The ferromagnetic (f): $m_1^A = m_1^B \cong m_2^A = m_2^B \neq 0$, The compensated (c) : $m_1^A = m_1^B \neq 0$ and $m_2^A = m_2^B \cong -m_1^A$, fundamental phases, and the f + p, f + c mixed phases for the FM/FM interaction. The p, f, antiferromagnetic (af): $m_1^A = -m_1^B, m_2^A = -m_2^B$, the surface (sf): $m_1^A = m_1^B \neq 0$, $m_2^A = m_2^B \cong -m_1^A \neq 0$ phases and the f + p, af+p, sf + f, sf + af mixed phases for the AFM/FM interaction. The p, af, and mixed (m): $m_1^A \cong m_2^A \neq 0$, $m_1^B \cong m_2^B \cong -m_1^A$ phases and the af + p, m+p, m+f, sf + f, sf + af mixed phases for the AFM/AFM interaction.

To study the effects of $D_A$, $D_B$ and $J_3$ on the dynamic phase diagrams (DPDs), one has to investigate the temperature dependence of the dynamic magnetizations ($M_{1,2}^{A,B}$) as a function of the reduced temperature (T) that are defined as

$$M_{1,2}^{A,B} = \frac{1}{2\pi}\int_0^{2\pi} m_{1,2}^{A,B}(\xi)d\xi. \quad (9)$$

Eq. (9) was solved by combining the numerical methods of the Adams-Moulton predictor corrector with Romberg integration to obtain the dynamic phase transition (DPT) points and also to characterize the nature of the transitions. From these detail solutions and investigations we find that the system undergoes either a first- or second-order phase transitions that depending on interaction parameters; hence we also obtained the DPT points. The DPDs are given in the (T, h) planes for the FM/FM, AFM/FM and AFM/AFM interactions, seen in Figs. 2-7. In the figures, the dashed and solid lines illustrate the first- and second-order phase transition lines, respectively. $T_R$, A, M and B are the dynamic tricritical, multicritical, tetracritical and critical end points, respectively. Finally, the TP represents the triple point.

Figs. 2 and 3 show the DPDs of the FM/FM interactions for the repulsive ($J_3$>0) and attractive ($J_3$<0) interlayer coupling constant, respectively, and $J_1$ =1.0, $J_2$ =1.0, various values

of $D_A$ and $D_B$. From Fig. 2, we have seen following interesting phenomena: (i) For $D_A = D_B=0$, the system contains the p, f and f+p phases as well as $T_R$ and B special critical points. The dynamic phase boundary between the f +p and f phases and between the f +p and p for high values of h are first-order lines. The dynamic boundary between the f and p phase and between the f +p and p for low values of h are second-order lines, seen Figs. 2(a) and (b). (ii) For $D_A \neq 0$ and $D_B =0$ or wise versa, the DPD is like to Fig. 2(a), except the B disappears and the first-order line between the p+f and f terminates at the $T_R$, illustrated Figs. 2 (c) and (d). (iii) For $D_A \neq 0$ and $D_B \neq 0$, the phase diagrams are similar to Fig. 2(c), except the A special critical points and the f+p appear for the low values of h and high values of T. The dynamic phase boundaries among the f, p+f and p phases are second order-phase lines (Fig.2 (d) and (e)). Moreover, if $D_A > D_B$, the A point and a new p+f mixed phase occur at lower values of h and higher values of T, compare Fig. 1 (c) with Fig 1 (e). For small values of $J_3$, the A critical point and p+f phase do not appear. Fig. 3 ($J_3<0$) illustrate the effect of $J_3$, if one compares with Fig. 2. The basic and important effects are that the c phase occurs instead of the f phase; compare Fig. 3 with Fig. 2. Moreover, the following important properties have been also observed: (i) The B point disappeared in Fig. 3 (b). (ii) The TP is observed in Fig. 3 (d). We should also mention that the behavior of Figs. 3 (a), (c) and (e) are akin to Figs. 2 (a), (c) and (e). Fig. 3 (f) displays more richer critical behaviors in which for high values of T and low values of h, the A, M special dynamic critical points and two more the p+c phases are observed. The dynamic boundaries among the phases are second-order lines.

Figs. 4 and 5 display the DPDs for the AFM/FM interactions for the repulsive ($J_3>0$) and attractive ($J_3<0$) interlayer coupling constant, respectively, $J_1$ =-1.0, $J_2$ =1.0 and various values of $D_A$ and $D_B$. From Fig. 4, we have seen following interesting phenomena: (i) For $D_A = D_B=0$, the system contains the p, f and p+f phases as well as the $T_R$ critical point. The dynamic phase boundaries among the p+f, f and p phases are first-order lines, but the boundary between the f and p phase is a second-order, seen Fig. 4(a). For small values of $J_3$, the TP point is also observed. (ii) For $D_A \neq 0$ and $D_B =0$ or wise versa, the DPD is similar to Fig. 2(a), except followings. The A dynamic critical point and the p+f mixed phase appear for the low values of h and high values of T, seen in Fig. 1 (c) and the new f+sf phase occurs at low values of T and h. (iii) For $D_A \neq 0$ and $D_B \neq 0$ (Figs. (e) and (f)), the phase diagrams are very similar to Fig. 4 (c), except the A special critical point and one more the p+f phase occur at high values of T and low values of h. (iv) For small values of the $J_3$, the sf+f mixed phase occurs at low values of T and h, and the boundary between the sf+f mixed and f phases is a second-order phase line (Fig. 4 (f). The behavior of DPDs in Figs. 5(a), (c) and (e) are similar to Figs. 4 (a), (c) and (e), but the difference is that the f phase turns out the c phase. Fig. 5 (b) displays the same behavior as Fig. 5 (a), except the c phase turns to the af and the TP point and the c+af mixed phase at low T appear. The DPD in Fig. 5 (d) is similar to Fig. 5 (b), except the reentrant behavior is observed. Fig. 5 (f) illustrates the same behavior as Fig. 5 (b), but differences are following. (i) The c+af at low T disappears and the new p+af phase is seen. (ii) The boundaries among the af, p+af and p phases are second-order lines.

Figs. 6 and 7 display the DPDs of the AFM/AFM interactions for the repulsive ($J_3>0$) and attractive ($J_3<0$) interlayer coupling constant, respectively, $J_1$ =-1.0, $J_2$ =-1.0 and various values of $D_A$ and $D_B$. First of all, only Fig. 6 (a), (c), (b) display a reentrant behavior. For $D_A = D_B=0$ (Fig. 6 (a) and (b)), the system contains the p, m and p+m phases as well as the $T_R$. The f+m mixed phase occurs for high values of $J_3$ (Fig. 6 (a)) and the TP point is seen for low values of $J_3$ (Fig. 6 (b)). Moreover, the dynamic phase boundaries among the p+m, m and p phases and the boundary between the f+m and m are first-order phase lines, but the dynamic boundary between the m and p phase is a second-order line. Fig. 6 (c) is like Fig. 6 (a), but the DPD in Fig. 6 (c) contains the new p+m phase and the TP, A points at high values of T. The boundary between the m and f+m, and the boundaries among m, p+m and p are second-order lines. The DPD in Fig. 6 (d) displays same behavior as Fig. 6(c), except the TP, A points and the f+m phase as well as the reentrant behavior do not occur. The topology of Fig. 6 (e) is very akin to

Fig. 6(c), except the f+m phase does not occur. The behavior in Fig. 6 (f) is very similar to Fig. 6(d), except the TP point also appears. The behavior of Fig.7 is similar to Fig. 6, except following two main differences: (i) The m phase turn out the c phase in Fig. 7 (a), (c), (e) and the af phase in Fig. 7 (b), (d), (f). (ii) The critical points appear for lower values of h.

In conclusion, we study influences of crystal-fields ($D_A$ and $D_B$) and interlayer coupling ($J_3$) interactions on the DPDs of the mixed spins (3/2, 2) bilayer system for the FM/FM, AFM/FM and AFM/AFM cases in the presence of a time-varying magnetic field within the GTS dynamics based on the MFT. We investigate the influence of the $D_A$, $D_B$ as well as $J_3$ on the DPDs and find that their effects on the dynamic magnetic critical properties of the DPDs more for the FM/FM, AFM/FM interaction, but less for the AFM/AFM. In particular, the sign and magnitudes of the $J_3$ mostly effects the phases that will be occurred in the system and the $D_A$ and $D_B$ mostly influence the critical behavior of the DPDs.

## Acknowledgments

This work has been carried out with support of Erciyes University Research Fund, Grant No: FBA- 2016-6324.

## References

[1] K. N. Chopra, A. M. Maini, Thin Films and Their Applications in Military and Civil Sectors, 2010, DRDO Monographs/Special Publications Series, New Delhi, India
[2] M. S. Wang, Y. Ji, S. L. Luo, L. X. Jiang, J. T. Ma, X. Xie, Y. Ping, J. J. Ge, Materials Science in Semiconductor Processing. **51**, 55 (2016).
[3] M. Bersweiler, K. Dumesnil, D. Lacour, M. Hehn, J. Physics- Condensed Matter **28**, 336005 (2016)
[4] M.Charilaou, C. Bordel, P. E. Berche, B. B. Maranville, P. Fischer, F. Hellman, Phys. Rev B **93**, 224408 (2016).
[5] R. Mansell, A. Mizrahi, A. Benguivin, R. P. Cowburn, IEEE Transactions on Magnetics, **52**, 2002904 (2016).
[6] J. J. Jin, S. H. Oh, W. Jo, J. Physics D-Applied Physics **49,** 125305 (2016).
[7] A. V. Svalov, G. V. Kurlyandskaya, V. O. Vaskovskiy, A. Larranaga, R. D. Della Pace, C. C. P. Cid, Superlattices and Microstructures **90,** 242 (2016).
[8] H. Jiang, S. Yan, J. T. Zhu, Z. H. Dong, Y. Zheng, Y. M. H. He, A. G. Li, Applied Surface Science **357,** 1180 (2015).
[9] S. Jung , T. Kim, H. Yim, Journal of Nanoscience and Nanotechnology **15,** 8739 (2015).
[10] M. Je, H. Choi Y. Wang, K. H. Yun, Y. C. Chung, Thin Solid Films **589**, 252 (2015)
[11] K. C. Kuiper, T. Roth, A. J. Schellekens, O. Schmitt, B. Koopmans, M. Cinchetti, M. Aeschlimann, Apply. Phys. Letts. 105, 202402 (2014).
[12] H. Turnow, H. Wendrock, S. Menzel, T. Gemming, J. Eckert, Thin Solid Films **561**, 48 (2014).
[13] T. Veres, L. Cser, V. Bodnarchuck, V. Ignatovich, Z. E. Horvath, B. Nagy, Thin Solid Films **540**, 69 (2013).
[14] G. P. Zhang, X. Q. Wang, G. H. Lu, L. Zhou, J. Huang, W. Chen, S. Z. Yang, Chin. Phys. B **22**, 035204 (2013).
[15] K. W. Chou, A. Puzic, H. Stoll, G. Schütz, B. W. Waeyenberge, T. Tyliszczak, K. Rott, G. Reiss, H. Brückl, I. Neudecker, D. Weiss, C. H. Back, J. Appl. Phys. **99**, 08F305 (2016).
[16] L. S. Huang, J. F. Hu, J. S. Chen, J. Magn. Magn. Mater. **324**, 1242 (2012).
[17] Z. Cao, X. Zhang, J. Appl. Phys. **39,** 5054 (2006).
[18] H.Magoussi, A. Zaim, M. Kerouad, Superlattices and Microstructures **89**, 188 (2016).

[19] E. Kantar, J Supercond Nov Magn **28**, 3387 (2015).
[20] E. Kantar, Chin. Phys. B **24**, 107501 (2015).
[21] D. S. Sabogal, J. D. D. Alzate, E. P. Restrepo, Physica A **434**, 60 (2015).
[22] Y. Yüksel, J. Magn. Magn. Mater. **385**, 47 (2015).
[23] T. Kaneyoshi, J. Magn. Magn. Mater. **339**, 260 (2015).
[24] T. Kaneyoshi, Phase Transitions 88, **121** (2015).
[25] N. Sarli, S. Akbudak, M. R. Ellialtioğlu, Physica B **452**, 18 (2014).
[26] T. Mayberry, K. Tauscher, M. Pleimling, Phys. Rev. B **90**, 011438 (2014).
[27] J. Jiang J. N. Chen, B. Ma, Z. Wang, Physica E **61**, 101 (2014).
[28] T. Kaneyoshi, J. Magn. Magn. Mater. **336**, 8 (2013).
[29] Z. X. Lu, B. H. Teng, X. H. Lu, Solid State Commun. **149**, 1176 (2009).
[30] E. A. Jagle, Phys. Rev. B **72**, 094406 (2005).
[31] A. Jabar, A. Belhaj, H. Labrim, L. Bahmad, N. Hassanain, J Supercond Nov Magn **28**, 2721 (2015).
[32] A. Jabar, A. Belhaj, H. Labrim, L. Bahmad, N. Hassanain, A. Benyoussef, Superlattices and Microstructures **78**, 171 (2015).
[33] E. Kantar, M. Ertaş, Solid State Commun. **188**, 71 (2014).
[34] Y. Yüksel, Physica B **436**, 1 (2014).
[35] N.Tahiri, H. Ez-Zahraouy, A. Benyoussef, Chin. Phys. B **20**, 017501 (2011).
[36] N. De La Espriella, C. A. Mercado, G. M. Buendia, J. Magn. Magn. Mater. **417**, 30 (2016).
[37] W. Wang , W. Jiang, D. Lv, F. Zhang, J. Phys. D **45**, 475002 (2012).
[38] A. Feraoun, A. Zaim, M. Kerouad, J Supercond Nov Magn **29**, 971 (2016).
[39] B. Deviren, Y. Polat, M. Keskin, Chin. Phys. B **20**, 060507 (2011).
[40] B. Ma, W. Jiang, IEEE Transactions on Magnetics **47**, 3118 (2011).
[41] O. Canko, E. Albayrak, Phys. Rev. E **75**, 011116 (2007).
[42] E. Albayrak, Ş. Yilmaz, Ş. Akkaya, J. Magn. Magn. Mater. **310**, 98 (2007).
[43] E. Albayrak, Ş. Akkaya, S. Yilmaz, Int. J. of Mod. Phys. B **22**, 4877 (2008).
[44] E. Albayrak, Ş. Yilmaz, Physica A **387**, 1173 (2008).
[45] E. Albayrak, Ş. Akkaya, S. Yilmaz, J. Physics-Condensed Matter **19**, 376212 (2007).
[46] M. Ertaş, E. Kantar, M. Keskin, J. Magn. Magn. Mater. **358**, 56 (2014).
[47] E. Vatansever, H. Polat, Thin Solid Films **589**, 778 (2015).
[48] B. O. Aktaş, U. Akinci, H. Polat, Phys. Rev. E 90, 012129 (2014).
[49] B. O. Aktaş, U. Akinci, H. Polat, Thin Solid Films **562**, 680 (2014).
[50] M. Ertaş, Modern Physics Letters B **29,** 1550236 (2015).
[51] K. I. Mazzitello, J. Candia, E. V. Albano, Phys. Rev E **91**, 042118 (2015).
[52] Y. Yuksel, Phys. Lett. A **377**, 2494 (2013).
[53] M. Ertaş. M. Keskin, Chin. Phys. B **22**, 120506 (2013).
[54] M. Ertaş, M. Keskin, Phys. Lett. A **376**, 2455 (2012).
[55] Ü. Temizer, M. Tülek, S. Yarar, Physica A **415**, 156 (2014).
[56] M. Ertaş, Y. Koçak, M. Keskin, Conferences of the International Journal of Arts & Sciences. **09(03)**, 145 (2016).
[57] M. Keskin. M. Ertaş, J Supercond Nov Magn., DOI 10.1007/s10948-017-4145-y

# List of Figure Captions

**Fig. 1.** Schematic representation of a two-layer square lattice: $L_1$ and $L_2$ refer to the upper and lower layers containing the spins labeled as $\sigma_i^A$, $\sigma_j^B$ and $S_{i'}^A$, $S_{j'}^B$

**Fig. 2.** Phase diagrams of the spin (3/2, 2) Ising system on two-layer square lattice in the (T, h) plane for the FM/FM interactions ($J_1 > 0$ and $J_2 > 0$), $J_1 = 1.0$, $J_2 = 1.0$, and $J_3=5$. The solid and dashed lines are the second- and first-order lines, respectively. $T_R$, B, TP and QP represent the dynamic tricritical, dynamic critical end, triple and quadruple points, respectively. a) $D_A= 0.0$ and $D_B= 0.0$, b) $D_A=-0.5$, $D_B= 0.0$; c) $D_A= 0.0$, $D_B= -0.5$; d) $D_A=- 0.5$, $D_B=- 0.25$ and e) $D_A= -0.25$ and $D_B=- 0.5$.

**Fig. 3.** Same as Fig. 2, but for $J_3=-0.25$. The special points are the dynamic multicritical (A) and dynamic tetracritical (M) points

**Fig. 4.** Same as Fig. 2, but for the AFM/FM interactions ($J_1< 1.0$ and $J_2>0$), $J_1=-1.0$, $J_2=1.0$ and $J_3=5$.

**Fig. 5.** Same as Fig. 4, but for $J_3=-0.25$.

**Fig.6.** Same as Fig. 2, but for the AFM/AFM interactions ($J_1< 1.0$ and $J_2<0$), $J_1=-1.0$, $J_2=-1.0$ and $J_3=5$.

**Fig. 7.** Same as Fig. 6, but for $J_3=-0.25$.

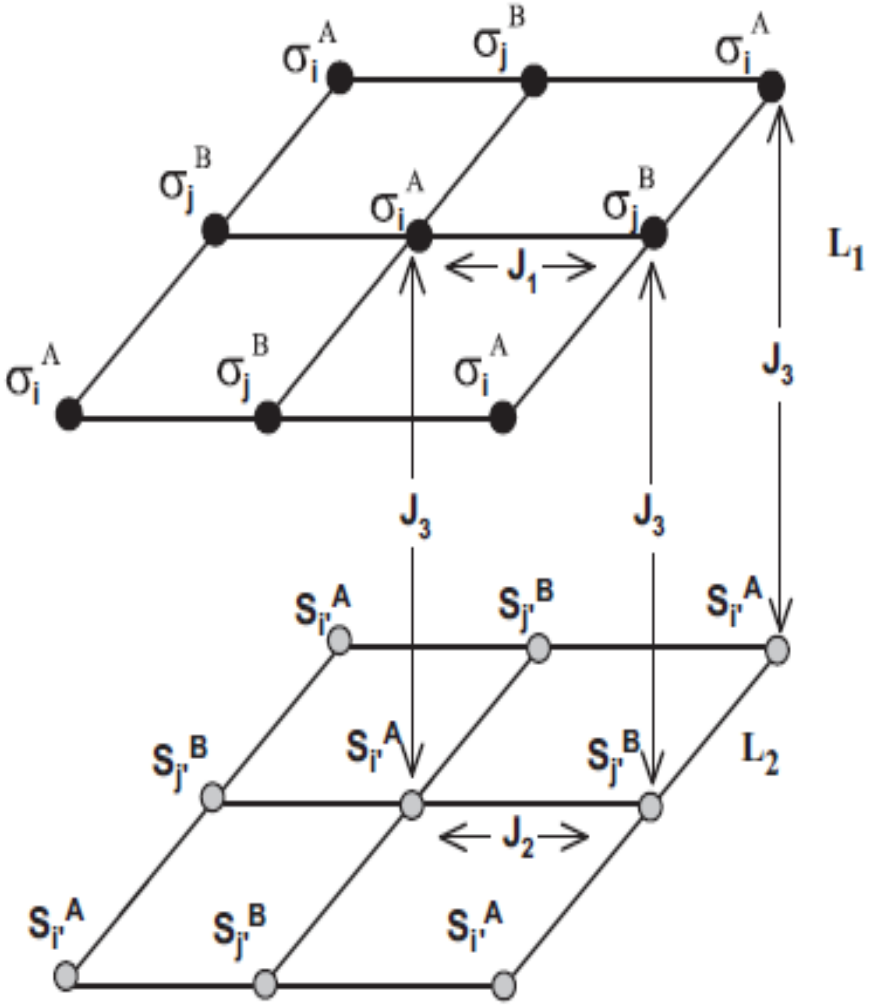


**Fig. 1**

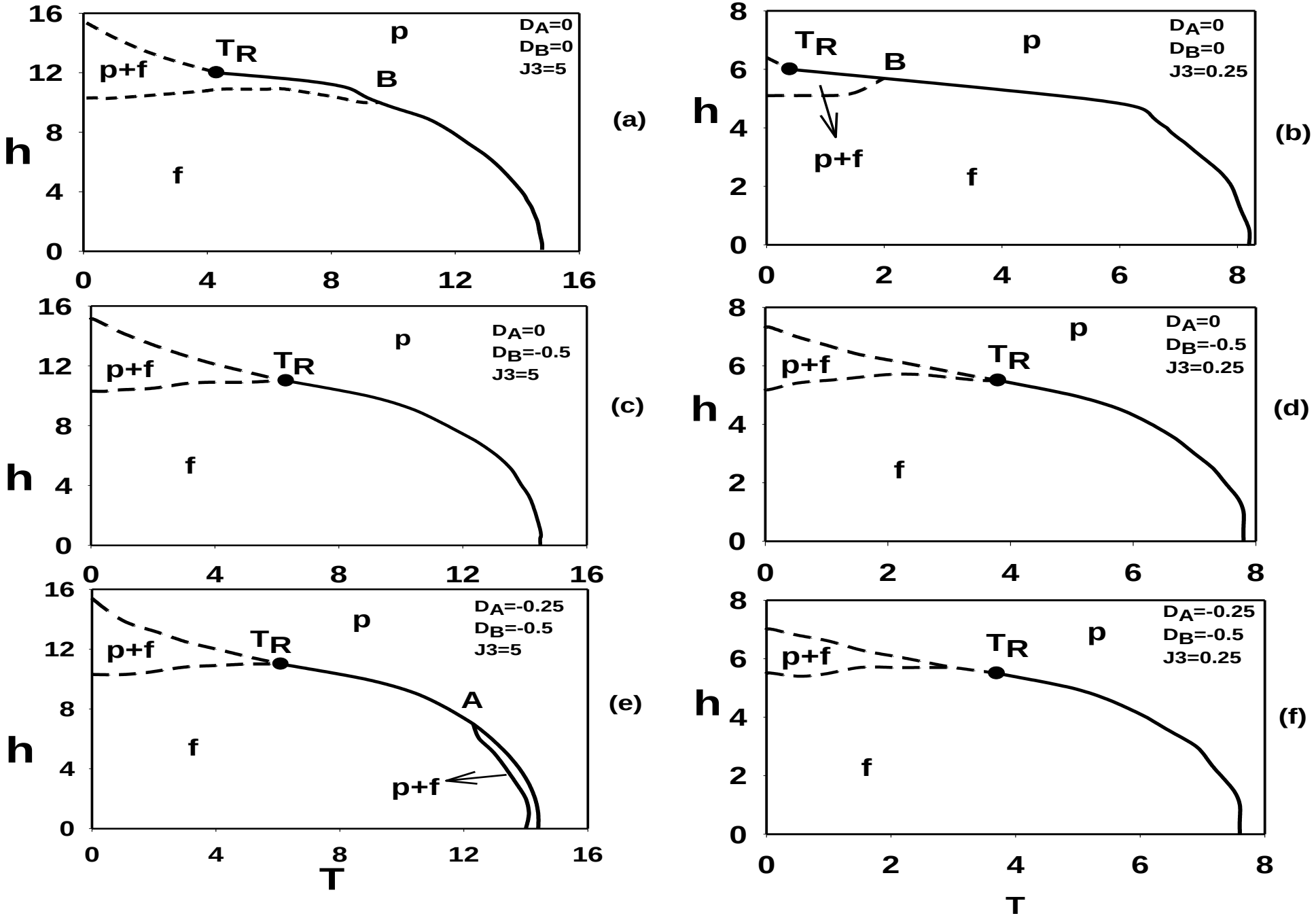


Fig. 2

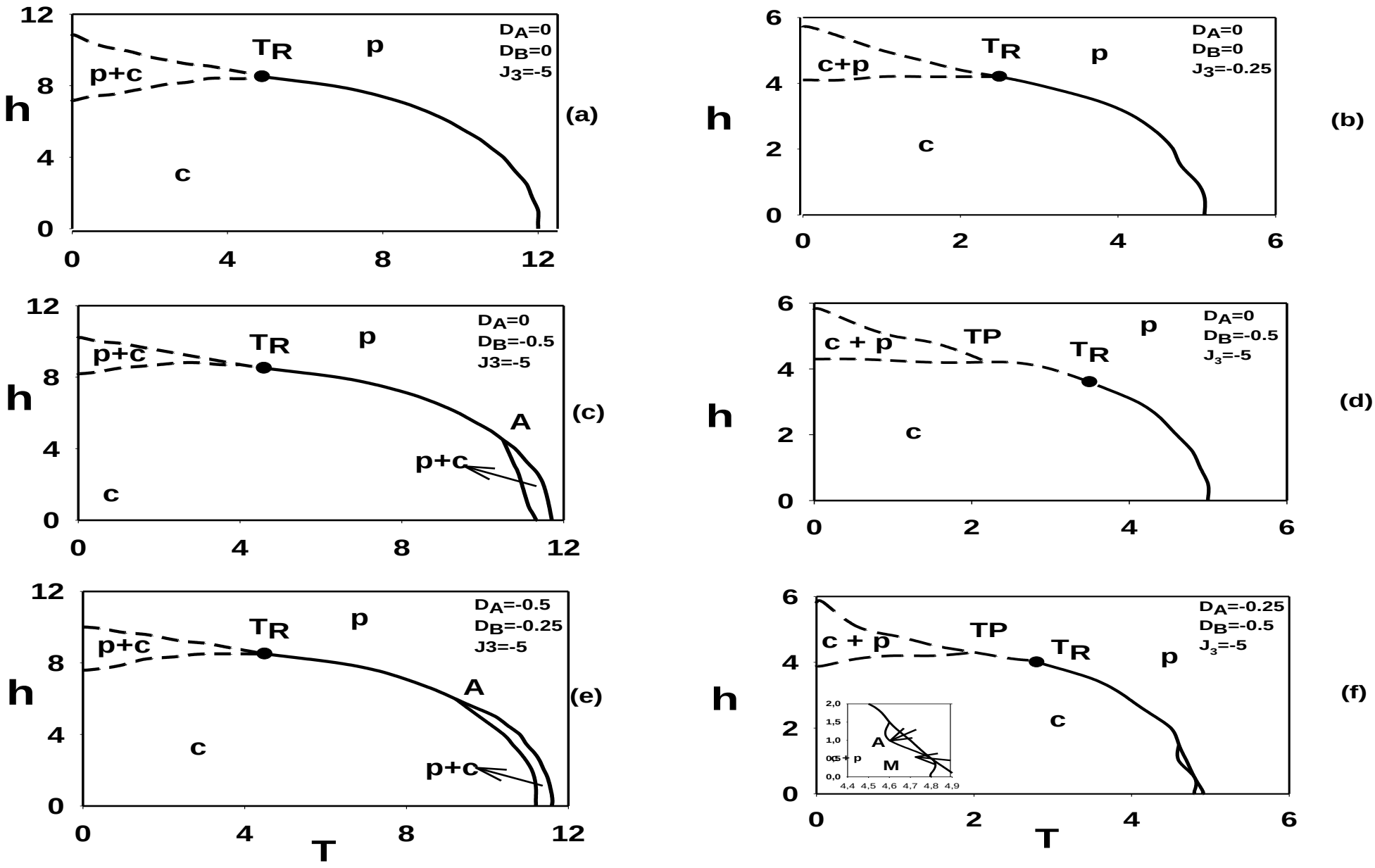


Fig. 3

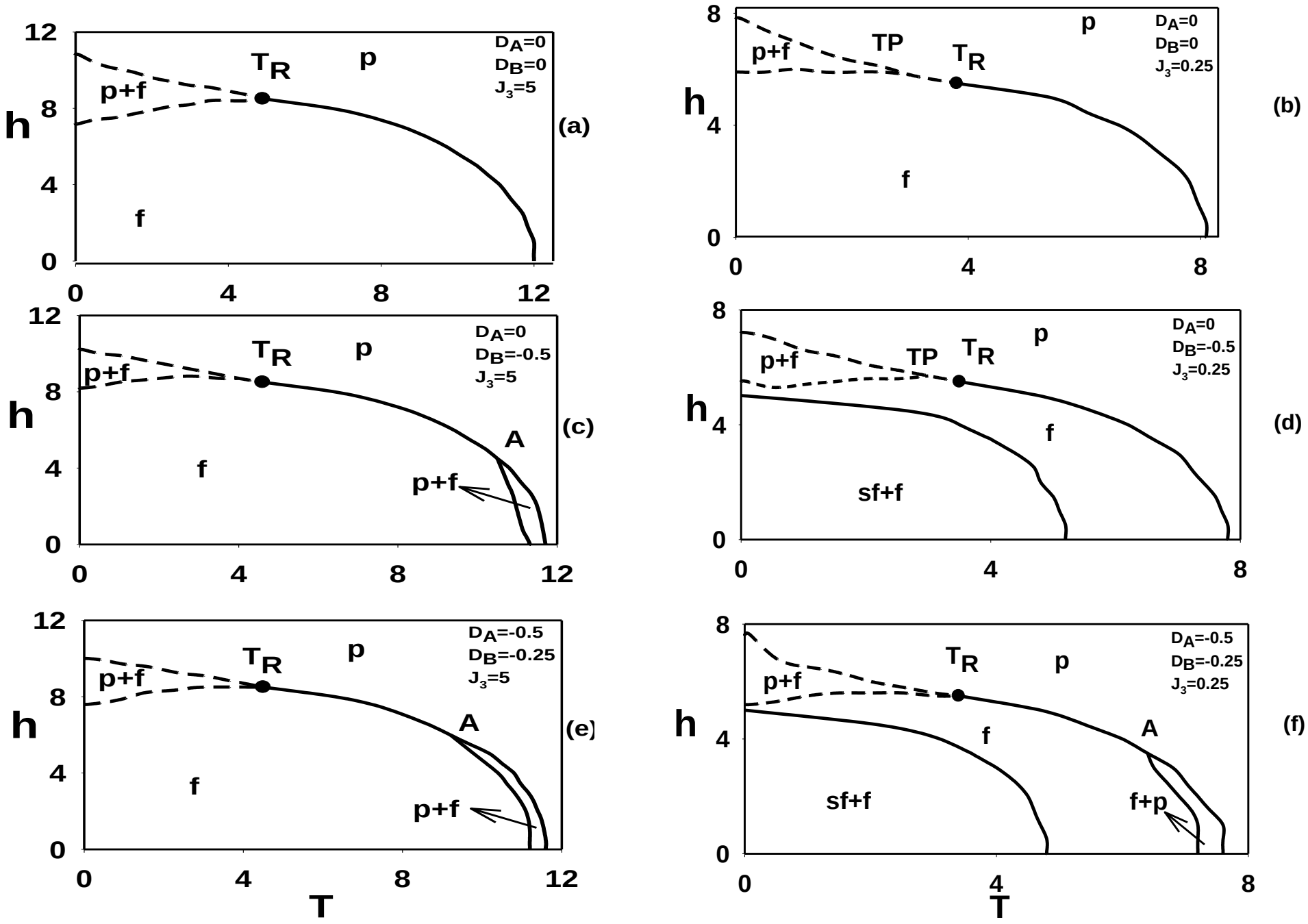


Fig. 4

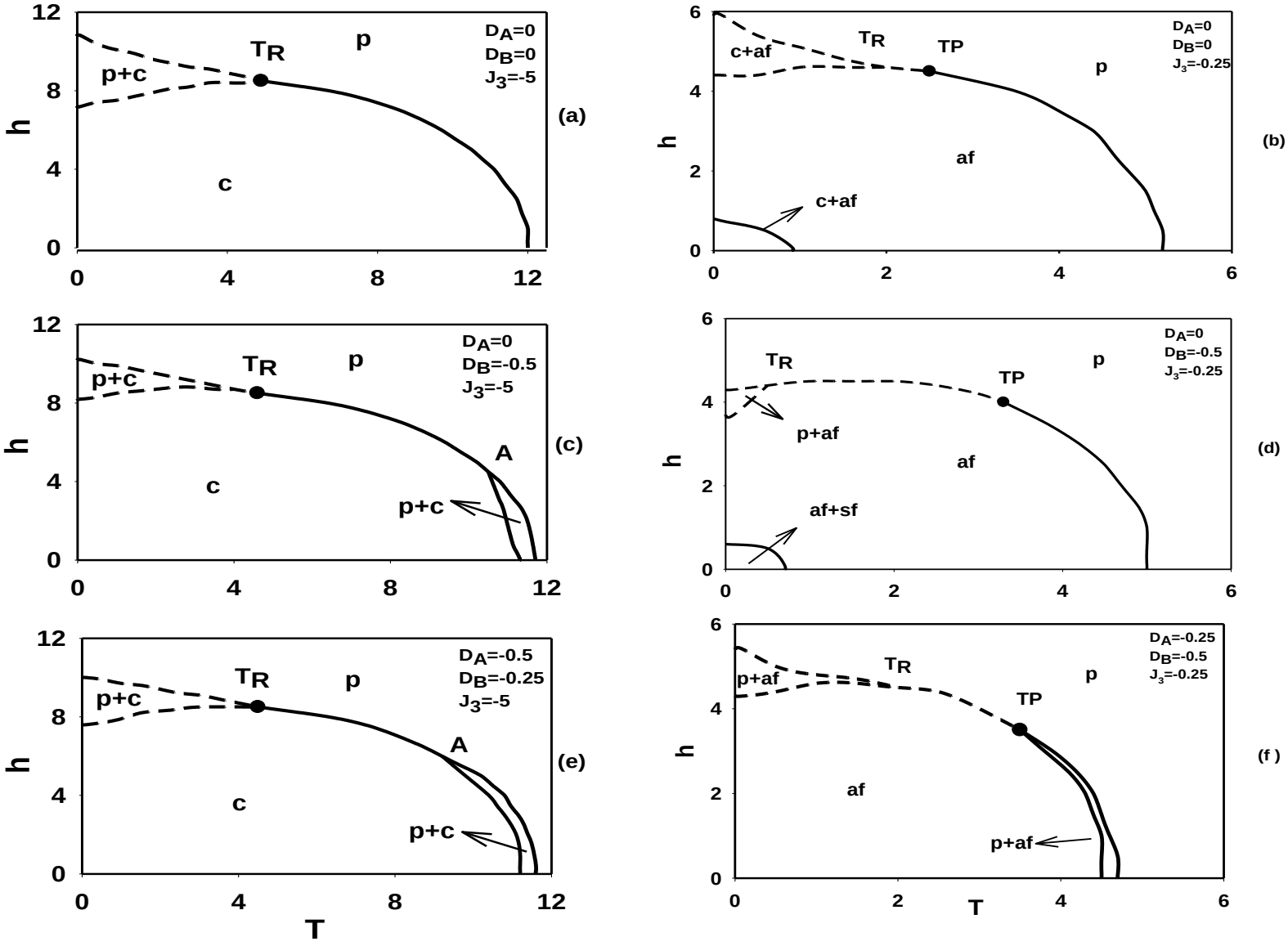


**Fig. 5**

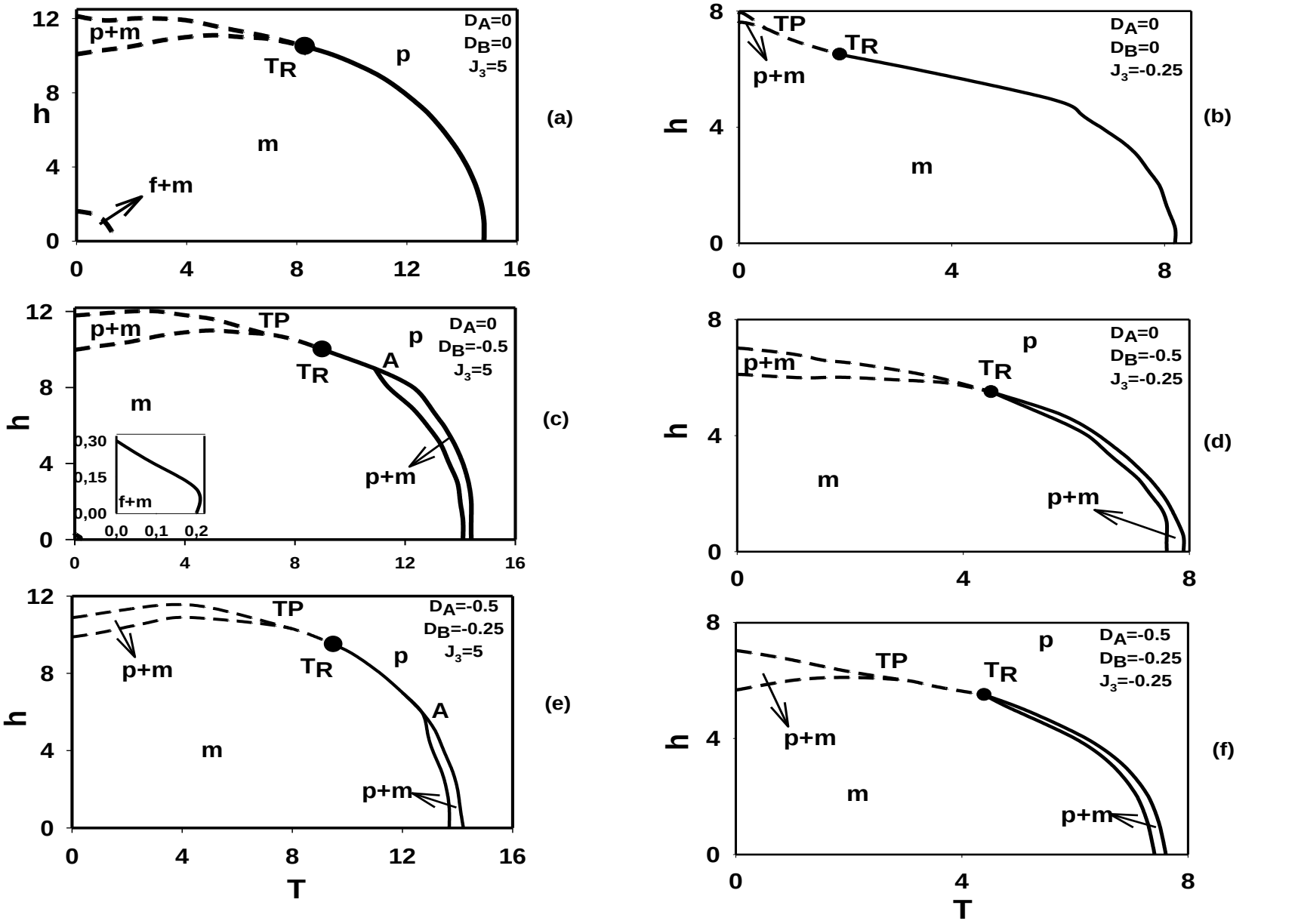


Fig.6

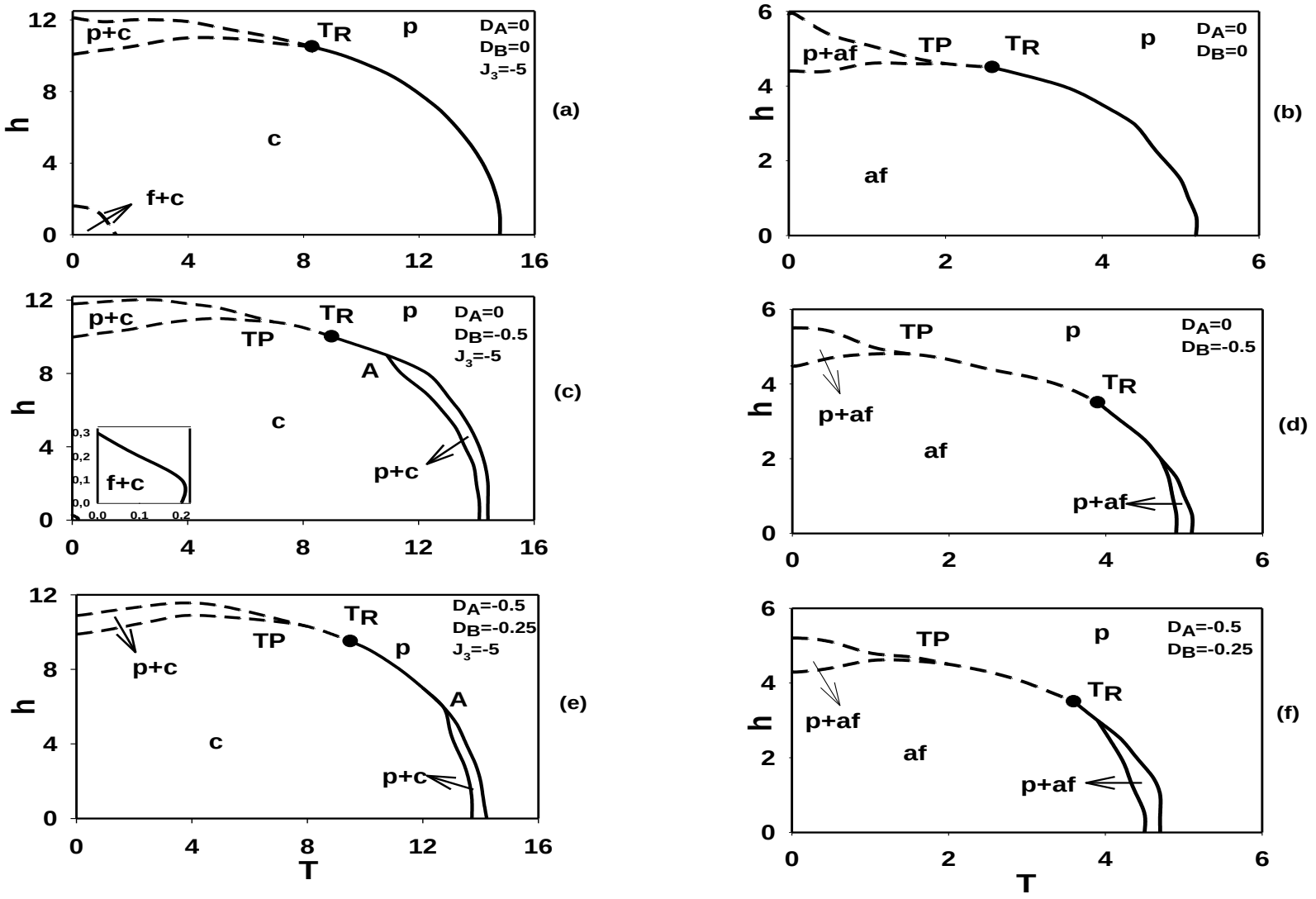


Fig. 7

EK-4

INTERNATIONAL SOCIETY FOR
ENGINEERING RESEARCH AND DEVELOPMENT

# Certificate of Session Chair

*This is to Certify that*

*Mustafa Keskin*

*Erciyes University, Kayseri, Turkey.*

*Joined the 65th ISERD International Conference*

*held in Mecca, Saudi Arabia on 23rd-24th January 2017.*

*as a Technical Session Chair and Invited Speaker.*

*Best wishes from ISERD.*

INTERNATIONAL SOCIETY FOR ENGINEERING RESEARCH & DEVELOPMENT
ISERD

Authorised By
CHAIRMAN / DIRECTOR

www.iserd.co

Paper ID: ISD-SIEMECA-23017-3132

INTERNATIONAL SOCIETY FOR ENGINEERING RESEARCH AND DEVELOPMENT

International Conference on

Science and Innovative Engineering

# Certificate

*This is to certify that Mustafa Keskin has presented a paper entitled "Dynamic Magnetic Hysteresis Behavior in a Mixed Spin (3/2, 2) Bilayer System Under a Time-Dependent Oscillating Magnetic Field" at the International Conference on Science and Innovative Engineering (ICSIE) held in Mecca, Saudi Arabia on 23rd-24th January 2017.*

INTERNATIONAL SOCIETY FOR ENGINEERING RESEARCH & DEVELOPMENT * ISERD.

Chairman
International Society for Engineering Research and Development

# DYNAMIC MAGNETIC HYSTERESIS BEHAVIOR IN A MIXED SPIN (3/2, 2) BILAYER SYSTEM UNDER A TIME-DEPENDENT OSCILLATING MAGNETIC FIELD

**[1]MEHMET ERTAS, [2]MUSTAFA KESKIN**

[1,2]Department of Physics, Erciyes University, 38039 Kayseri, Turkey
E-mail: [1]mehmetertas@erciyes.edu.tr, [2]keskin@erciyes.edu.tr

**Abstract**- We study dynamic magnetic hysteresis properties of the mixed spin-3/2 and spin-2 Ising model on a two-layer square lattice within the framework of dynamic mean-field calculations based on the Glauber –type stochastic. We obtain the hysteresis loops for different reduced temperatures as well as investigate the effect of frequencies on the hysteresis behavior. We also study the temperature dependence of the coercive field and remanent magnetization. We compare our results with some theoretical and experimental works and observe a quantitatively good agreement with some theoretical and experimental results.

**Keywords**: The mixed spin (3/2, 2) bilayer system; Dynamic magnetic hysteresis; coercively; remanent magnetization Mean-field approach based on the Glauber–type stochastic dynamics.

## I.INTRODUCTION

The dynamic magnetic hysteresis (DMH) or the dynamics of magnetization reversal is of great importance in both technical applications, such as developing memory storage devices and high frequency devices applications as well as academic research [1-2]. The DMH is defined as the dependence of the hysteresis loop area on the frequency and the amplitude of the applied magnetic field [3]. The DMH has important technological implications such as for high frequency devices applications [2-3].The DMH behaviors of various materials, such as Co films on a Cu (001) surface [4, 5], ferromagnetic NiFe, Co layers and NiFe/Cu/Co(001) spin-valve structures [6], ultrathin epitaxial Fe/GaAs(001) [7], permalloy thin films [8], [Co/Pt]3 magnetic multilayers [9], Fe- films [10], etc, have been experimentally investigated. Theoretically, the DMH has been mostly investigated by Ising models, such as spin-1/2 (see [11-18] and references therein), spin-1 [19-20], spin-3/2 [21] and mixed spin Ising systems (see [22- 25] and references therein) as well as some other methods (see [26-31] and references therein).

On the other hand, the mixed spin (3/2, 2) system is one of the important mixed spin systems which have been used to investigate molecular-based magnetic materials and ferrimagnetisim. They also display new and rich critical phenomena that cannot be observed in the single-spin Ising systems. . The mixed spin (3/2, 2) Ising corresponds to the Prussian blue of the type FeII 1.5 [CrIII(CN)6]. nH2O [32]. The equilibrium behaviors of the systems have been studied to explain various physical phenomena and critical properties within some methods in equilibrium statistical physics, such as the mean-field theory (MFT) [33-35], the effective-field theory [36-37], and Monte Carlo calculations [38-39]. Moreover, dynamic phase diagrams of the system has been constructed by the Glauber-type stochastic (GTS) dynamics based on the MFT, also called the dynamic mean-field theory (DMFT) [40-41].

In this talk, we will present the DMH behaviors the mixed spin (3/2, 2) Ising system within the DMFT. We will also discuss the temperature dependence of the coercive field and remanent magnetization. In the next section, we briefly describe the model and formulation. In Sec. 3 we give the numerical results with discussions and a brief conclusion.

## II.MODEL AND FORMULATION

The mixed spin (3/2, 2) Ising system with a two-layers, namely L1 and L2, on a square lattices is shown Fig. 1. Each layer of the system is also a two-sublattice system (A and B) with spin variables , , = ±3/2, ±1/2 occupy L1 layer and , , = ±2, ±1, 0 L2 layer; hence, the system can be depicted with four sublattice magnetizations or four magnetizations that are introduced as follows:

$$m_1^A \equiv \left\langle \sigma_i^A \right\rangle,\ m_1^B \equiv \left\langle \sigma_j^B \right\rangle,\ m_2^A \equiv \left\langle S_{i'}^A \right\rangle,\ m_2^B \equiv \left\langle S_{j'}^B \right\rangle,$$

where<¨>is the thermal expectation value. Each layer has N sites and interacts with its nearest-neighbor (NN) and the corresponding adjacent spins in the other layer whose sites are labeled by i, i′, j and j′, as seen in Fig. 1.

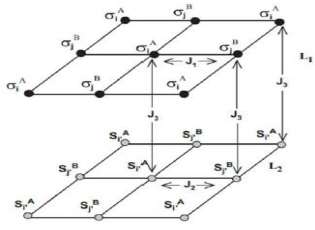

**Fig. 1. The sketch of a two-layer square lattice. L1 and L2 represent to the upper and lower layers.**

The mixed spin (3/2, 2) Ising Hamiltonian of such a bilayer square lattice system can be written as

$$\mathcal{H} = -J_1\sum_{<ij>}\sigma_i^A\sigma_j^B - J_2\sum_{<i'j'>}S_{i'}^A S_{j'}^B$$
$$-J_3\left(\sum_{<ii'>}\sigma_i^A S_{i'}^A + \sum_{<jj'>}\sigma_j^B S_{j'}^B\right)$$
$$-D\left(\sum_{<i>}\left(\sigma_i^A\right)^2 + \sum_{<i'>}\left(S_{i'}^A\right)^2 + \sum_{<j>}\left(\sigma_j^B\right)^2 + \sum_{<j'>}\left(S_{j'}^B\right)^2\right)$$
$$-H\left(\sum_{<i>}\sigma_i^A + \sum_{<j>}\sigma_j^B + \sum_{<i'>}S_{i'}^A + \sum_{<j'>}S_{j'}^B\right), \qquad (1)$$

where <ij> and <i′j′> indicate a summation over all pairs of nearest-neighboring sites of each layer. J1 and J2 are exchange constants for the first and second layer, respectively, which are also called intralayer coupling constants, and J3 represents the interlayer coupling constant over all the adjacent neighboring sites of layers, as illustrated in Fig. 1. H is a time-dependent oscillating external magnetic field: H= H0cos(wt), where H0 and w = 2πν are the amplitude and the angular frequency of the oscillating field, respectively. D is the crystal-field interaction. The system is in contact with an isothermal heat bath at absolute temperature TA.

Now, we employ the GTS dynamics to obtain DMFT equations. The system evolves according to the GTS process at a rate of 1/τ transitions per unit time. We define and as the probability that the system has σ- and S- spin configurations in each layer at time t. If is the probability per unit time that the ith spin changes from the values to , while the others, i.e., and spins on sublattice B, remain momentarily fixed, then we may write the master equation that describes the interaction between the spins and the heat bath as

$$\frac{d}{dt}P_1^A(\sigma_1^A,\sigma_2^A,...,\sigma_N^A;t) =$$
$$-\sum_i\left(\sum_{\sigma_i^A\neq\sigma_i^{A'}}W_i^A(\sigma_i^A\to\sigma_i^{A'})\right)P_1^A(\sigma_1^A,\sigma_2^A,...,\sigma_i^A,...,\sigma_N^A;t)+$$
$$\sum_i\left(\sum_{\sigma_i^A\neq\sigma_i^{A'}}W_i^A(\sigma_i^{A'}\to\sigma_i^A)P_1^A(\sigma_1^A,\sigma_2^A,...,\sigma_i^{A'},...,\sigma_N^A;t)\right), \qquad (2)$$

Since the system is in contact with a heat bath at absolute temperature TA, the probability of change of state per unit time of each spin would be given by the Boltzmann factor as

$$W_i^A(\sigma_i^A\to\sigma_i^{A'}) = \frac{1}{\tau}\frac{\exp(-\beta\Delta E(\sigma_i^A\to\sigma_i^{A'}))}{\sum_{\sigma_i^{A'}}\exp(-\beta\Delta E(\sigma_i^A\to\sigma_i^{A'}))}, \qquad (3)$$

where β=1/kBTA kB being the Boltzmann factor, $\sum_{\sigma_i^{A'}}$ is the sum over the four possible values of = ±3/2, ±1/2 and represents the change in the energy of the system and defines as

$$\Delta E_i^A(\sigma_i^A\to\sigma_i^{A'}) = -(\sigma_i^{A'}-\sigma_i^A)(J_1\sum_{j'}\sigma_j^B + J_3\sum_i S_{i'}^A + H)$$
$$-D\left(\left(\sigma_i^{A'}\right)^2 - \left(\sigma_i^A\right)^2\right), \qquad (4)$$

The probabilities satisfy the detailed balance condition. Using Eqs. (1)-(4), we obtain the dynamic equation for $m_1^A$

$$\Omega\frac{d}{d\xi}m_1^A = -m_1^A + \frac{3\exp\left(\frac{4d}{T}\right)\sinh\left[\frac{3a_1}{2T}\right] + \exp\left(-\frac{d}{T}\right)\sinh\left[\frac{a_1}{2T}\right]}{2\exp\left(\frac{d}{T}\right)\cosh\left[-\frac{3a_1}{2T}\right] + 2\exp\left(-\frac{d}{T}\right)\cosh\left[\frac{a_1}{2T}\right]}, \qquad (5)$$

$$\xi = wt,\ T = (\beta J_1)^{-1},\ h = H_0/J_1,\ d = D/J_1,\ \Omega = \tau w$$

$$\text{and } a_1 = zm_1^B + \frac{J_3}{J_1}m_2^A + h\cos\xi \text{ .We fixed } z = 4.$$

The other dynamic equations for $m_1^B$, $m_2^A$ and $m_2^B$ can be similarly calculated and found as

$$\Omega\frac{d}{d\xi}m_1^B = -m_1^B + \frac{3\exp\left(\frac{d_B}{T}\right)\sinh\left[\frac{3a_2}{2T}\right] + \exp\left(-\frac{d}{T}\right)\sinh\left[\frac{a_2}{2T}\right]}{2\exp\left(\frac{d}{T}\right)\cosh\left[-\frac{3a_2}{2T}\right] + 2\exp\left(-\frac{d}{T}\right)\cosh\left[\frac{a_2}{2T}\right]}, \qquad (6)$$

$$\Omega\frac{d}{d\xi}m_2^A = -m_2^A + \frac{2\exp\left(\frac{4d}{T}\right)\sinh\left[\frac{2a_3}{T}\right] + \exp\left(\frac{d}{T}\right)\sinh\left[\frac{2a_3}{T}\right]}{\exp\left(\frac{4d}{T}\right)\cosh\left[\frac{2a_3}{T}\right] + \exp\left(\frac{d}{T}\right)\cosh\left[\frac{2a_3}{T}\right] + 1/2}, \qquad (7)$$

$$\Omega\frac{d}{d\xi}m_2^B = -m_2^B + \frac{2\exp\left(\frac{4d}{T}\right)\sinh\left[\frac{2a_4}{T}\right] + \exp\left(\frac{d}{T}\right)\sinh\left[\frac{a_4}{T}\right]}{\exp\left(\frac{4d}{T}\right)\cosh\left[\frac{2a_4}{T}\right] + \exp\left(\frac{d}{T}\right)\cosh\left[\frac{a_4}{T}\right] + 1/2}, \qquad (8)$$

$$\text{Where } a_2 = zm_1^A + \frac{J_3}{J_1}m_2^B + h\cos\xi,$$
$$a_3 = \frac{J_2}{J_1}zm_2^B + \frac{J_3}{J_1}m_1^A + h\cos\xi,$$
$$a_4 = \frac{J_2}{J_1}zm_2^A + \frac{J_3}{J_1}m_1^B + h\cos\xi.$$

Now, we should define the dynamic hysteresis loop area to investigate the DMH behaviors and it is define as

$$A = -\oint m_{1,2}^{A,B}(t)\,dh = -h_0 w \int_0^{\tau} m_{1,2}^{A,B}(t)\cos(wt)dt. \quad (9)$$

Moreover,

$$m_T = (m_1^A + m_1^B + m_2^A + m_2^B)/4. \quad (10)$$

Results of numerical solutions and discussions will be given in Section III.

## III. RESULTS AND DISCUSSIONS

We solved Eq. (9) by combining the numerical methods of Adams-Moulton-predictor-corrector with the Romberg integration for a given set of system parameters and presented in Figs. 2 and 3.

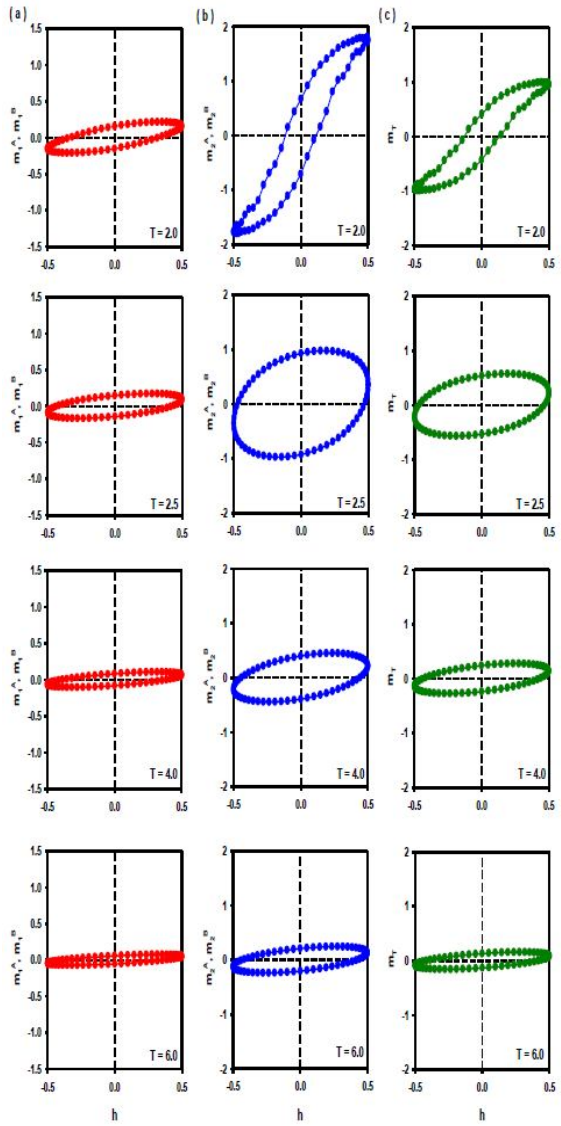


**Fig. 2.The DMH behaviors at different reduced temperatures.**

Fig. 2 illustrates dynamic magnetic hysteresis loops for w=0,11π, J1=-1, J2=0.1, J3=0.5, D=1 at T=2, 2.5, 4 and 6 for the submagnetizations and total magnetization. From this figure, one can see that the dynamic magnetic hysteresis loop areas increase as the temperature increases and at a certain temperature loop areas decrease with increasing the temperature that is in a good, quantitatively, agreement with some theoretical [15-17,24,25] results as well as experimental reports [5].

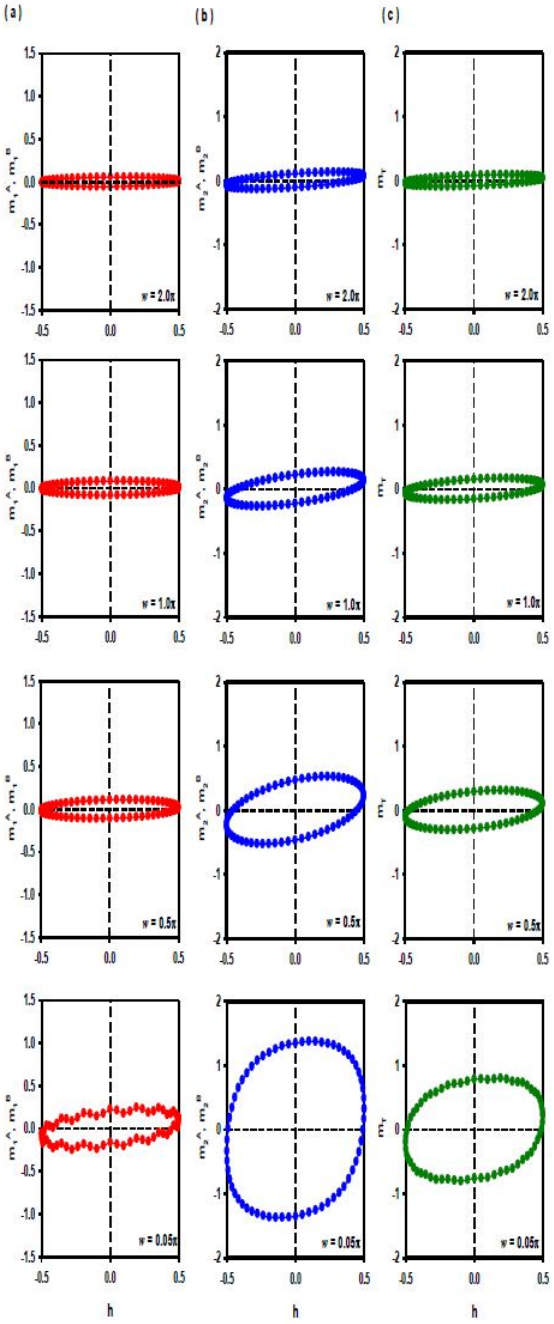


**Fig. 3. The DMH behaviors at various frequencies.**

Fig. 3 is obtained for J1=-1, J2=0.1, J3=0.5, d=1, T= 1.95 and various values of w; hence we investigate the effects of the frequencies on DMH behaviors. The results display that as the frequency is increased, the area of hysteresis loops decrease.. The results are also quantitatively good agreement some theoretical results [16, 24, 29] and experimental reports [4, 5, 7].

Finally, Fig. 4 shows the thermal behaviors of the coercivities and remanent magnetizations for

w=0,11π, J1=-1, J2=0.1, J3=0.5, d=1, and different reduced temperatures from 2 to 6. The figure illustrates that if the temperature is increased, the coercivity also increased up to a certain values of temperature and, with further increase of temperature, the coercivity very smoothly decreases. The remanent magnetization also displays similar behaviors as the coercivity field.

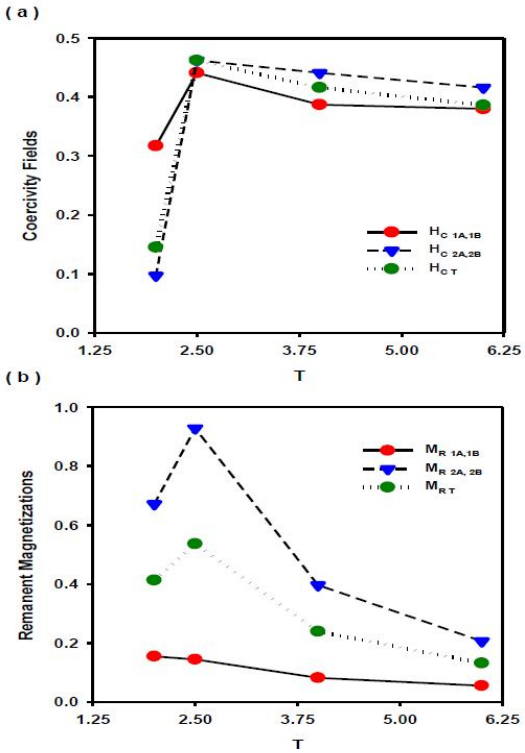


**Fig. 4 a) The coercivity field and b) the remanent magnetizations, versus the reduced temperatures for the same parameters as in Fig 2.**

The similar behaviors have been seen in some theoretical [24] results and the experimental report for the low and intermediate dynamic regimes [7]. We should also mention that the high coercivities correspond to the magnetically hard materials and low coercivities to the magnetically soft ones.

In conclusion, we study the DMH loop behaviors at different reduced temperatures and as well as investigate the effect of frequencies on the hysteresis behavior. We also investigate the temperature dependence of the coercive field and remanent magnetization. We observe that our results are in a good agreement with some theoretical and experimental results. More details of our results, such as influence of thickness and crystal-field interaction, will be appeared in the future communication due to the page limitation here. We hope that this work gives some light into theoretical and experimental research for investigation of the DMH behaviors.

## ACKNOWLEDGMENTS

This work was supported by Erciyes University Research Fund, Grant No: FBA- 2016-6324.

## REFERENCES

[1] Z. Zhu, Y. Sun, Q. Zhang, J. M. Liu, ”Dynamics and scaling of low-frequency hysteresis loops in nanomagnets” Phys. Rev. B, Vol. 76, pp. 014439, July 2007.

[2] G. Bertotti, Hysteresis in Magnetism, Academic Press, San Diego, 1998.

[3] K. Chakrabarti and M. Acharyya, “Dynamic transitions and hysteresis”, Rev. Mod. Phys. Vol. 71, pp. 847-860, April 1999.

[4] Q. Jiang, H. N. Yang, G. C. Wang, “Scaling and dynamics of low-frequency hysteresis loops in ultrathin Co films on a Cu(100) surface”, Phys. Rev. B, Vol. 52, pp. 14911-14916, November 1995.

[5] J. S. Suen, M. H. Lee, G.Teeter and J. L. Eskine, “Magnetic hysteresis dynamics of thin Co films on Cu(001) surface”, Phys. Rev. B vol. 59, pp. 4249-4259, February 1999.

[6] W. Y. Lee, A. Samed, T. A. Moore and J. A. C. Bland, “Dynamic hysteresis behavior in epitaxial spin-valve structures”, J. Appl. Phys. Vol. 87, pp. 6600-6602, May 2000.

[7] T. A. Moore, G. Wastlbauer, and J. A. C. Blanda, E. Cambril, M. Natali, D. Decanini and Y. Chen,” Antidot density-dependent reversal dynamics in ultrathin epitaxial Fe/GaAs(001)”, J. Appl. Phys. Vol. 39, pp. 8746-8748, May 2003.

[8] C. Nistor, E. Faraggi and J. L. Erskine, “Magnetic energy loss in permalloy thin films and microstructures”, Phys. Rev. B, Vol. 72, pp. 014404-1-014404-8, July 2005.

[9] D.T. Robb, Y.H. Xu, O. Hellwig, J. McCord, A. Berger, M.A. Novotny and P.A. Rikvold, “Evidence for a dynamic phase transition in [Co/Pt]3 magnetic multilayers”, Phys. Rev. B, Vol. 78, pp. 134422-134428, October 2008.

[10] N. J. Steinke, T. A. Moore, R. Mansell, J. A. C. Bland and C. H. W. Barnes, “Nonuniversal dynamic magnetization reversal in the Barkhausen-dominated and mesofrequency regimes”, Phys. Rev. B, Vol. 86, pp. 184434-1-184434-8, November 2012.

[11] W.S. Lo and R.A. Pelcovits, “Ising model in a time-dependent magnetic field”, Phys. Rev. A, Vol. 42, pp. 7471-7475, September 1990.

[12] M. Acharyya, “Nonequilibrium phase transition in the kinetic Ising model: Is the transition point the maximum lossy point?” Phys. Rev. E, Vol. 58, pp. 179-186, July 1998.

[13] S.W. Sides, P.A. Rikvold, and M.A. Novonty, “Kinetic Ising model in an oscillating field: Avrami theory for the hysteretic response and finite-size scaling for the dynamic phase transition”, Phys. Rev. E, Vol. 59, pp. 2710-2730, March 1999.

[14] M.Y. Sun, X. Chen, S. Dong, K.F. Wang and J. -M. Liu, “Dynamic hysteresis of magnetic aggregates with non-integer dimension”, J. Magn. Magn. Mater. Vol. 321, pp. 2429-2432, March 2009.

[15] B. Deviren, Y. Şener and M. Keskin, “Dynamic magnetic properties of the kinetic cylindrical Ising nanotube”, Physica A, Vol. 392, pp. 3969-3983, May 2013.

[16] Y. Yüksel, “Monte Carlo simulations of dynamic phase transitions in ultrathin Blume–Capel films” Phys. Lett. A, vol.377, pp. 2494-25-04, August 2013.

[17] B. O. Aktaş, Ü. Akıncı and H. Polat, “Dynamic hysteresis features of Ising-type thin films”, Phys. Rev. E,Vol. 90, pp. 012129, July 2014.

[18] M. Ertaş, E. Kantar, Y. Kocakaplan and M. Keskin, “Dynamic magnetic properties in the kinetic Ising ferromagnet on triangular lattice within the effective-field theory and using Glauber-type stochastic Dynamics”, Physica A, vol. 444, pp. 732-743, February2016.

[19] B. Deviren and M. Keskin, “Dynamic magnetic hysteresis behavior and dynamic phase transition in the spin-1 Blume–Capel model” J. Magn. Magn. Mater. Vol. 324, pp. 1051-1062, March 2012.

[20] M. Ertaş and M. Keskin,” The dynamic magnetic hysteresis behaviors of the Blume-Capel under the presence of an oscillating magnetic field : The path probability approach”,

International Journal of Advances in Science Engineering and Technology, vol. 3, pp. 41-44, July 2015.
[21] E. Kantar and M. Ertaş, "Influence of frequency on the kinetic spin-3/2 cylindrical Ising nanowire system in an oscillating Field", J Supercond Nov Magn. Vol. 28, pp. 2529-2538, August 2015.
[22] A. Bukharov, A. S. Ovcihinnikov, N. V. Baranov and K. Inoue, "Magnetic hysteresis in molecular Ising ferrimagnet: Glauber dynamic approack", Eur. Phys. J. B vol. 70, pp. 369-375, July 2009.
[23] M. Ertaş, M. Keskin and B. Deviren, "Multicritical dynamic phase diagrams and dynamic hysteresis loops in a mixed spin-2 and spin-5/2 Ising ferrimagnetic system with repulsive biquadratic coupling: Glauber dynamic approach", J. Stat. Phys. Vol. 146, pp. 1244-1262, February 2012.
[24] M. Ertaş and M. Keskin," Dynamic hysteresis features in a two-dimensional mixed Ising system", Phy. Letts A, Vol. 379, pp. 1576-1583, April 2015.
[25] M. Batı and M. Ertaş," Dynamic magnetic hysteresis properties in a two-Dimensional mixed Ising system designed with integer and half-integer spins", J Supercond Nov Magn. Vol. 29, pp. 2835-2841, November 2016.
[26] R. Hu, A. K. Soh, G. P. Zheng and Y. Ni,"Micromagnetic modelling studies on the effects of stress on magnetization reversal and dynamic hysteresis", J. Magn. Magn. Mater. Vol. 301, pp. 458-468, August 2005.
[27] D. Ribbenfjard and G. Engdahl, "Novel method for modelling of dynamic hysteresis", IEEE Trans. Magn., vol. 44, pp. 854-857, June 2008.
[28] M.Y. Sun, X. Chen, S. Dong, K.F. Wang and J. -M. Liu, "Dynamic hysteresis of magnetic aggregates with non-integer dimension", J. Magn. Magn. Mater. Vol. 321, pp. 2429-2432, March 2009.
[29] G.T. Landi "Dynamic symmetry loss of high-frequency hysteresis loops in sing-domain particles with uniaxial anisotropy", J. Magn. Magn. Mater. Vol. 324, pp. 466-470, February 2012.
[30] B. Ourai, S.V. Titov, H. El Mrabti and Y.P. Kalmykov, "Nonlinear susceptibility and dynamic hysteresis loops of magnetic nanoparticles with biaxial anisotropy", J. Appl. Phys., Vol. 113, pp. 053903-053913, February 2013.
[31] I.S. Poperechny, Y.L. Raikher and V.I. Stepanov, "Dynamic hysteresis of a uniaxial superparagnet: Semi-adiabatic approximation", Physica B, Vol. 435, pp. 58-61, February 2014.
[32] K. Hashimoto, S. Ohkoshi, "Design of novel magnets using Prussian blue analogues", Philos. Trans. R. Soc. London A, Vol. 357, pp. 2977-3003, November 1999.
[33] Bobak and J. Dely, "Phase transitions and multicritical points in the mixed spin-3/2 and spin-2 Ising system with a single-ion anisotropy", J. Magn. Magn. Mater. Vol. 310, pp. 1419-1421, March 2007.
[34] H. Miao, G. Wei and J. Geng, "Phase transition and multicritical points in the mixed spin-3/2 and spin-2 Ising model different sing-ion anisotropies", J. Magn. Magn. Mater. vol. 321, pp. 4139-4144, 2009.
[35] F. Abubrig, "Magnetic properties of a mixed-spin-3/2 and spin-2 Ising ferrimagnetic system in an applied longitudinal magnetic field", World Journal of Condensed Matter Physics, Vol 3, pp. 111-118, May 2013.
[36] B. Deviren, E. Kantar, M. Keskin, "Magnetic properties of a mixed-spin-3/2 and spin-2 Ising ferrimagnetic system within the effective-field theory", Journal of the Korean Physical Society, Vol. 56, 1738-1747, June 2010.
[37] B. Deviren, Y. Polat, M. Keskin, "Phase diagrams in the mixed spin-3/2 and spin-2 Ising system with two alter-native layers within the effective-field theory", Chin. Phys. B, Vol. 20, pp. 060507-1—06057-13, June 2011.
[38] Jabar, A. Belhaj, H. Labrim, L. Bahmad and N. Hassanain, "Monte Carlo study of a Blume-Capel mixed thin film with four-spin interaction", J Supercond Nov Magn Vol. 28, pp. 2721-2730, September 2015.
[39] Jabar, A. Belhaj, H. Labrim, L. Bahmad, N. Hassanain and A. Benyoussef, "Mixed spin thin films in the Blume-Emery-Griffiths model with biquadratic exchange interactions: A Monte Carlo study", Superlattices and Microstructres, Vol. 78, pp. 171-182, February 2015.
[40] M. Keskin and Y. Polat, "Phase diagrams of a nonequilibrium mixed spin-3/2 and spin-2 Ising system in an oscillating magnetic field", J. Magn. Magn. Mater. Vol. 321, pp. 3905-3912, December 2009.
[41] Ü. Temizer, M. Tülek and S. Yarar, "Dynamic phase diagrams of the mixed Ising bilayer system consisting of spin-3/2 and spin-2", Physica A, Vol. 415, pp.156-171, December 2014.

★★★

J Supercond Nov Magn
DOI 10.1007/s10948-017-4145-y

ORIGINAL PAPER

# Dynamic Magnetic Hysteresis Behaviors in a Mixed Spin (3/2, 2) Bilayer System with Different Crystal-Field Interactions

**Mustafa Keskin**[1] · **Mehmet Ertaş**[1]

Received: 3 March 2017 / Accepted: 22 April 2017


**Abstract** Dynamic magnetic hysteresis (DMH) behaviors of the mixed spin-3/2 and spin-2 Ising bilayer system with different crystal-field interactions on a two-layer square lattice is studied by the use of dynamic mean field calculations based on the Glauber-type stochastic. The hysteresis loops are obtained for different reduced temperatures ($T$), magnetic field amplitudes ($h$), frequencies ($w$) and interlayer coupling constants ($J_3$). Influences of the $T$, $h$, $w$ and $J_3$ on the DMH properties are investigated. We also study the temperature, frequency and interlayer coupling interaction dependence of the coercive field and remanent magnetization. We compare our results with some theoretical and experimental works and observe a quantitatively good agreement with some theoretical and experimental results.

**Keywords** Mixed spin (3/2, 2) bilayer system · Dynamic magnetic hysteresis · Coercive field · Remanent magnetization · Glauber-type stochastic · Mean field theory

## 1 Introduction

The dynamic magnetic hysteresis (DMH) or the dynamics of magnetization reversal is of great importance in advanced technological applications, such as developing memory storage devices and high-frequency device applications as well as academic research [1–4]; hence, they have been intensively studied topics both theoretically and experimentally. The DMH is often referred to as the dependence of the hysteresis loop area on the frequency and the amplitude of the applied magnetic field [3]. The DMH behaviors of various materials, such as Co films on a Cu(001) surface [5, 6]; epitaxial single ferromagnetic face-centered cubic (fcc) NiFe(001), fcc Co(001) layers and NiFe/Cu/Co(001) spin valve structures [7]; epitaxial Fe/GaAs(001) and Fe/InAs(001) ultrathin films [8]; ultrathin epitaxial Fe/GaAs(001) [9]; permalloy thin films [10, 11]; [Co/Pt]3 magnetic multilayers [12]; thick Fe and thick CoFe films [13]; Fe thin films [14, 15]; a single crystalline compound $Co_7(TeO_3)_4Br_6$, [16]; BiGdFeCoO films [17]; and the ternary intermetallic compound DyMnSi2 [18], have been investigated. Theoretically, the DMH has been mostly investigated by two classes of models: (1) Ising-type models, such as spin-1/2 (see [19–31] and references therein), spin-1 [32, 33], spin-3/2 [34] and mixed spin Ising systems (see [35–39] and references therein), and (2) extended domain wall models (see [40–45] references therein). The DMH is also studied using some other methods, such as the time-dependent Landau-Lifshitz-Gilbert equation [46–48], the semi-adiabatic approximation [49] and the dynamic Preisach model [50]. On the other hand, the mixed spin (3/2, 2) system is one of the important mixed spin systems which have been employed to study molecular-based magnetic materials and ferromagnetism. They also illustrate new and rich critical phenomena that cannot be observed in the single-spin Ising systems. The mixed spin (3/2, 2) Ising corresponds to the Prussian blue of the $FeII_{1.5}[CrIII(CN)_6]\cdot nH_2O$ type [51].

The equilibrium behaviors of the systems have been studied to explain various physical phenomena and critical properties within some methods in equilibrium statistical

✉ Mustafa Keskin
keskin@erciyes.edu.tr

[1] Department of Physics, Erciyes University, 38039 Kayseri, Turkey

Published online: 04 May 2017

physics, such as the mean field theory (MFT) based on the Bogoliubov inequality for the Gibbs free energy [52–55], the effective field theory [56, 57] and Monte Carlo calculations [58, 59]. The exact formulation of the system on the Bethe lattice within the exact recursion equations was given, and that of some magnetic properties of the system has been investigated [60, 61]. Moreover, the dynamic phase transitions (DPTs) of the system have been studied and the dynamic phase diagrams (DPDs) have been constructed by the Glauber-type stochastic (GTS) dynamics based on the MFT, also called the dynamic mean field theory (DMFT) [62–64]. In particular, Keskin and Polat [62] studied the DPTs and presented the DPDs of the mixed spin (3/2, 2) Ising system on square lattice in an oscillating magnetic field. Temizer et al. [63] only investigated the DPTs and constructed the DPDs of the mixed spin (3/2, 2) system on the bilayer square lattice for the same crystal-field interactions ($D_A = D_B = D$) in detail. Recently, Keskin and Koçak [64] examined the influences of crystal-field ($D_A$ and $D_B$) and interlayer coupling interaction on the DPDs of the mixed spin (3/2, 2) system on the bilayer square lattice. Therefore, the DMH behaviors, which are of great importance in advanced technological applications, of the mixed spin (3/2, 2) Ising system on the bilayer square lattice, to the best of our knowledge, have not been investigated.

In this paper, we investigate the DMH behaviors of the mixed spin-3/2 and spin-2 Ising model with different crystal-field interactions on a two-layer square lattice within the framework of dynamic mean field calculations based on the Glauber-type stochastic. In particular, we investigate the influences of the reduced temperatures, frequencies, interlayer coupling constants ($J_3$) and crystal-field interactions on the DMH properties. We also study the temperature, frequency and interlayer coupling interaction dependence of the coercive field and remanent magnetization.

## 2 Model and Formulations

We consider a mixed spin-3/2 and Spin-2 Ising system with two layers, i.e. $L_1$ and $L_2$, on a square lattices, as seen in Fig. 1. Each layer of the system is also a two-sublattice system (A and B) with spin variables $\sigma_i^A$ and $\sigma_i^B = \pm 3/2,\ \pm 1/2$ occupying $L_1$ layer and $S_j^A$ and $S_j^B = \pm 2,\ \pm 1,\ 0$ occupying $L_2$ layer. Therefore, the system can be depicted with four sublattice magnetizations which are introduced as follows: $m_1^A \equiv \langle \sigma_i^A \rangle$, $m_1^B \equiv \langle \sigma_j^B \rangle$, $m_2^A \equiv \langle S_{i'}^A \rangle$, $m_2^B \equiv \langle S_{j'}^B \rangle$, where $\langle ... \rangle$ is the thermal expectation value. Each layer has $N$ sites and interacts with its nearest-neighbor (NN) and the corresponding adjacent spins in the other layer whose sites are labeled by $i$, $i'$, $j$ and $j'$, as seen in Fig. 1.

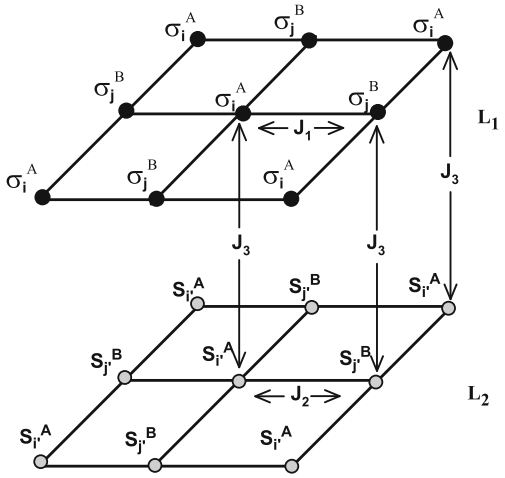


**Fig. 1** Schematic representation of a two-layer square lattice. $L_1$ and $L_2$ refer to the upper and lower layers containing spin variables $\sigma_i^A$ and $\sigma_i^B = \pm 3/2,\ \pm 1/2$ occupying $L_1$ layer and $S_j^A$ and $S_j^B$

The Hamiltonian of the mixed spin (3/2, 2) bilayer square lattice system can be written as

$$\begin{aligned}\mathcal{H} = & -J_1 \sum_{<ij>} \sigma_i^A \sigma_j^B - J_2 \sum_{<i'j'>} S_{i'}^A S_{j'}^B \\ & -J_3 \left( \sum_{<ii'>} \sigma_i^A S_{i'}^A + \sum_{<jj'>} \sigma_j^B S_{j'}^B \right) \\ & -D_A \left( \sum_{<i>} \left(\sigma_i^A\right)^2 + \sum_{<i'>} \left(S_{i'}^A\right)^2 \right) \\ & -D_B \left( \sum_{<j>} \left(\sigma_j^B\right)^2 + \sum_{<j'>} \left(S_{j'}^B\right)^2 \right) \\ & -H \left( \sum_{<i>} \sigma_i^A + \sum_{<j>} \sigma_j^B + \sum_{<i'>} S_{i'}^A + \sum_{<j'>} S_{j'}^B \right) \end{aligned} \quad (1)$$

where $<ij>$ and $<i'j'>$indicate a summation over all pairs of nearest-neighboring sites of each layer. $J_1$ and $J_2$ are exchange constants for the first and second layers, respectively, which are also called intralayer coupling constants, and $J_3$ is the interlayer coupling constant over all the adjacent neighboring sites of layers, as seen in Fig. 1. $H$ is an oscillating external magnetic field which is given as follows: $H = H_0 \cos(wt)$, where $H_0$ and $w = 2\pi\nu$ are the amplitude and the angular frequency of the oscillating field, respectively. $D_A$ and $D_B$ are the crystal fields for sites on A lattice and for sites on B lattice, respectively. The system is in contact with an isothermal heat bath at absolute temperature ($T_A$).

To obtain the set of mean field dynamic equations for magnetizations, we apply the Glauber-type stochastic dynamics. Thus, the system evolves according to a Glauber-type stochastic process at a rate of $1/\tau$ transitions per unit time. Since the derivation of the dynamic equations was extensively described for this mixed system [62, 63] and also

the other mixed systems [36, 37], in here, we will only give a brief summary. For this purpose, we define $P(\sigma_1, \sigma_2, \ldots, \sigma_N, S_1, S_2, \ldots, S_N; t)$ as the probability that the system has $\sigma$- and $S$-spin configurations in each layer $\sigma_1, \sigma_2, \ldots, \sigma_N, S_1, S_2, \ldots, S_N$ at time $t$. If $W_i\left(\sigma_i^{\mathrm{A}} \rightarrow \sigma_i^{\mathrm{A}'}\right)$ is the probability per unit time that the $i$th spin changes from the values $\sigma_i^{\mathrm{A}}$ to $\sigma_i^{\mathrm{A}'}$, the others, i.e. $(S_1, S_2, \ldots, S_N)$ and spins on sublattice B, remain momentarily fixed and then we may write the master equation that describes the interaction between the spins and the heat bath as

$$\begin{aligned}\frac{d}{dt}P_1^{\mathrm{A}}\left(\sigma_1^{\mathrm{A}},\sigma_2^{\mathrm{A}},\ldots,\sigma_{\mathrm{N}}^{\mathrm{A}};t\right) = -\sum_i\left(\sum_{\sigma_i^{A}\neq\sigma_i^{A\prime}} W_i^{\mathrm{A}}(\sigma_i^{\mathrm{A}}\rightarrow\sigma_i^{\mathrm{A}'})\right)\\ \times P_1^{\mathrm{A}}\left(\sigma_1^{\mathrm{A}},\sigma_2^{\mathrm{A}},\ldots,\sigma_i^{\mathrm{A}},\ldots,\sigma_N^{\mathrm{A}};t\right)\\ +\sum_i\left(\sum_{\sigma_i^{\mathrm{A}}\neq\sigma_i^{\mathrm{A}'}} W_i^{\mathrm{A}}\left(\sigma_i^{\mathrm{A}'}\rightarrow\sigma_i^{\mathrm{A}}\right)\right.\\ \left.\times P_1^{\mathrm{A}}\left(\sigma_1^{\mathrm{A}},\sigma_2^{\mathrm{A}},\ldots,\sigma_i^{\mathrm{A}'},\ldots,\sigma_{\mathrm{N}}^{\mathrm{A}};t\right)\right)\end{aligned} \tag{2}$$

Since the system is in contact with a heat bath at absolute temperature ($T_{\mathrm{A}}$), each spin can change from the value $\sigma_i^{\mathrm{A}}$ to $\sigma_i^{\mathrm{A}'}$ with the probability per unit time by the Boltzmann constant

$$W_i^{\mathrm{A}}\left(\sigma_i^{\mathrm{A}}\rightarrow\sigma_i^{\mathrm{A}'}\right) = \frac{1}{\tau}\frac{\exp\left(-\beta\Delta E\left(\sigma_i^{\mathrm{A}}\rightarrow\sigma_i^{\mathrm{A}'}\right)\right)}{\sum\limits_{\sigma_i^{\mathrm{A}'}}\exp\left(-\beta\Delta E\left(\sigma_i^{\mathrm{A}}\rightarrow\sigma_i^{\mathrm{A}'}\right)\right)} \tag{3}$$

where $\beta = 1/k_{\mathrm{B}}T_{\mathrm{A}}$ ($k_{\mathrm{B}}$ being the Boltzmann factor, the sum ranges the four possible values of $\sigma_i^{\mathrm{A}\prime} = \pm 3/2,\ \pm 1/2$) and

$$\begin{aligned}\Delta E_i^{\mathrm{A}}\left(\sigma_i^{\mathrm{A}}\rightarrow\sigma_i^{\mathrm{A}'}\right) = -\left(\sigma_i^{\mathrm{A}'}-\sigma_i^{\mathrm{A}}\right)\\ \times\left(J_1\sum_{j'}\sigma_{j'}^{\mathrm{B}}+J_3\sum_i S_{i'}^{\mathrm{A}}+H\right)\\ -\left(\left(\sigma_i^{\mathrm{A}'}\right)^2-\left(\sigma_i^{\mathrm{A}}\right)^2\right)D_{\mathrm{A}}\end{aligned} \tag{4}$$

is the change in the energy of the system when the $\sigma_i$-spin changes. The probabilities satisfy the detailed balance condition. Using (1)–(4), we obtain the dynamic equation for $m_1^{\mathrm{A}}$

$$\begin{aligned}\Omega\frac{d}{d\xi}m_1^{\mathrm{A}} = -m_1^{\mathrm{A}}\\ +\frac{3\exp\left(\frac{4d_{\mathrm{A}}}{T}\right)\sin h\left[\frac{3}{2T}\left(zm_1^{\mathrm{B}}+\frac{J_3}{J_1}m_2^{\mathrm{A}}+h\cos\xi\right)\right]+\exp\left(-\frac{d_{\mathrm{A}}}{T}\right)\sin h\left[\frac{1}{2T}\left(zm_1^{\mathrm{B}}+\frac{J_3}{J_1}m_2^{\mathrm{A}}+h\cos\xi\right)\right]}{2\exp\left(\frac{d_{\mathrm{A}}}{T}\right)\cos h\left[-\frac{3}{2T}\left(zm_1^{\mathrm{B}}+\frac{J_3}{J_1}m_2^{\mathrm{A}}+h\cos\xi\right)\right]+2\exp\left(-\frac{d_{\mathrm{A}}}{T}\right)\cos h\left[\frac{1}{2T}\left(zm_1^{\mathrm{B}}+\frac{J_3}{J_1}m_2^{\mathrm{A}}+h\cos\xi\right)\right]}\end{aligned} \tag{5}$$

where $\xi = wt$, $T = (\beta J_1)^{-1}$, $h = H_0/J_1$, $d_{\mathrm{A}} = D_{\mathrm{A}}/J_1$ and $\Omega = \tau w$. We fixed $z = 4$ and $w = 2\pi v$.

The other mean field dynamical equations for $m_1^{\mathrm{B}}$, $m_2^{\mathrm{A}}$ and $m_2^{\mathrm{B}}$ can be similarly calculated and obtained as

$$\begin{aligned}\Omega\frac{d}{d\xi}m_1^{\mathrm{B}} = -m_1^{\mathrm{B}}\\ +\frac{3\exp\left(\frac{d_{\mathrm{B}}}{T}\right)\sin h\left[\frac{3}{2T}\left(zm_1^{\mathrm{B}}+\frac{J_3}{J_1}m_2^{\mathrm{B}}+h\cos\xi\right)\right]+\exp\left(-\frac{d_{\mathrm{B}}}{T}\right)\sin h\left[\frac{1}{2T}\left(zm_1^{\mathrm{A}}+\frac{J_3}{J_1}m_2^{\mathrm{B}}+h\cos\xi\right)\right]}{2\exp\left(\frac{d_{\mathrm{B}}}{T}\right)\cos h\left[-\frac{3}{2T}\left(zm_1^{\mathrm{A}}+\frac{J_3}{J_1}m_2^{\mathrm{B}}+h\cos\xi\right)\right]+2\exp\left(-\frac{d_{\mathrm{B}}}{T}\right)\cos h\left[\frac{1}{2T}\left(zm_1^{\mathrm{A}}+\frac{J_3}{J_1}m_2^{\mathrm{B}}+h\cos\xi\right)\right]}\end{aligned} \tag{6}$$

$$\begin{aligned}\Omega\frac{d}{d\xi}m_2^{\mathrm{A}} = -m_2^{\mathrm{A}}\\ +\frac{2\exp\left(\frac{4d_{\mathrm{A}}}{T}\right)\sin h\left[\frac{2}{T}\left(\frac{J_2}{J_1}zm_2^{\mathrm{B}}+\frac{J_3}{J_1}m_1^{\mathrm{A}}+h\cos\xi\right)\right]+\exp\left(\frac{d_{\mathrm{A}}}{T}\right)\sin h\left[\frac{1}{T}\left(\frac{J_2}{J_1}zm_2^{\mathrm{B}}+\frac{J_3}{J_1}m_1^{\mathrm{A}}+h\cos\xi\right)\right]}{\exp\left(\frac{4d_{\mathrm{A}}}{T}\right)\cos h\left[\frac{2}{T}\left(\frac{J_2}{J_1}zm_2^{\mathrm{B}}+\frac{J_3}{J_1}m_1^{\mathrm{A}}+h\cos\xi\right)\right]+\exp\left(\frac{d_{\mathrm{A}}}{T}\right)\cos h\left[\frac{1}{T}\left(\frac{J_2}{J_1}zm_2^{\mathrm{B}}+\frac{J_3}{J_1}m_1^{\mathrm{A}}+h\cos\xi\right)\right]+1/2}\end{aligned} \tag{7}$$

$$\begin{aligned}\Omega\frac{d}{d\xi}m_2^{\mathrm{B}} = -m_2^{\mathrm{B}}\\ +\frac{2\exp\left(\frac{4d_{\mathrm{B}}}{T}\right)\sin h\left[\frac{2}{T}\left(\frac{J_2}{J_1}zm_2^{\mathrm{A}}+\frac{J_3}{J_1}m_1^{\mathrm{B}}+h\cos\xi\right)\right]+\exp\left(\frac{d_{\mathrm{B}}}{T}\right)\sinh\left[\frac{1}{T}\left(\frac{J_2}{J_1}zm_2^{\mathrm{A}}+\frac{J_3}{J_1}m_1^{\mathrm{B}}+h\cos\xi\right)\right]}{\exp\left(\frac{4d_{\mathrm{B}}}{T}\right)\cos h\left[\frac{2}{T}\left(\frac{J_2}{J_1}zm_2^{\mathrm{A}}+\frac{J_3}{J_1}m_1^{\mathrm{B}}+h\cos\xi\right)\right]+\exp\left(\frac{d_{\mathrm{B}}}{T}\right)\cos h\left[\frac{1}{T}\left(\frac{J_2}{J_1}zm_2^{\mathrm{A}}+\frac{J_3}{J_1}m_1^{\mathrm{B}}+h\cos\xi\right)\right]+1/2}\end{aligned} \tag{8}$$

where $d_B = D_B/J_1$.

Now, we will define the dynamic hysteresis loop area to investigate the DMH behaviors and it is defined as

$$A = -\oint m_{1,2}^{A,B}(t)\,dh = -h_0 w \oint m_{1,2}^{A,B}(t)\cos(wt)dt \quad (9)$$

On the other hand, the total magnetization is defined as

$$m_T \equiv \left(m_1^A + m_1^B + m_2^A + m_2^B\right)/4 \quad (10)$$

Solution of results and discussions will be given in Section 3. In numerical calculations, since we fixed $J_1 = |1|$, $d_A = D_A$ and $d_B = D_B$.

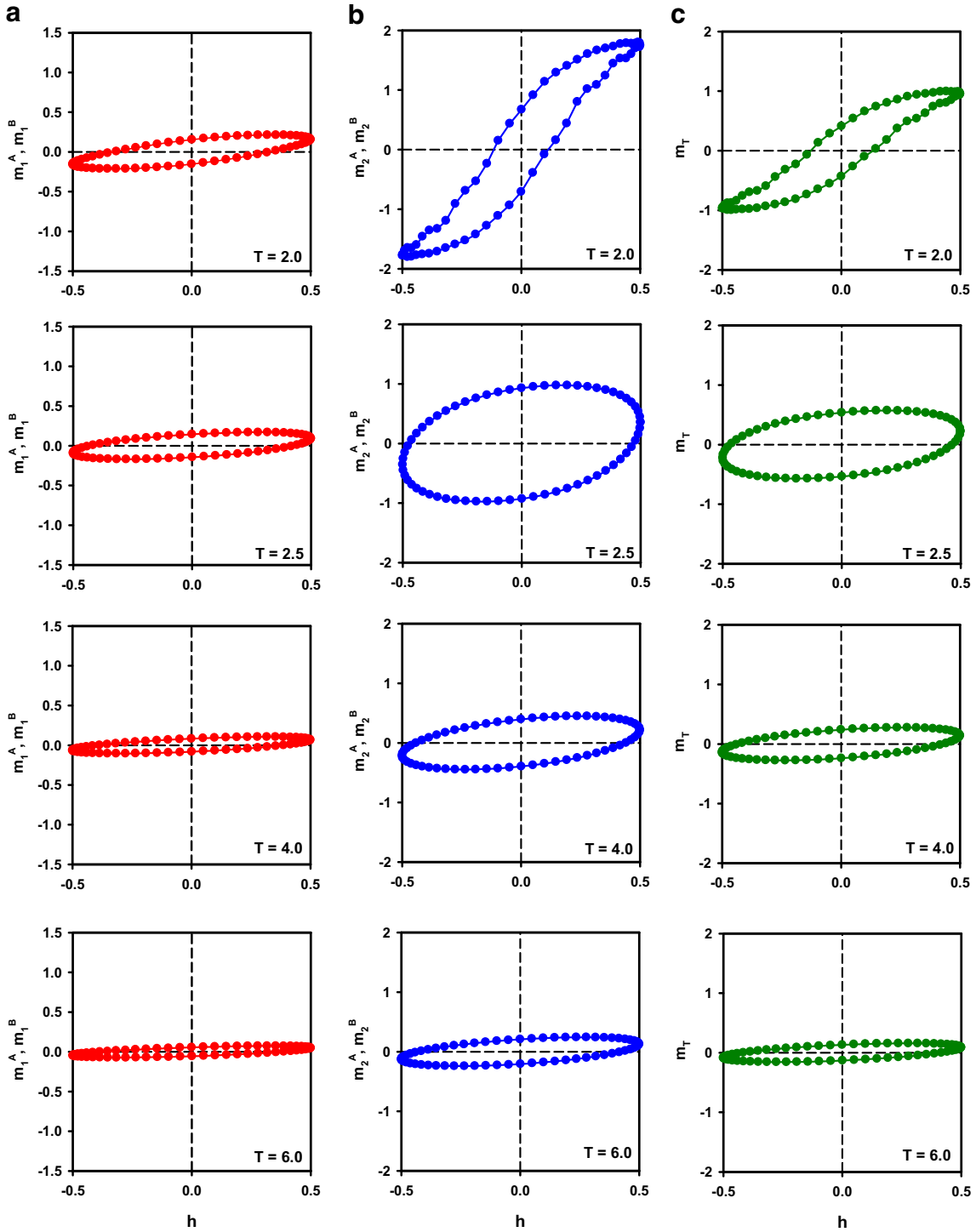


**Fig. 2** **a** For $m_1A$, $m_1B$; (**b**) for $m_2A$, $m_2B$ and (**c**) for $m_T$. The DMH behaviors at different reduced temperatures for $w = 0.11\pi$, $J_1 = -1$, $J_2 = 0.1$, $J_3 = 0.5$ and $d_A = d_B = 1$ at $T = 2$, 2.5, 4 and 6

## 3 Results and Discussions

We numerically solve (9) and (10) and present the DMH behaviors (Figs. 2, 3, 4, 5 and 6) as well as the dynamic coercivity field and remanent magnetization behaviors (Figs. 7 and 9). We should have mentioned that if the loop area is wide and big, which corresponds to hard magnet, it is desirable for permanent magnets, magnetic recording and memory devices. If the loop area is thinner and narrower that corresponds to soft magnet, it is useful for transformer

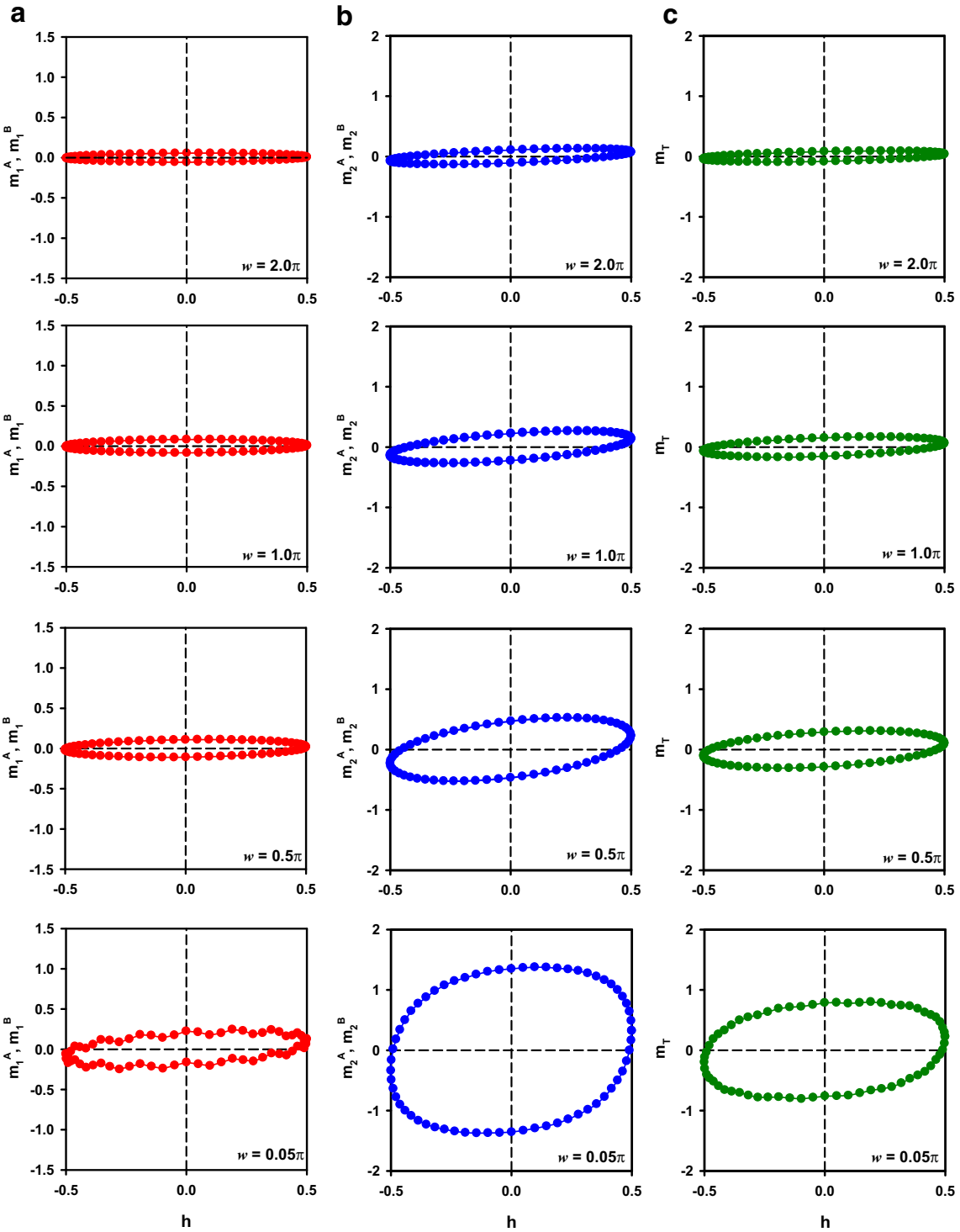


**Fig. 3** **a** For $m_1A$, $m_1B$; (**b**) for $m_2A$, $m_2B$ and (**c**) for $m_T$. The DMH behaviors for different angular frequencies for $J_1 = -1$, $J_2 = 0.1$, $J_3 = 0.5$ and $d_A = d_B = 1$ at $T = 1.95$

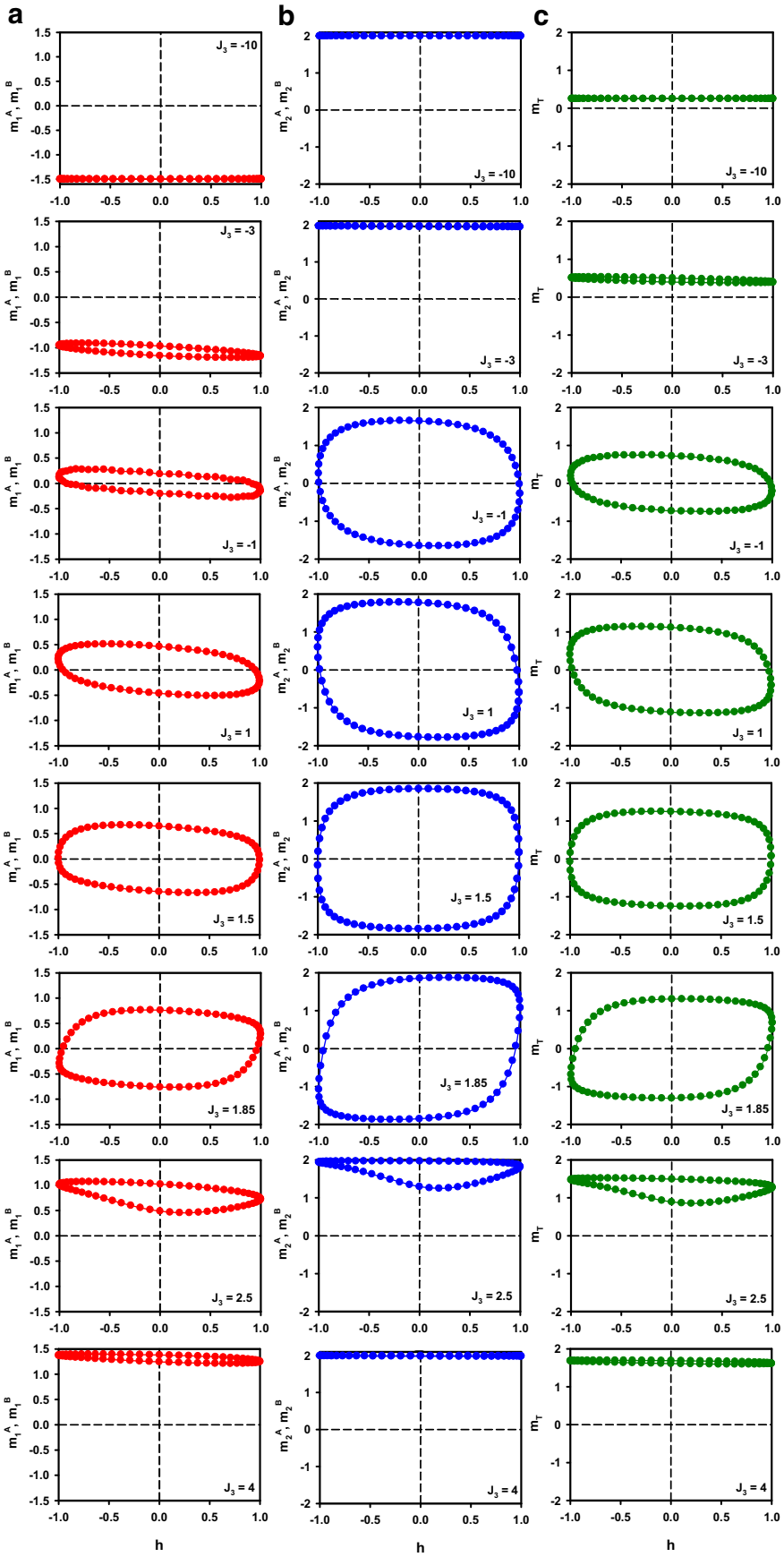


**Fig. 4** **a** For $m_1A$, $m_1B$; (**b**) for $m_2A$, $m_2B$ and (**c**) for $m_T$. The DMH behaviors for different values of the interlayer coupling constant for $w = 0.11\pi$, $J_1 = -1$, $J_2 = 0.1$ and $d_A = d_B = 1$ at $T = 1.95$

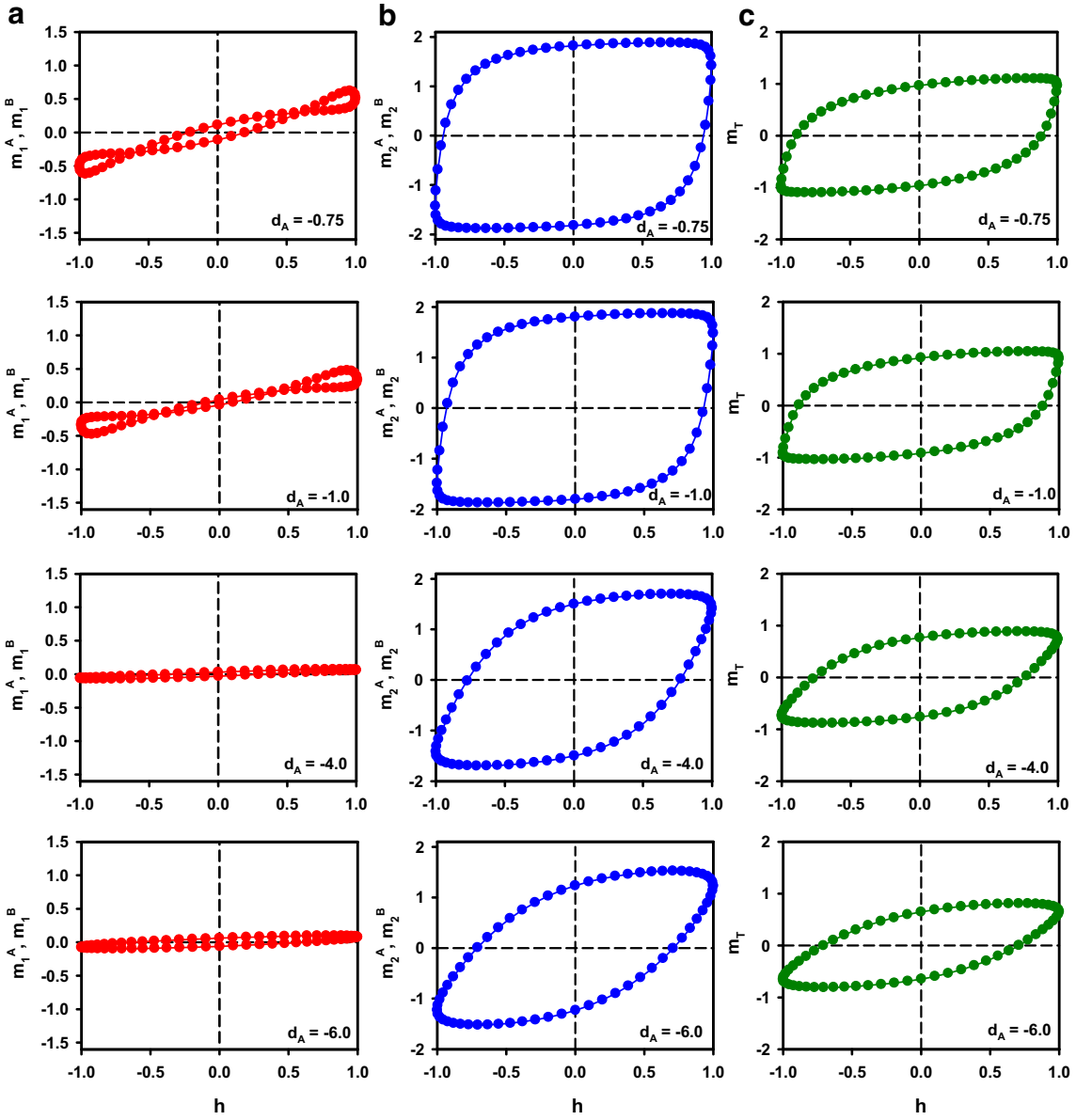


**Fig. 5** **a** For $m_1A$, $m_1B$; (**b**) for $m_2A$, $m_2B$ and (**c**) for $m_T$. The DMH behaviors for different crystal field values of $d_A$ for $w = 0.04\pi$, $J_1 = -0.3$, $J_2 = 0.1$, $J_3 = 1$, $h = 1$, $T = 2$ and $d_B = 1$

and motor cores to minimize the energy dissipation with the alternating fields associated with AC applications. On the other hand, the high coercivities correspond to the magnetically hard materials and low coercivities to the magnetically soft ones.

Figure 2 illustrates DMHs for $w = 0.11\pi$, $J_1 = -1$, $J_2 = 0.1$, $J_3 = 0.5$ and $d_A = d_B = 1$ at $T = 2$, 2.5, 4 and 6 for the submagnetizations and total magnetization. From this figure, one can see that the dynamic magnetic hysteresis loop areas increase as the temperature increases at a certain temperature and then loop areas decrease with increasing temperature that is in a good, quantitatively, agreement with some theoretical results [32, 33, 36, 37, 39, 42, 43]. For very small values of temperatures, the areas of loops are very small and, as the temperatures increase, the areas of loops also increase until the critical temperature is reached. Then, areas of loops become smaller as temperatures increase; finally, the loops disappeared for very high values of temperatures, namely much bigger than $T_c$. One should also mention that at $T_c$, the system undergoes from the ordered (paramagnetic) phase to the disordered (ferrimagnetic) phase. Therefore, the areas of loops are large for the temperature below and above $T_c$, and as the temperature moves away from the $T_c$ (either becomes larger or smaller), the areas of loops turn to smaller and eventually vanished. The physical reason why the area of hysteresis loop at first increases and then decreases in Fig. 2 may be as follows: since $J_1$ is negative, the spin configuration in the $L_1$ plane

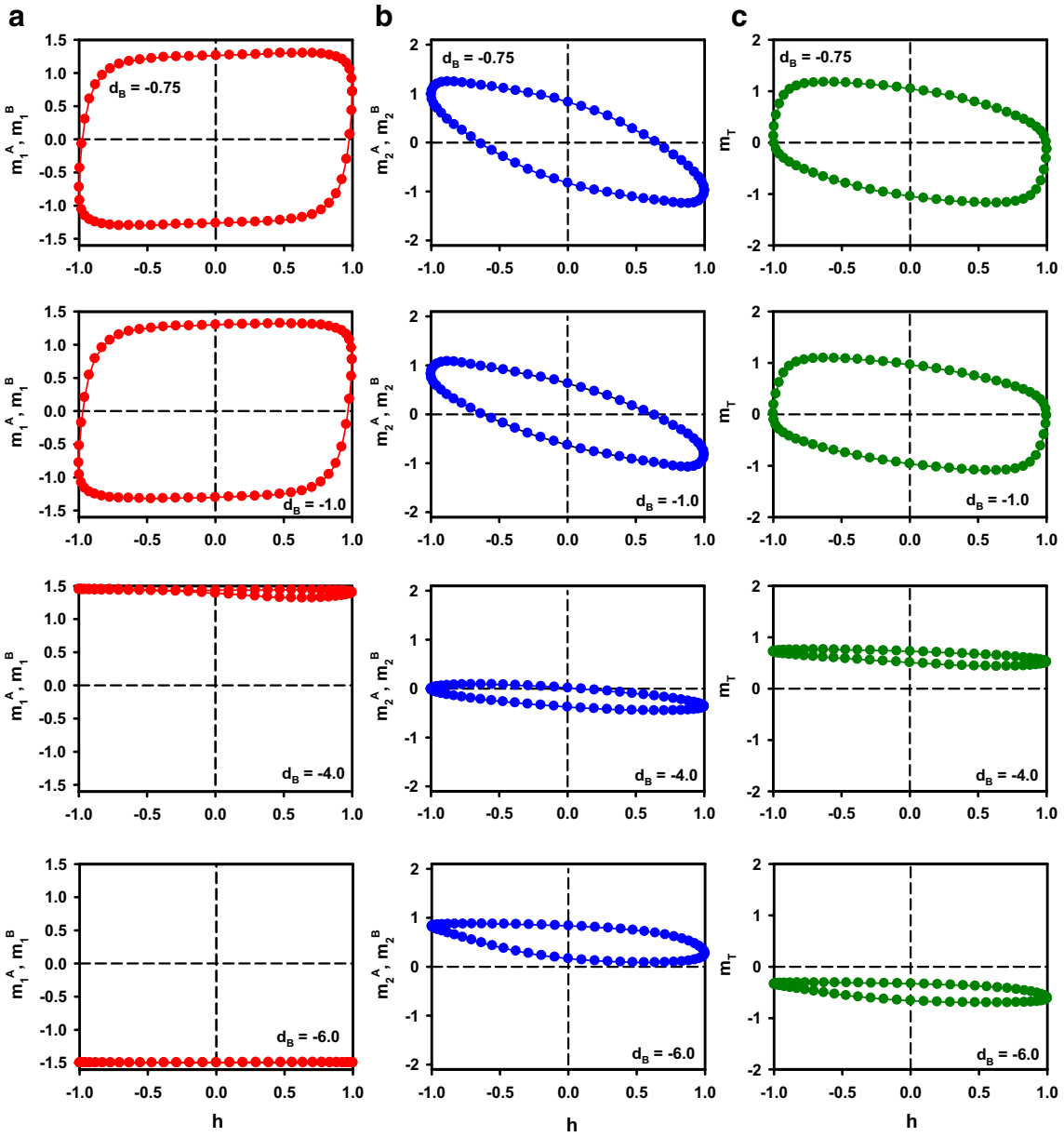


**Fig. 6** The same as Fig. 5, but different crystal field values of $d_B$ and $d_A = 1$

must be antiferromagnetic, and since $J_3$ is positive, the spin configuration in the $L_2$ plane must be ferrimagnetic, so that at the ground state, the spin configuration in both $L_1$ and $L_2$ layers must be frustrated. Because of this fact, at the ground state, both magnetizations in each layer must be very small. However, with the increase of $T$, the frustration of spin configurations in each layer is released due to the thermal agitation. The total magnetization must, at first, increase from the saturation magnetization at $T = 0.0$ K. However, because the thermal agitation becomes strong at a finite temperature, the total magnetization must decrease with the increase of $T$ and reduces to zero at its transition temperature. In other words, roughly saying, the area of hysteresis loop is proportional to the magnitude of total magnetization, so that the area of hysteresis loop at first increase and then, at a finite temperature, it starts to decrease and reduces to zero at its transition temperature. Although this explanation is completely for the static case, it will be also satisfied for the present dynamic case. This fact can be seen very clearly in Figs. 2 and 3 in Ref. [39]. We also mention that, in general, the physical origins of hysteresis loop areas are due to the following factors that affect the domain structure: (1) the exchange interaction that is the spin-spin interactions, favoring long-range ordering over macroscopic distances and the most important interaction between atomic magnetic moments; (2) magnetocrystalline

anisotropy that defines preferred directions in the lattice along which the magnetization can lie and also refers to the directional dependence exhibited in measurements of magnetic properties. Moreover, it is due to interactions with lattice. (3) The magnetostatic energy is the self-energy of a magnetic body, and it leads to anisotropy and formation of domains. It prefers zero magnetization or zero total moment on average. The more information about the physical origins of hysteresis loop areas can be found in Ref. [65]. Moreover, larger loops correspond to hard magnets that are desirable for permanent magnets, magnetic recording and memory devices and thinner loops are useful for transformer and motor cores to minimize the energy dissipation with the alternating fields associated with AC applications. We should also mention that in increasing the DMH loops, the area with decreasing temperatures has been experimentally reported for thin Co films on Cu(001) [6] and bulk ferromagnet $Co_7(TeO_3)_4Br_6$. Figure 3 is obtained for $J_1 = -1$, $J_2 = 0.1$, $J_3 = 0.5$, $d_A = d_B = 1$, $T = 1.95$ and various values of $w$, namely $w = 2\pi$, $w = 1\pi$, $w = 0.5\pi$ and $w = 0.05\pi$; hence, we investigate the effects of the frequencies on DMH behaviors. The results display that as the frequency is increased, the area of hysteresis loops is also increased. The results are also quantitatively in good agreement with some theoretical results [23, 24, 42, 43, 48] and the experimental reports for thin Co films on Cu(001) [6], ultrathin epitaxial Fe/GaAs(001) [9] and Fe thin films [14]. Figure 4 displays behaviors of the DMHs for $w = 0.11\pi$, $J_1 = -1$, $J_2 = 0.1$, $d_A = d_B = 1$, $T = 1.95$ and different values of $J_3$, i.e. $J_3 = -1.0, -3, -1, 1, 1.5, 1.85, 2.5$ and 4. In here, it should be mentioned that $J_3$ corresponds to the thickness of layers in experimental works. For $J_3 < 0$, the area of hysteresis loops is increasing with the decreasing negative values of $J_3$, but for $J_3 > 0$, the area of hysteresis

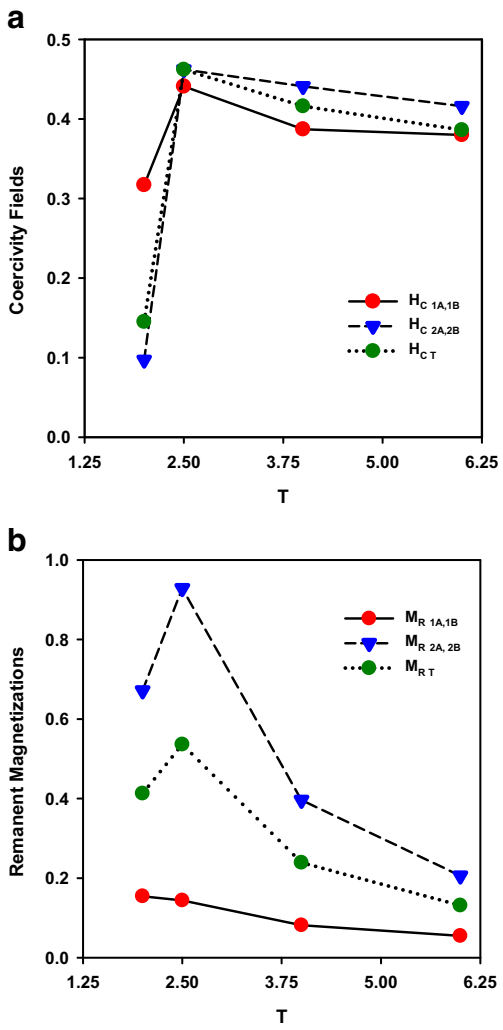


**Fig. 7** **a** The coercivity fields. **b** The remanent magnetizations, versus the reduced temperature for the same parameters as in Fig. 2

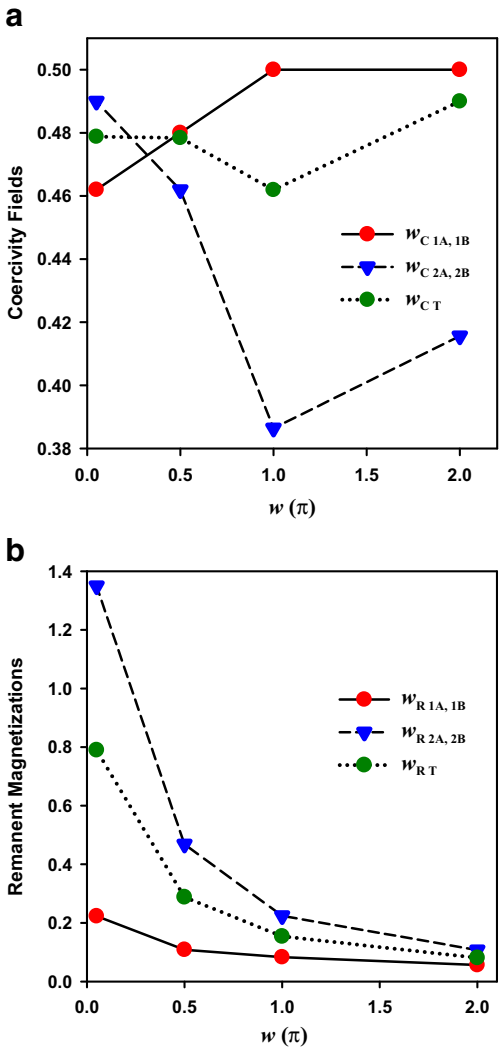


**Fig. 8** The same as Fig. 7, but versus the angular frequency for the same parameters as in Fig. 3

loops is decreasing with the increasing values of $J_3$; the area of hysteresis loops is decreasing with the increasing values of $J_3$ at a certain value of $J_3$ and then starting to decrease. Figures 5 and 6 show the influence of the crystal-field interactions on the DMH properties for $d_A$ and $d_B$, respectively. Figure 5 is presented for $w = 0.04\pi$, $J_1 = -1$, $J_2 = 0.1$, $J_3 = 0.5$, $T = 2$ and $d_B = 1$ for the different values of $d_A$ that are $-0.75$, $-1.0$, $-4.0$ and $-6.0$. The DMH loops increase with increasing values of $d_A$. Moreover, at low negative values of $d_A$, triple loops have been observed for $m_1^A$ and $m_1^B$. Figure 6 displays for $w = 0.04\pi$, $J_1 = -1$, $J_2 = 0.1$, $J_3 = 0.5$, $T = 2$ and $d_A = 1$ for different values of $d_B$, namely $d_B = -0.75$, $-1.0$, $-4.0$ and $-6.0$. The topology of Fig. 6 is similar to that of Fig. 5, except the triple loops are not observed: $m_1^A$ and $m_1^B$.

Finally, Fig. 7 shows the coercivity fields and remanent magnetizations versus the reduced temperature and it illustrates that if the temperature is increased, the coercivity also increases up to certain values of temperature and, with a further increase of temperature, the coercivity decreases very smoothly. The remanent magnetization also displays similar behaviors, except the $m_1^A$ and $m_1^B$ decrease smoothly with the temperature. Figures 8 and 9 illustrate the variation of the coercivities and remanent magnetizations with the frequency and the interlayer coupling constant ($J_3$), respectively.

In conclusion, we investigate the DMH loop behaviors at different reduced temperatures, frequencies, interlayer coupling constants and crystal-field interactions. We also investigate the variation of the coercive field and remanent magnetization with the reduced temperature and the interlayer coupling constant. We observe that our results are in good agreement with some theoretical and experimental results. We hope that this work gives some light into theoretical and experimental research for investigation of the DMH behaviors. We also hope our results could shed light on the development of magnetic device application, in particular developing memory storage devices and high-frequency device applications.

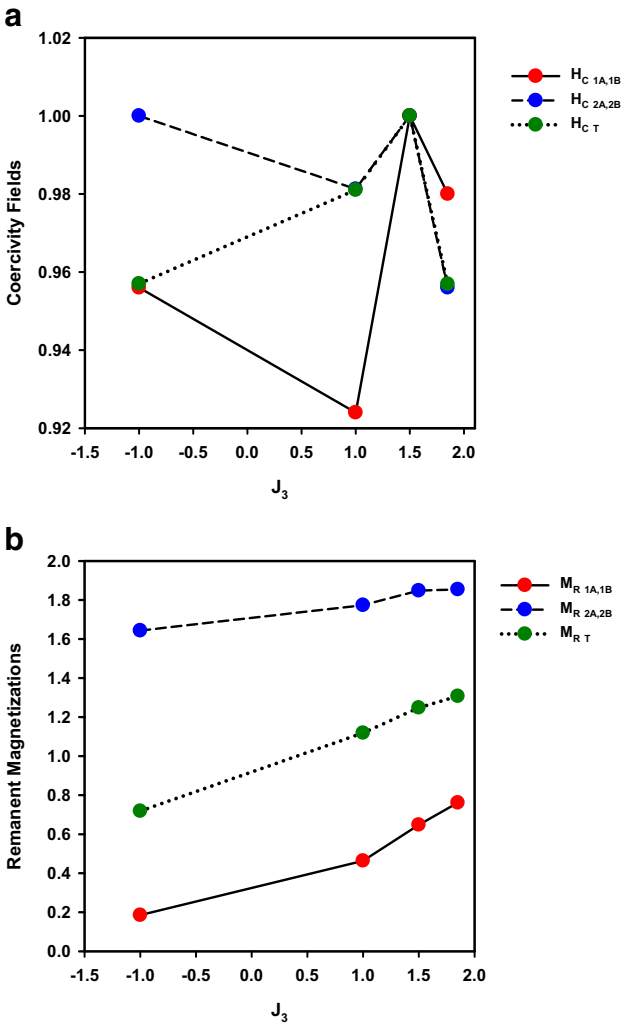


**Fig. 9** The same as Fig. 7, but versus the interlayer coupling constant for the same parameters as in Fig. 4

**Acknowledgments** This work was supported by the Erciyes University Research Fund (Grant No. FBA-2016-6324).

## References

1. Zhu, Z., Sun, Y., Zhang, Q., Liu, J.M.: Phys. Rev. B **76**, 014439 (2007)
2. Bertotti, G.: Hysteresis in magnetism. Academic, San Diego (1998)
3. Chakrabarti, K., Acharyya, M.: Rev. Mod. Phys. **71**, 847 (1999)
4. Moore, T.A., Bland, J.A.C.: J. Phys. Condens. Matter. **16**, R1369 (2004)
5. Jiang, Q., Yang, H.N., Wang, G.C.: Phys. Rev. B **52**, 14911 (1995)
6. Suen, J.S., Lee, M.H., Teeter, G., Eskine, J.L.: Phys. Rev. B **59**, 4249 (1999)
7. Lee, W.Y., Samed, A., Moore, T.A., Bland, J.A.C., Choi, B.C.: J. Appl. Phys. **87**, 6600 (2000)
8. Moore, T.A., Rothman, J., Xu, Y.B., Bland, J.A.C.: J. Appl. Phys. **89**, 7018 (2001)
9. Moore, T.A., Wastlbauer, G., Blanda, J.A.C., Cambril, E., Natali, M., Decanini, D., Chen, Y.: J. Appl. Phys. **93**, 8746 (2003)
10. Nistor, C., Faraggi, E., Erskine, J.L.: Phys. Rev. B **72**, 014404 (2005)
11. Moore, T.A., Hayward, T.J., Tse, D.H.Y., Bland, J.A.C., Castano, F.J., Ross, C.A.: J. Appl. Phys. **97**, 063910 (2005)
12. Robb, D.T., Xu, Y.H., Hellwig, O., McCord, J., Berger, A., Novotny, M.A., Rikvold, P.A.: Phys. Rev. B **78**, 134422 (2008)
13. Steinke, N.J., Moore, T.A., Mansell, R., Bland, J.A.C., Barnes, C.H.W.: Rev. B **86**, 184434 (2012)
14. Suen, J.S., Eskine, J.L.: Phys. Rev. Lett. **18**, 3567 (1997)
15. Cao, Y., Xu, K., Jiang, W., Droubay, T., Ramuhalli, P., Edwards, D., Johnson, B.R., McCloy, J.: J. Magn. Magn. Mater. **395**, 361 (2015)
16. Prester, M., Živkovic, I., Drobac D., Surija, V., Pajic, D., Berger, H.: Phys. Rev. B **84**, 064441 (2011)
17. Kuang, D., Tang, P., Yang, S., Zhang, Y.: J. Magn. Magn. Mater. **397**, 33 (2016)

18. Dos Reis, D.C., Franca, E.L.T., De Paula, V.G., Dos Santos, A.O., Coelho, A.A., Cardoso, L.P., Da Silva, L.M.: J. Magn. Magn. Mater. **424**, 84 (2017)
19. Acharyya, M.: Phys. Rev. E **58**, 1798 (1998)
20. Sides, S.W., Rikvold, P.A., Novonty, M.A.: Phys. Rev. E **59**, 271 (1999)
21. Acharyya, M.: Nonequilibrium phase transitions in model ferromagnets: A review. Int. J. Modern Phys. C **16**, 1631–1635 (2005)
22. Sun, M.Y., Chen, X., Dong, S., Wang, K.F., Liu, J.-M.: J. Magn. Magn. Mater. **321**, 2429 (2009)
23. Punya, A., Yimnirum, R., Laoratanakul, P., Laosiritaworn, Y.: Phys. B **405**, 3482 (2010)
24. Wang, L., Teng, B.H., Rong, Y.H., Lu, Y., Wang, Z.C.: Solid State Commun. **152**, 1641 (2012)
25. Yüksel, Y.: Phys. Lett. A **377**, 2494 (2013)
26. Deviren, B., Şener, Y., Keskin, M.: Phys. A **392**, 3969 (2013)
27. Aktaş, B.O., Aknc, Ü., Polat, H.: Phys. Rev. E **90**, 012129 (2014)
28. Ertaş, M., Kantar, E., Kocakaplan, Y., Keskin, M.: Phys. A **444**, 732 (2015)
29. Kantar, E.: J. Supercond. Nov. Magn. **28**, 3387 (2015)
30. Yüksel, Y.: J. Magn. Magn. Matter. **389**, 34 (2015)
31. Vatansever, E., Polat, H.: Thin Films **589**, 789–782 (2015)
32. Deviren, B., Keskin, M.: J. Magn. Magn. Mater. **324**, 1051 (2012)
33. Ertaş, M., Keskin, M.: Int. J. Adv. Sci. Eng. Technol. **3**, 41 (2015)
34. Kantar, E., Ertaş, M.: J. Supercond. Nov. Magn. **28**, 2529 (2015)
35. Bukharov, A.A., Ovcihinnikov, A.S., Baranov, N.V., Inoue, K.: Eur. Phys. J. B **70**, 369 (2009)
36. Ertaş, M., Keskin, M., Deviren, B.: J. Stat. Phys. **146**, 1244–1262 (2012)
37. Ertaş, M., Keskin, M.: Phy. Lett. A **379**, 1576 (2015)
38. Ertaş, M.: Superlattice. Microtuructures **85**, 734 (2015)
39. Bat, M., Ertaş, M.: Phys. B **513**, 40 (2017)
40. Cerruti, B., Zapperi, S.: Phys. Rev. B **75**, 064416 (2007)
41. Carrey, J., Mehdaoui, B., Respaund, M.: J. Appl. Phys. **109**, 08392 (2011)
42. Landi, G.T., Santos, A.D.: J. Appl. Phys. **111**, 07D121 (2012)
43. Landi, G.T.: J. Magn. Magn. Mater. **324**, 466 (2012)
44. El Mrabti, H., Dejardin, P.M., Titov, S.V., Kalmykov, Y.P.: Phys. Rev. B **85**, 094425 (2012)
45. Ourai, B., Titov, S.V., El Mrabti, H., Kalmykov, Y.P.: J. Appl. Phys. **113**, 053903 (2013)
46. Dimitrov, D., Veysin, G.M.: Phys. Rev. B **50**, 3077 (1994)
47. Hu, R., Soh, A.K., Zheng, G.P., Ni, Y.: J. Magn. Magn. Mater. **301**, 458 (2006)
48. Zhu, Z., Sun, Y., Zhang, Q., Liu, J.M.: Phys. Rev. B **76**, 014439 (2007)
49. Poperechny, I.S., Raikher, Y.L., Stepanov, V.I.: Phys. B **435**, 58 (2014)
50. de la Barriere, O., Ragusa, C., Appino, C., Fiorilo, F., LoBue, M., Mazaleyrat, F.: Phys. B **435**, 80 (2014)
51. Hashimoto, K., Ohkoshi, S.: Philos. Trans. R. Soc. Lond. A **357**, 2977 (1999)
52. Bobak, A., Dely, J.: J. Magn. Magn. Mater. **310**, 1419 (2007)
53. Miao, H., Wei, G., Geng, J.: J. Magn. Magn. Mater. **321**, 4139 (2009)
54. Wei, G., Miao, H.: Commun. Theor. Phys. **51**, 756 (2009)
55. Abubrig, F.: World J. Condens. Matter Phys. **3**, 111 (2013)
56. Deviren, B., Kantar, E., Keskin, M.: J. Korean Phys. Soc. **56**, 1738 (2010)
57. Deviren, B., Polat, Y., Keskin, M.: Chin. Phys. B **20**, 060507 (2011)
58. Jabar, A., Belhaj, A., Labrim, H., Bahmad, L., Hassanain, N.: J. Supercond. Nov. Magn. **28**, 2721 (2015)
59. Jabar, A., Belhaj, A., Labrim, H., Bahmad, L., Hassanain, N., Benyoussef, A.: Superlattice. Microstructures **78**, 171 (2015)
60. Albayrak, E.: Phys. B **391**, 47 (2007)
61. Karimou, M., Yessoufou, R., Hontinfinde, F.: World J. Condens. Matter Phys. **5**, 187 (2015)
62. Keskin, M., Polat, Y.: J. Magn. Magn. Mater. **321**, 3905 (2009)
63. Temizer, Ü., Tülek, M., Yarar, S.: Phys. A **415**, 156–171 (2014)
64. Keskin, M., Koçak, Y. Phase transitions (submitted)
65. Mitchler, P.D.: Characterization of hysteresis in magnetic systems: A Preisach approach. Ph.D Thesis, Department of Physics and Astronomy, University of Manitoba, Winnipeg, Manitoba (2000)

**EK-7**

# Sixth Bozok Science Workshop

**Studies from Nuclei to Nanomaterials with Applications**

**(Altıncı Bozok Bilim Çalıştayı: Çekirdekten Nanomalzemelere Araştırmalar ile Uygulamaları)**

**23-25 August 2017 / 23-25 Ağustos 2017**

**Yozgat, Turkey**

---

02.08.2017

**Sayın, Prof. Dr. Mustafa KESKIN**

Bozok Üniversitesi bünyesinde 23 – 25 Ağustos 2017 tarihlerinde düzenlenecek olan "Altıncı Bozok Bilim Çalıştayı: Çekirdekten Nanomalzemelere Araştırmalar ile Uygulamaları – BBÇ2017 (Sixth Bozok Science Workshop: Studies from Nuclei to Nanomaterials with Applications – BSW2017)" isimli toplantıya çalışmalarınızı sunmak üzere gönderdiğiniz "DYNAMIC MAGNETIC HYSTERESIS BEHAVIORS IN A MIXED SPIN (3/2, 2) BILAYER SYSTEM WITH DIFFERENT CRYSTAL-FIELD INTERACTIONS" başlıklı özetiniz sözlü sunum olarak kabul edilmiştir. Toplantıda görüşmek ümidiyle, katkı ve katılımlarınızdan dolayı teşekkür ederim.

Saygılarımla,

Prof. Dr. Mustafa BÖYÜKATA
Çalıştay Başkanı

---

**Bilgi için:** bsw.bozok.edu.tr, **e-posta:** bsw@bozok.edu.tr, **Tel:** 0-354-2421021, **Faks:** 0-354-2421022

**Abstract: Bozok Science Workshop 2017, Yozgat, August 23-25, 2017**

# DYNAMIC MAGNETIC HYSTERESIS BEHAVIORS IN A MIXED SPIN (3/2, 2) BILAYER SYSTEM WITH DIFFERENT CRYSTAL-FIELD INTERACTIONS

**Mustafa Keskin[1] *, Mehmet Ertaş[1]**

[1] *Department of Physics, Erciyes University, 38039 Kayseri, Turkey*
*keskin@erciyes.edu.tr; mehmetertas@erciyes.edu.tr*

**Abstract:** We investigate the dynamic magnetic hysteresis loop behaviors of the mixed spin-3/2 and spin-2 Ising model with different crystal-field interactions under a time-varying magnetic field on a two-layer square lattice within the framework of dynamic mean-field calculations based on the Glauber–type stochastic dynamics. The dynamic magnetic hysteresis loops are obtained for different reduced temperatures (T), magnetic field amplitudes (h), frequencies (*w*) and interlayer coupling constants ($J_3$). Influences of the T, h, w and $J_3$ on the dynamic magnetic hysteresis loop properties are investigated. We also study the temperature, frequency and interlayer coupling interaction dependence of the coercive field and remanent magnetization. We compare our results with some theoretical and experimental works and observe a quantitatively good agreement with some theoretical and experimental results.

**This work was supported by Erciyes University Research Fund, Grant No: FBA- 2016-6324.**

**Keywords:** Mixed spin (3/2, 2) bilayer system, dynamic magnetic hysteresis, coercive field, remanent magnetization, Glauber-type stochastic dynamics, mean-field theory

* ***Corresponding author****; e-mail: keskin@erciyes.edu.tr, phone:90(352)2076660 -33105, fax:90(352)4374931*

EK-8

# Manuscript Details

| | |
|---|---|
| **Manuscript number** | MAGMA_2017_2169 |
| **Title** | Dynamic magnetic properties of the Ising bilayer system consisting of spin-3/2 and spin-5/2 atoms with a crystal-field interaction in an oscillating field |
| **Article type** | Full Length Article |


**Abstract**

Dynamic magnetic properties of the Ising bilayer system consisting of the mixed spin (3/2, 5/2) atoms with a crystal-field interaction in an oscillating field on a two-layer square lattice is studied by the use of dynamic mean-field theory based on the Glauber–type stochastic. Dynamic phase transition temperatures are obtained and dynamic phase diagrams are presented in three different planes. The frequency dependence of dynamic hysteresis loops are also investigated in detail. We compare the results with some available theoretical and experimental works and observe a quantitatively good agreement with some theoretical and experimental results.



| | |
|---|---|
| **Keywords** | Mixed spin (3/2, 5/2) bilayer system, dynamic phase diagrams, dynamic magnetic hysteresis, Glauber-type stochastic dynamics |



| | |
|---|---|
| **Corresponding Author** | Mustafa Keskin |
| **Corresponding Author's Institution** | Erciyes University |
| **Order of Authors** | Mustafa Keskin, Mehmet Ertaş |
| **Suggested reviewers** | Rachid Masrour, Ersin Kantar, Gloria Buendia, NICOLAS DE LA ESPRIELLA |


## Submission Files Included in this PDF

**File Name [File Type]**

Cover Letter.doc [Cover Letter]

Manuscript.doc [Manuscript File]

Fig. 1.doc [Figure]

Fig. 2.docx [Figure]

Fig. 3.docx [Figure]

Fig. 4.docx [Figure]

Fig. 5.docx [Figure]

Fig. 6.docx [Figure]

To view all the submission files, including those not included in the PDF, click on the manuscript title on your EVISE Homepage, then click 'Download zip file'.

ERCIYES UNIVERSITY
**DEPARTMENT OF PHYSICS**
**38039 KAYSERI-TURKEY**

PHONE: 90 (352) 2076666 Ext: 33105
FAX: 90 (352) 4374931
E-Mail: keskin@erciyes.edu.tr

August 08, 2017

Prof. Dr. S.D. Bader
Materials Science Division
Argonne National Laboratory
IL 60439
USA
Email: jmmm@anl.gov

Dear Prof. Dr. Bader

We hereby respectfully submit a manuscript entitled "**Dynamic magnetic properties of the Ising bilayer system consisting of spin-3/2 and spin-5/2 atoms with a crystal-field interaction in an oscillating field**" by M. Ertaş and myself for publication in **Journal of Magnetism and Magnetic Materials.**

Looking forward to hearing from you soon.

Sincerely yours,

Mustafa Keskin
Professor of Physics

# Dynamic magnetic properties of the Ising bilayer system consisting of spin-3/2 and spin-5/2 atoms with a crystal-field interaction in an oscillating field

**Mustafa Keskin and Mehmet Ertaş**

*Department of Physics, Erciyes University, 38039 Kayseri, Turkey*

## Abstract

Dynamic magnetic properties of the Ising bilayer system consisting of the mixed spin (3/2, 5/2) atoms with a crystal-field interaction in an oscillating field on a two-layer square lattice is studied by the use of dynamic mean-field theory based on the Glauber–type stochastic. Dynamic phase transition temperatures are obtained and dynamic phase diagrams are presented in three different planes. The frequency dependence of dynamic hysteresis loops are also investigated in detail. We compare the results with some available theoretical and experimental works and observe a quantitatively good agreement with some theoretical and experimental results.

*Keywords:* Mixed spin (3/2, 5/2) bilayer system, dynamic phase diagrams, dynamic magnetic hysteresis, Glauber-type stochastic dynamics

## 1. Introduction

The mixed spin systems are the one of the most actively studied topics in theoretical condensed matter physics for about three decades. The reasons are that these systems are mainly related to the potential technological applications in the area of thermomagnetic recording [1] as well as have less translational symmetry than their single spin counterparts; hence exhibit many new critical phenomena that cannot be observed in the single-spin Ising systems. Moreover, they are also the prototypical systems that have been used to investigate bimetallic molecular systems based magnetic materials [2]. The mixed spins (3/2, 5/2) system is the one of the well-known mixed spin Ising systems that have been studied or used a model to examine the magnetic properties of some physical systems. One of the early study of the system was made by Zhang *et al*. [3] who investigated the phase diagram and internal energy of the mixed spins (3/2, 5/2) system on the honeycomb lattice by the effective-field theory (EFT). The exact solution of the system was done by Albayrak and Yigit [4, 5] that they presented the phase diagrams for various coordination numbers. Yessoufou *et al.* [6] studied the mixed spins (3/2, 5/2) Ising model with two possible crystal fields on the two-fold Cayley tree by means of exact recursion relations, and a first- and second-order phase transitions are obtained. De La Espriella and Buendia [7] studied the ground state phase diagrams of the system in detail. Ma and Jiang [8] investigated surface effects on the magnetization and the

phase diagrams of the mixed spins (3/2, 5/2) Ising model on 3D layered honeycomb lattice. De La Espriella and Buendia [9] also studied the magnetic properties, such as thermal magnetizations, compensation temperatures and phase diagrams, of the system on square lattice. Mohamad [10] studied the compensation phenomenon for the mixed spins (3/2, 5/2) Ising ferromagnetic system in presence of external magnetic field. Masrour *et al.* [11] used the mixed spins (3/2, 5/2) Ising system as a model to study the size effect on magnetic properties of a nano-graphane bilayer structure within the Monte Carlo simulations (MCS). Iwashita *et al.* [12] studied magnetizations, the specific heat, the critical temperature and phase diagrams of the Blume-Emery-Griffiths model with S=5/2 and 3/2 on 2D square lattice by the MCS, extensively. De La Espriella Velez *et al.* [13] analyzed the magnetic behavior of Ising model of the mixed spins (3/2, 5/2) on square lattice by the MCS. Reyes *et al.* [14] examined the magnetic properties of a ferromagnetic mixed spins (3/2, 5/2) Ising model by the MCS. Masrour *et al.* [15] have investigated and compared the thermal magnetizations, magnetic susceptibilities of the system on decorated square and triangular lattices by the MCS. Luo *et al.* [16] have applied the MCS to study the internal energy and specific heat of a nano-graphene bilayer with a honeycomb structure using the mixed spins (3/2, 5/2) Ising system. Wang *et al.* [17] investigated the effects system parameters on the magnetization, the susceptibility, the blocking temperature and hysteresis loops of the nano-graphene bilayer with a honeycomb structure which consisting of spin-3/2 and spin-5/2 atoms. The compensation behavior and phase diagram of the mixed spins (2/3, 5/2) Ising ferromagnetic system in graphene layer was studied within the MCS by Alzate-Cardona *et al.* [18]. Very recently, Benhouria *et al.* studied the dielectric properties of the mixed spins (3/2, 5/2) Ising ferrielectric nanowires by use of the MCS. Finally, it is also worth whiling mention that the mixed spins (3/2, 5/2) model comes out to be suitable to the understanding of particular biological compounds, e.g. some experimental studies indicate that the mixed spins (3/2, 5/2) model is behind the unusual magnetic properties of certain types of ferric heme proteins [19-22]. Heme proteins are utilized as a synthetic base to design novel biomaterials with important potential applications in optical communications, and are considered as the base for nanoporous catalytic materials [23], in addition to their important role in oxygen transport by blood. Moreover, the NMR studies demonstrate that the azide complex of iron (III) porphycene is a mixed spins (3/2, 5/2) system [24].

Although considerable advances have been done in understanding the equilibrium magnetic properties of the mixed spins (3/2, 5/2) Ising system, it is necessary and meaningful to investigate the dynamic magnetic properties of the system. As far as we know, only one work

have been done by Deviren and Keskin [25] who studied the dynamic phase transitions and the dynamic compensation temperatures of the system with a crystal-field interaction in an oscillating field on a hexagonal lattice within the dynamic mean-field theory (MFT) based on the Glauber–type stochastic dynamics (GTSD) that has been also called the dynamic mean-field theory (DMFT). Therefore, the aim of the present paper is to investigate dynamic magnetic properties, such as dynamic phase transition, dynamic phase diagrams and dynamic hysteresis loops behavior, of the Ising bilayer system consisting of the mixed spin (3/2, 5/2) atoms with the crystal-field interaction under a time-varying magnetic field on a two-layer square lattice by using the DMFT.

## 2. Mixed bilayer square lattice consisting of spin-3/2 and spin-5/2 atoms

The Ising bilayer model (IBM) on a two-layer square lattice which is an extension of its one-layer version is considered; hence one considers two identical layers (A and B) of square lattices (upper layer) and (lower layer) with different spins with values of $\sigma_i$ (or $\sigma_{i'}$) $\pm 3/2, \pm 1/2$ and with values of $S_j$ (or $S_{j'}$) $\pm 5/2, \pm 3/2, \pm 1/2$, respectively, shown in Fig. 1. The Hamiltonian of the IBM is defined as:

$$= -J_1 \sum_{<i'j'>} \sigma_{i'}\sigma_{j'} - J_2 \sum_{<ij>} S_i S_j - J_3 \left( \sum_{<ii'>} \sigma_{i'} S_i + \sum_{<jj'>} \sigma_{j'} S_j \right) - \left( \sum_{<i'>} \sigma_{i'} + \sum_{<j'>} \sigma_{j'} + \sum_{<i>} S_i + \sum_{<j>} S_j \right) \quad (1)$$
$$- H \left( \sum_{<i'>} \sigma_{i'} + \sum_{<j'>} \sigma_{j'} + \sum_{<i>} S_i + \sum_{<j>} S_j \right),$$

where first and second summations are over all nearest-neighbor sites of each layer, namely, upper and lower layers. $J_1$ and $J_2$ are intralayer bilinear coupling constants and $J_3$ is the interlayer coupling constant over all the adjacent neighboring sites of layers. H is a time-dependent oscillating external magnetic field: $H(t)=H_0 \cos(wt)$, where $H_0$ and $w = 2\pi\nu$ are the amplitude and the angular frequency of the oscillating field, respectively. The system is in contact with an isothermal heat bath at absolute temperature $T_A$. The order parameters of the (IBM) is defined as: $m_1^A \equiv \langle \sigma_i \rangle$, $m_1^B \equiv \langle \sigma_j \rangle$, $m_2^A \equiv \langle S_{i'} \rangle$, $m_2^B \equiv \langle S_{j'} \rangle$. $\langle\ \rangle$ is the thermal expectation value, and A and B denote the two sublattices of the layers.

Now, we can apply the dynamic mean-field theory (MFT) based on the Glauber–type stochastic dynamics (GTSD), namely the DMFT, to obtain the mean-field dynamic equation of motion. So, the system evolves according to a GTS process at a rate of $1/\tau$ transitions per

unit time. $P(\sigma_1,\sigma_2,...,\sigma_N, S_1, S_2,..., S_N; t)$ as the probability is defined that the system has the σ- and S- spin configurations of each layer $\sigma_1,\sigma_2,...,\sigma_N, S_1, S_2,..., S_N,$ at time t.

If we let $W_i(\sigma_i^A \to \sigma_i^{A'})$ be the probability per unit time that the *i*th spin changes from the value $\sigma_i^A$ to $\sigma_i^{A'}$, while the others, i.e., $(S_1,S_2,...,S_N)$ and spins on sublattice B, remain momentarily fixed, then we may write the master equation that describes the interaction between the spins and the heat bath as

$$\frac{d}{dt}P_1^A(\sigma_1^A,\sigma_2^A,...,\sigma_N^A;t) = -\sum_i\left(\sum_{\sigma_i^A\neq\sigma_i^{A'}} W_i^A(\sigma_i^A \to \sigma_i^{A'})\right)P_1^A(\sigma_1^A,\sigma_2^A,...,\sigma_i^A,...,\sigma_N^A;t)$$
$$+\sum_i\left(\sum_{\sigma_i{}^A\neq\sigma_i{}^{A'}} W_i^A(\sigma_i{}^{A'} \to \sigma_i{}^A)P_1^A(\sigma_1{}^A,\sigma_2{}^A,...,\sigma_i{}^{A'},...,\sigma_N{}^A;t)\right), \qquad (2)$$

where $W_i^A(\sigma_i^A \to \sigma_i^{A'})$ is the probability per unit time that *i*th spin changes from the values $\sigma_i^A$ to $\sigma_i^{A'}$. In this sense Glauber model is stochastic. Since the system is in contact with a heat bath at absolute temperature $T_A$, each spin can change from the value $\sigma_i{}^A$ to $\sigma_i{}^{A'}$ with the probability per unit time

$$W_i^A(\sigma_i^A \to \sigma_i^{A'}) = \frac{1}{\tau}\frac{\exp(-\beta\Delta E(\sigma_i^A \to \sigma_i^{A'}))}{\sum_{\sigma_i^{A'}}\exp(-\beta\Delta E(\sigma_i^A \to \sigma_i^{A'}))} \qquad (3)$$

where $\beta = 1/k_B T_A$, $k_B$ being the Boltzmann factor, $\sum_{\sigma_i^{A'}}$ is the sum over the five possible values of $\sigma_i{}^{A'} = \pm 3/2, \pm 1/2$ and

$$\Delta E_i^A(\sigma_{i'}^A \to \sigma_{i'}^{A'}) = -(\sigma_{i'}^{A'} - \sigma_i{}^A)(J_1\sum_{j'}\sigma_{j'}^B + J_3\sum_i S_i^A + H) - \left(\left(\sigma_{i'}^{A'}\right)^2 - \left(\sigma_{i'}{}^A\right)^2\right)D \qquad (4)$$

gives the change in the energy of the system when the $\sigma_i$-spin changes. The probabilities satisfy the detailed balance condition. Using Eqs. (1)-(4), we obtain the dynamic equation for $m_l^A$,

$$\Omega\frac{d}{d\xi}m_1^A=-m_1^A$$
$$+\frac{3\exp\left(\frac{d}{T}\right)\sinh\left[\frac{3}{2T}\left(zm_1^B+\frac{J_3}{J_1}m_2^A+h\cos\xi\right)\right]+\exp\left(-\frac{d}{T}\right)\sinh\left[\frac{1}{2T}\left(zm_1^B+\frac{J_3}{J_1}m_2^A+h\cos\xi\right)\right]}{2\exp\left(\frac{d}{T}\right)\cosh\left[-\frac{3}{2T}\left(zm_1^B+\frac{J_3}{J_1}m_2^A+h\cos\xi\right)\right]+2\exp\left(-\frac{d}{T}\right)\cosh\left[\frac{1}{2T}\left(zm_1^B+\frac{J_3}{J_1}m_2^A+h\cos\xi\right)\right]}, \quad (5)$$

where $m_1^A\equiv\left\langle\sigma_{i'}^A\right\rangle$, $m_1^B\equiv\left\langle\sigma_{j'}^B\right\rangle$, $m_2^A\equiv\left\langle S_i^A\right\rangle$, $m_2^B\equiv\left\langle S_j^B\right\rangle$, $\xi=wt$, $T=(\beta J_1)^{-1}$, $h=H_0/J_1$, $d=D/J_1$ and $\Omega=\tau w$. We fixed $\tau=1$, $z=4$ and $w=2\pi\nu$.

The other three mean–field dynamical equations for $m_1^B$, $m_2^A$ and $m_2^B$ can be similarly obtained as

$$\Omega\frac{d}{d\xi}m_1^B=-m_1^B$$
$$+\frac{3\exp\left(\frac{d}{T}\right)\sinh\left[\frac{3}{2T}\left(zm_1^A+\frac{J_3}{J_1}m_2^B+h\cos\xi\right)\right]+\exp\left(-\frac{d}{T}\right)\sinh\left[\frac{1}{2T}\left(zm_1^A+\frac{J_3}{J_1}m_2^B+h\cos\xi\right)\right]}{2\exp\left(\frac{d}{T}\right)\cosh\left[-\frac{3}{2T}\left(zm_1^A+\frac{J_3}{J_1}m_2^B+h\cos\xi\right)\right]+2\exp\left(-\frac{d}{T}\right)\sinh\left[\frac{1}{2T}\left(zm_1^A+\frac{J_3}{J_1}m_2^B+h\cos\xi\right)\right]}, \quad (6)$$

$$\Omega\frac{d}{d\xi}m_2^A=-m_2^A$$
$$+\frac{5\sinh\left[\frac{5}{2T}\left(\frac{J_2}{J_1}zm_2^B+\frac{J_3}{J_1}m_1^A+h\cos\xi\right)\right]+3\exp\left(-\frac{4d}{T}\right)\sinh\left[\frac{3}{2T}\left(\frac{J_2}{J_1}zm_2^B+\frac{J_3}{J_1}m_1^A+h\cos\xi\right)\right]+\exp\left(-\frac{6d}{T}\right)\sinh\left[\frac{1}{2T}\left(\frac{J_2}{J_1}zm_2^B+\frac{J_3}{J_1}m_1^A+h\cos\xi\right)\right]}{2\cosh\left[\frac{5}{2T}\left(\frac{J_2}{J_1}zm_2^B+\frac{J_3}{J_1}m_1^A+h\cos\xi\right)\right]+2\exp\left(-\frac{4d}{T}\right)\cosh\left[\frac{3}{2T}\left(\frac{J_2}{J_1}zm_2^B+\frac{J_3}{J_1}m_1^A+h\cos\xi\right)\right]+\exp\left(-\frac{6d}{T}\right)\cosh\left[\frac{1}{2T}\left(\frac{J_2}{J_1}zm_2^B+\frac{J_3}{J_1}m_1^A+h\cos\xi\right)\right]}, \quad (7)$$

$$\Omega\frac{d}{d\xi}m_2^B=-m_2^B$$
$$+\frac{5\sinh\left[\frac{5}{2T}\left(\frac{J_2}{J_1}zm_2^A+\frac{J_3}{J_1}m_1^B+h\cos\xi\right)\right]+3\exp\left(-\frac{4d}{T}\right)\sinh\left[\frac{3}{2T}\left(\frac{J_2}{J_1}zm_2^A+\frac{J_3}{J_1}m_1^B+h\cos\xi\right)\right]+\exp\left(-\frac{6d}{T}\right)\sinh\left[\frac{1}{2T}\left(\frac{J_2}{J_1}zm_2^A+\frac{J_3}{J_1}m_1^B+h\cos\xi\right)\right]}{2\cosh\left[\frac{5}{2T}\left(\frac{J_2}{J_1}zm_2^A+\frac{J_3}{J_1}m_1^B+h\cos\xi\right)\right]+2\exp\left(-\frac{4d}{T}\right)\cosh\left[\frac{3}{2T}\left(\frac{J_2}{J_1}zm_2^A+\frac{J_3}{J_1}m_1^B+h\cos\xi\right)\right]+\exp\left(-\frac{6d}{T}\right)\cosh\left[\frac{1}{2T}\left(\frac{J_2}{J_1}zm_2^A+\frac{J_3}{J_1}m_1^B+h\cos\xi\right)\right]}. \quad (8)$$

Therefore, a set of mean-field dynamical equations for the order parameters are obtained. Numerical solutions of Eqs. (5)-(8) gives the phases in the system that will be given in the next section.

On the other hand, to characterize the nature of the dynamic phase transition (DPT), calculate dynamic phase transition temperatures (DPTTs) and to present dynamic phase diagrams (DPDs), we have to investigate the thermal behavior of the dynamic magnetizations ($M_{1,2}^{A,B}$) that are defined as

$$M_{1,2}^{A,B} = \frac{1}{2\pi}\int_0^{2\pi} m_{1,2}^{A,B}(\xi)d\xi. \qquad (9)$$

Finally, in order to examine dynamic magnetic hysteresis behaviors, one should define the dynamic hysteresis loop area that defined as

$$A = -\oint m_{1,2}^{A,B}(t)\,dh = -h_0 w \oint m_{1,2}^{A,B}(t)\cos(wt)dt\,. \qquad (10)$$

Moreover, the total magnetization is

$$m_T \equiv (m_1^A + m_1^B + m_2^A + m_2^B)/4\,. \qquad (11)$$

Solution of all these equations will be presented in Section 3.

**3. Solution and discussion**

To obtain the phases in the system, we investigate the stationary solutions Eqs. (5)-(8) when the system parameters ($J_1$, $J_2$, $J_3$, d, h, w ) are varied. Since the solution of these kinds of equations is extensively discussed and given in Refs. [26-29] we will not discuss or explain them here and present any figures. The stationary solutions of these equations give that the system exhibits three different fundamental solutions or phases, namely, the paramagnetic (p), ferromagnetic (f) and ferrimagnetic (i), and a one mixed phase or coexistence, i.e. the i + p mixed phase in which i and p phases coexist.

Eq. (9) is solved and investigated to characterize the nature (first- or second-order) of the DPT, calculate the DPTTs and present the DPDs. Few interesting results are plotted in Fig. 2. Figs. 2 (a) and (b) display that the system undergoes a second- and first-order DPT, respectively, because of $M_{1,2}^{A,B}$ decrease to zero continuously as the reduced temperature (T) increases in Fig. 2 (a) and $M_{1,2}^{A,B}$ decrease to zero discontinuously as T increases in Fig. 2 (b). Tc=6.61 and Tt=4.76 are the second- and first-order DPTTs, respectively. Figs. 2 (c) and (d) are calculated for $J_1$ =1.0, $J_2$ =0.1, $J_3$=1.0, d=1.0, h=0.5, w=10 π and two different initial values. Figs. 2 (c) and (d) illustrate that system undergoes a second-order phase transition at $Tc_1$=6.21 and $Tc_2$=6.75, respectively. If we consider Fig. 1(d) with Fig. 2 (c), we see that the system undergoes two successive second-order DPTs in which the first one is from the i phase to the i+p mixed phase at $Tc_1$ and the second one from the i + p mixed phase to the p phase at $Tc_2$ = 6.75 that can be seen in Fig. 3 (c) for h = 0.5, explicitly. Similarly, Figs. 1(e) and (f) are constructed for $J_1$ =1.0, $J_2$ =0.1, $J_3$=1.0, d=1.0, h=5.5, w=10 π and two different initial values.

If we take into account Fig. 2 (e) with Fig. 1 (f), we see that the system undergoes a first-order DPT from the i+ p mixed phase to the p phase at $T_t = 1.34$ which can be clearly seen in Fig. 3 (c) for h=5.5.

Figs. (3) - (5) illustrate the DPDs for three different planes. In the figures, the solid and dashed lines indicate the second- and first-order DPTTs, respectively and TP and QP and the solid circle are the dynamic triple, quadrupole and tricritical points. Fig. 3 is constructed in the (T, h) plane for different values of w and three different topological behaviors are found. For small values w, the system undergoes a first-order phase transition for low values of T, and a second-order transition for values of T; the transition from the i phase to the p phase; hence the system exhibits the dynamic tricritical (DTRC) behavior. For very low T and very high h values, two different TP points and the i + p mixed phase appear. Moreover, the reentrant behavior also seen in this region where as the T is lowered, the system passes from the p phase to the i+p phase, and back to the p phase again. Fig. 3 (b) is similar to the Fig. 3 (a) except that two TP points disappeared and the i + p region becomes large. Similar DPD has been reported in the some mixed Ising systems [26, 30-34] as well as single spin Ising systems [35-38], except the i phase becomes the ferromagnetic (f) phase. Fig. 3 (c) displays two DTRC behavior and for low values of h the system undergoes two successive second-order phase transitions, namely the i phase to the i+p mixed phase then the p phase and for high values of h the system undergoes two successive first-order phase transitions, i.e. the i phase to the i + p mixed phase then the p phase. Very similar DPD was reported in the mixed spins (1, 3/2) [35] and (1/2, 1) [39] Ising systems. Fig. 4 shows the DPD in the (T, d) plane for three different values of w. For small values of w ($w=0.05\ \pi$) in Fig. 4 (a), only p and i phases exists and the dynamic phase boundary between them is the dynamic first-order phase line. For $w=2.0\pi$ (Fig. 4(b)), the system exhibits the DTRC behavior in which the high values of T system undergo a second-order phase transition from the p phase to the i phase. For low values of the system passes on two successive first-order phase transitions, i.e. the i phase to the i+p mixed phase then the p phase. Alike DPD was obtained in the mixed spin systems [26, 40] and the Blume-Capel model [41], except the i phase is the f phase. Fig. 4 (c) obtained for $w=10.0\ \pi$ that exhibits two DTRC behavior in which for high values of T the system passes on two successive second-order phase transitions, namely the p phase to the i+p mixed phase then the i phase and for low values of T the system undergoes two successive first-order phase transitions, i.e. the p phase to the i+p mixed phase then the i phase. Similar DPD was obtained in Ref. [34]. The DPDs in the (T, w/ $\pi$) plane are presented for the three values of h (Fig. 5). For h=0.1, the DPD contains the p, i and i +p phase and the dynamic phase boundaries among

these phase are the second-order lines, illustrated in Fig. 5 (a). Fig. 5 (b) calculated for h=1.5, the system displays the DTRC behavior in which for high values of T the second-order phase transition occurs from the p phase to the i phase. Low and very low values of T, the system undergoes the first-order phase transitions from the p phase to the i phase and from the i+p phase to the p phase, respectively. Fig. 5 (c) is the one of the interesting DPD that observed for h=2.5 in which comprises three DTRC and one QP as well as two different the i+p mixed phases. The system undergoes the second- and firs-order phase transitions for very high values of T and very low values of T, respectively. The phase boundaries among p, i+p and i phases for very low values of T are first-order lines. The temperatures between two DTCR points for high values of T, the system undergoes a first-order phase transition from the p phase to the i phase, but for low values of T the system passes on two successive phase transitions, namely the p phase to the i+p mixed phase with a second-order and the i + p phase to the i phase with a first-order.

We also investigate dynamic magnetic hysteresis (DMH) or the dynamics of magnetization reversal behavior that is of great importance for developing memory storage devices and high frequency devices applications as well as academic research [42-43]. Fig. 6 illustrates the DMH loops behavior for $J_1$=-0.3, $J_2$=0.1, $J_3$=1.0, d = - 1.0, h=1 and T=0.1 for various values of w/π for the submagnetizations ($m_{1,2}^{A,B}$) and total magnetization ($m_T$). Blue and red colors indicate the $m_1^A, m_1^B$ and $m_2^A, m_2^B$, respectively. First of all, we can observe that as the frequency is decreased, the area of DMH loops is increase. These behaviors are also quantitatively good agreement some theoretical obtained results in Refs. [44-49) as well as the experimental reports for thin Co films on Cu (001) [50], ultrathin epitaxial Fe/GaAs(001) [51] and Fe thin films [52]. For w=1.0 π, the $m_1^A, m_1^B$ exhibits the dynamic triple loops behavior, but for w=0.4 π, the $m_2^A, m_2^B$ display. Moreover, the $m_T$ exhibits the triple loops behavior for w=0.6 π. The dynamic triple hysteresis loops behavior has been also observed in some recent theoretical works on Ising systems [53–55].

In conclusion**,** we study investigate the DPTs, DPDs and DMH loops behavior of the Ising bilayer system consisting of the mixed spin (3/2, 5/2) atoms with the crystal-field interaction under a time-varying magnetic field on a two-layer square lattice by using the DMFT. We also compare the results with available theoretical and experimental works and find that some of our DPDs are very similar to the DPDs obtained in the mixed and single Ising systems. The DPDs of Fig. 3 (a), Fig. 4 (a) and Fig. 5 are observed for the first time in this system as far as we know. Similar DMH loops behavior are also reported by some

theoretical and experimental works. Moreover, although the dynamic triple hysteresis loops behavior was reported to be observed in some recent theoretical studies, unfortunately, best of our knowledge, we could not see any experimental works of the DPT that reported this behavior. Finally, we hope that these results will shed some light into theoretical and especially experimental research for investigation of the DPTs, DPDs and DMH loops behaviors.

**Acknowledgments**

This work was supported by the Erciyes University Research Funds, Grant No: FBA-2016-6324.

**References**

[1] M. Monsuripur, J. Appl. Phys. **61** (1987) 1580.

[2] O. Kahn, in: E. Coronado, et al., (Eds.), From Molecular Assemblies to the Devices, Kluwer Academic Publishers, Dordrecht, 1996.

[3] Q. Zhang, G. Z. Wei, Y. Gu, phys. status sol.(b) **242** (2005) 924.

[4] E. Albayrak, A. Yiğit, Phys. Lett. A **353** (2006)121.

[5] E. Albayrak, A. Yiğit, phys. status sol. (b) **244** (2007) 748.

[6] R. A. Yessoufou, H. S. Amoussa, F. Hontinfinde, Cent. Eur. J. Phys. **7** (2009) 555.

[7] N. De La Espriella, G. M. Buendía, Physica A **389** (2010) 2725.

[8] B. Ma, W. Jiang, IEEE TRANSACTIONS ON MAGNETIC **47** (2011) 3118.

[9] N. De La Espriella, G. M. Buendía, J. Phys.: Condens. Matter **23** (2011) 176003.

[10] H. K. Mohamad, J. Magn. Magn. Mater. **323** (2011) 61.

[11] R. Masrour, L. Bahmad, A. Benyoussef, J. Magn. Magn. Mater. **324** (2012) 3991.

[12] T. Iwashita, H. Arai, Y. Ito, Y. Muraoka, J. Magn. Magn. Mater. **325** (2013) 57.

[13] N. De La Espriella Velez J. Madera Yancez, M. S. Paez Mesa, Revista Mexicane de Fisica **60** (2014) 419.

[14] J. A. Reyes, N. De La Espriella, G. M. Buendía, phys. status sol.(b) **252** (2015) 2268.

[15] R. Masrour, A. Jabar, A. Benyoussef, M. Hamedoun, J. Magn. Magn. Mater. **410** (2016) 223.

[16] X. H. Luo, W. Wang, D. D. Chen, S. Y. Xu, Physica B **491** (2016) 51.

[17] W. Wang, R. Liu, D. Lv, X. H. Luo, Super. Micr. **98** (2016) 458.

[18] J. D. Alzate-Cardona, D. Sabogal-Suarez, E. Restrepo-Parra, J. Magn. Magn. Mater. **429**

(2017) 34.

[19] M. M. Maltempo, T. H. Moss, Rev. Biophys. **9** (1976) 18.

[20] L. B. Dugad, V. R. Marathe, S. Mitra, Proc. Indian Acad. Sci. **95** (1985) 189.

[21] R. Weiss, A. Gold, J. Terner, Chem. Rev. **106** (2006) 2550.

[22] Y. Zeng, G. A. Caignan, R. A. Bunce, J. C. Rodriguez, A. Wilks, M. Rivera, J. Am. Chem. Soc. **127** (2005) 9794 .

[23] N. A. Rakow, K. S. Suslick, Nature **406** (2000) 710.

[24] S. Neya, A. Takahashi, H. Ode, T. Hoshino, M. Hata, A. Ikezaki, Y. Ohgo, M. Takahashi, H. Hiramatsu, T. Kitagawa, Y. Furutani, H. Kandori, N. Funasaki, M. Nakamura, Eur. J. Inorg. Chem. **20** (2007) 3188.

[25] B. Deviren, M. Keskin, J. Stat. Phys. **140** (2010) 934.

[26] M. Keskin, M. Ertaş, O. Canko, Phys. Scr. **79** (2009) 025501.

[27] M. Keskin, M. Ertaş, J. Stat. Phys. **139** (2010) 333.

[28] M. Ertaş, M. Keskin, Physics Letters A **376** (2012) 2455.

[29] E. Kantar, M. Ertaş, M. Keskin, J. Magn. Magn. Mater. **361** (2014) 61.

[30] M. Keskin, E. Kantar, O. Canko, Phys. Rev. E **77** (2008) 051130.

[31] B. Deviren, M. Keskin, O. Canko, J. Magn. Magn. Mater. **321** (2009) 458.

[32]T. Korkmaz, Ü. Temizer, J. Magn. Magn. Mater. **324** (2012) 3875.

[33] M. Ertaş, M. Keskin, Physica B **470-471** (2015) 76.

[34] E. Kantar, M. Ertaş, J. Supercond. Nov. Magn. **29** (2016) 2319.

[35] T. Tome, M. J. de Oliveira, Phys. Rev. A **41** (1990) 4251.

[36] G. M. Buendia, E. Machado, Phys. Rev. E **58** (1998) 1260.

[37] X. Shi, G. Wei, L. Li, Phys. Lett. A **372** (2008) 5922.

[38] G. Gulpinar, E. Vatansever, M. Ağartıoglu, Physica A **391** (2012) 3574.

[39] M. Ertaş, M. Keskin, Physica A **437** (2015) 430.

[40] A. Özkılıç, Ü. Temizer, J. Magn. Magn. Mater. **330** (2013) 55.

[41] M. Keskin, O. Canko, Ü. Temizer, J. Exp. Theo. Phys. **104** (2007) 936.

[42] G. Bertotti, Hysteresis in Magnetism, Academic Press, San Diego, 1998.

[43] Z. Zhu, Y. Sun, Q. Zhang, J. M. Liu, Phys. Rev. B 76 (2007) 014439.

[44] L. Wang, B.H.Teng, Y.H.Rong , Y.Lu, Z.C.Wang, Solid State Commun. **152** (2012) 1641.

[45]Y. Yüksel, Phys. Lett. A **377** (2013) 2494.

[46] G.T. Landi and A.D. Santos, J. Appl. Phys. **111** (2012) 07D121.

[47] G.T. Landi, J. Magn. Magn. Mater. **324** (2012) 466.

[48] Z. Zhu, Y. Sun, Q. Zhang, J. M. Liu, Phys. Rev. B **76** (2007) 014439.

[49] M. Keskin, M. Ertaş, J. Supercond. Nov. Magn. doi:10.1007/s10948-016-3551-x (in press)

[50] J. S. Suen, J. L. Eskine, Phys. Rev. Lett. **18** (1997) 3567.

[51] J. S. Suen, M. H. Lee, G.Teeter, J. L. Eskine, Phys. Rev. B **59** (1999) 4249.

[52] T. A. Moore, G. Wastlbauer, J. A. C. Blanda, E. Cambril, M. Natali, D. Decanini, Y. Chen, J. Appl. Phys. **93** (2003) 8746.

[53] Y. Yüksel, E. Vatansever, H. Polat, J. Phys.: Condens. Matter 24 (2012) 436004.

[54] M. Ertaş, J. Supercond. Nov. Magn. **30** (2017) 1839.

[55] M. Batı, M. Ertaş, Physica B **513** (2017) 40.

**List of the figure captions**

**Fig. 1.** Schematic representation of a bilayer square lattice system: $L_1$ and $L_2$ refer to the upper and lower layers containing with spin variables $\sigma_i^A$ , $\sigma_i^B$ = ±3/2, ±5/2 occupy $L_1$ layer and $S_j^A$ , $S_j^B$ .

**Fig. 2.** Reduced temperature dependence of the dynamic magnetizations $M_{1,2}^{A,B}$. $T_C$ and Tt are the dynamic second- and first-order phase transition temperatures. **(a)** $J_1$ =1.0, $J_2$ =0.1, $J_3$=1.0, d=1.0, h=0.1, w=0.05 π. **(b)** $J_1$ =1.0, $J_2$ =0.1, $J_3$=1.0, d=1.0, h=0.8, w=0.05 π. **(c)** and **(d)** $J_1$ =1.0, $J_2$ =0.1, $J_3$=1.0, d=1.0, h=0.5, w=10.0 π and two different initial values. **(e)** and **(f)** $J_1$ =1.0, $J_2$ =0.1, $J_3$=1.0, d=1.0, h=5.5, w=10.0 π and two different initial values.

**Fig. 3.** Dynamic phase diagrams of the system in the (T, h) plane for $J_1$ =1.0, $J_2$ =0.1, $J_3$=1.0, d=1.0, h=1.0. The solid and dashed lines are the second- and first-order lines, respectively. TP and QP and the solid circle represent the dynamic triple, quadrupole and tricritical points, respectively. **(a)** w=0.05 π, **(b)** w=2.0 π, **(c)** w=10.0 π.

**Fig. 4.** Same as Fig. 3, but in the (T, d) plane for $J_1$ =1.0, $J_2$ =0.1, $J_3$=1.0, d=1.0, h=2.0. **(a)** w=0.05 π, **(b)** w=2.0 π, **(c)** w=10.0 π.

**Fig. 5.** Same as Fig. 4, but in the (T, w/π) plane for $J_1$ =1.0, $J_2$ =0.1, $J_3$=1.0, d=1.0. **(a)** h=0.1, **(b)** h=1.5, **(c)** h=2.5.

**Fig. 6.** The DMH behaviors for various angular frequencies and $J_1$=-0.3, $J_2$=0.1, $J_3$=1.0, d= -1.0, h=1.0, T=0.1. Blue and red colors indicate the $m_1^A, m_1^B$ and $m_2^A, m_2^B$, respectively.

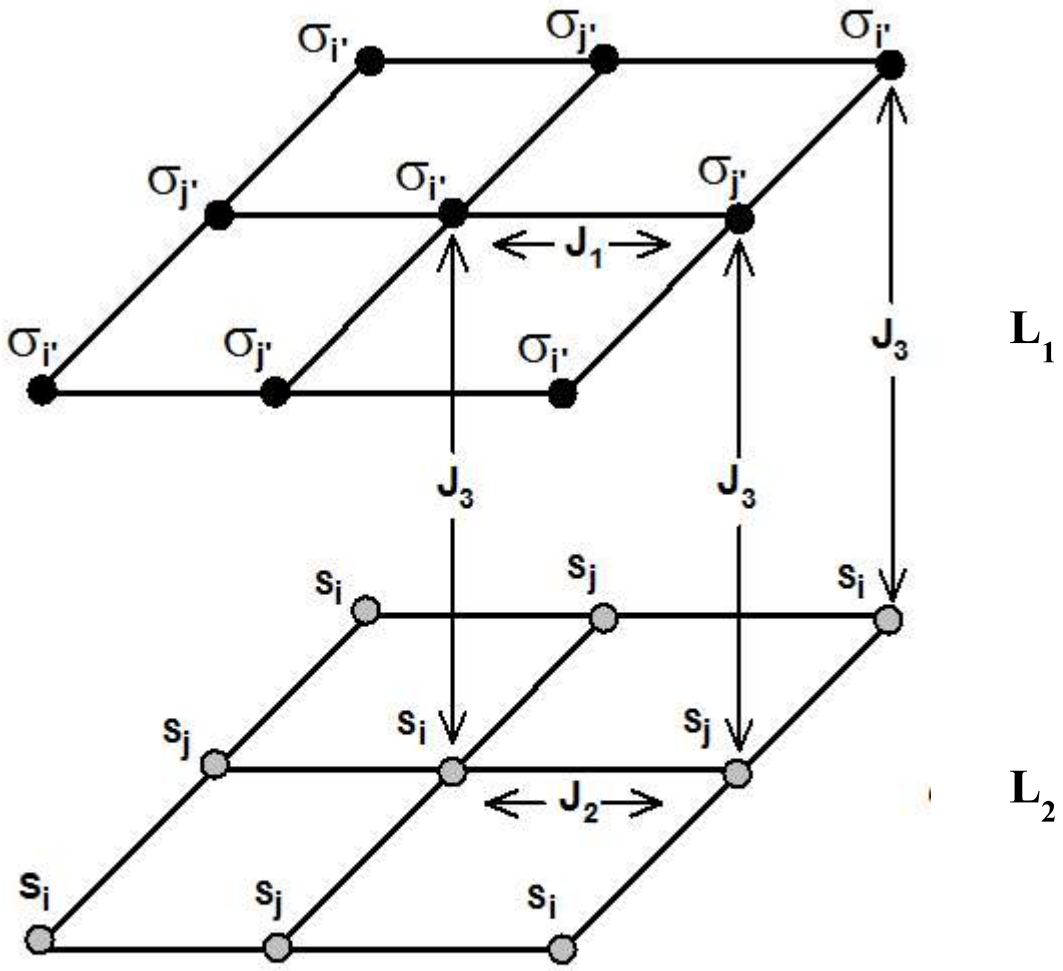
σi'
σj'
σi'
σj'
σi'
σj'
J1
σi'
σj'
σi'
J3
L1
J3
J3
si
sj
si
sj
si
sj
J2
L2
si
sj
si

**Fig. 1**

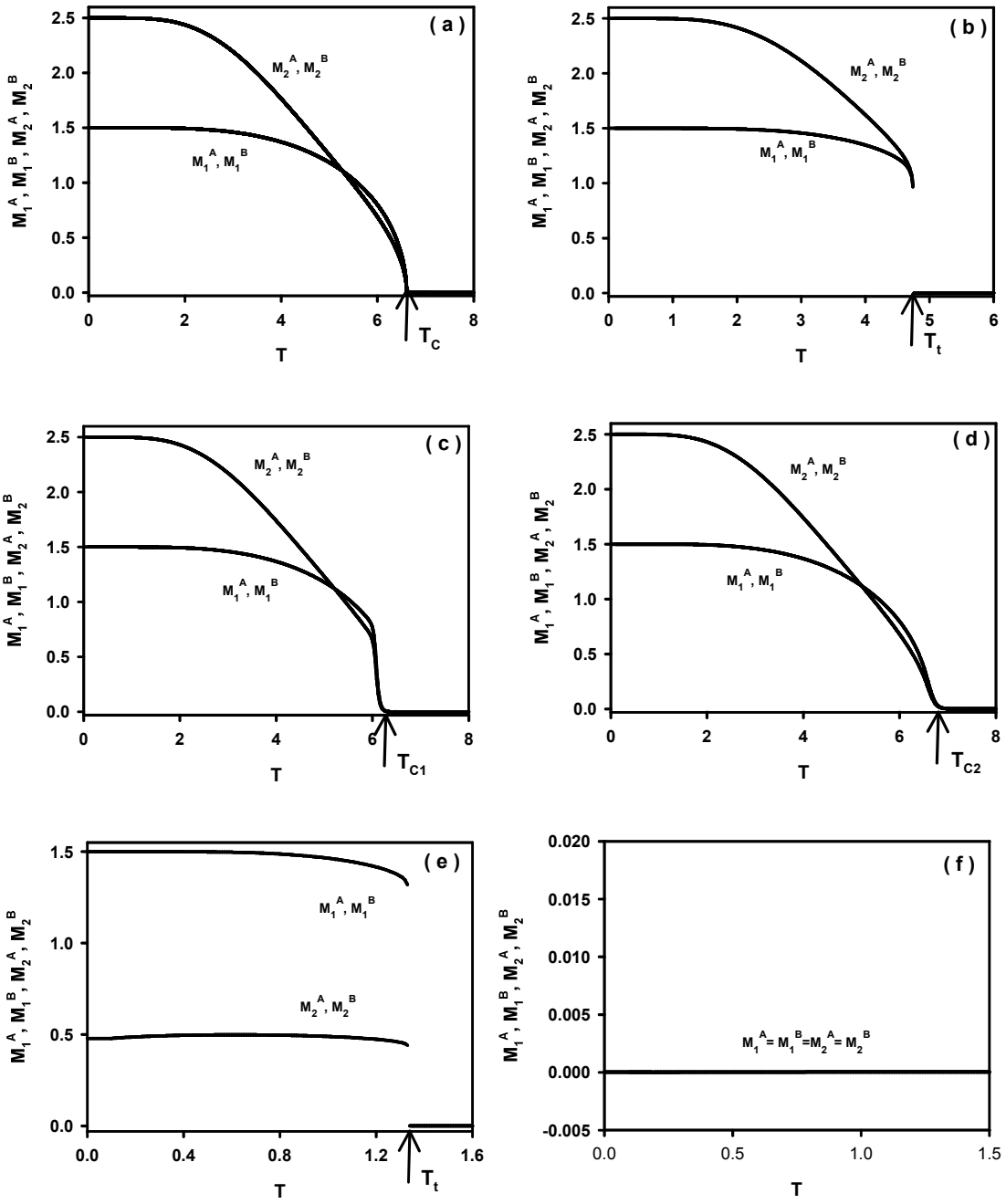
(a)
(b)
(c)
(d)
(e)
(f)
$M_1^A, M_1^B, M_2^A, M_2^B$
$M_2^A, M_2^B$
$M_1^A, M_1^B$
$M_1^A = M_1^B = M_2^A = M_2^B$
T
$T_C$
$T_t$
$T_{C1}$
$T_{C2}$

**Fig. 2**

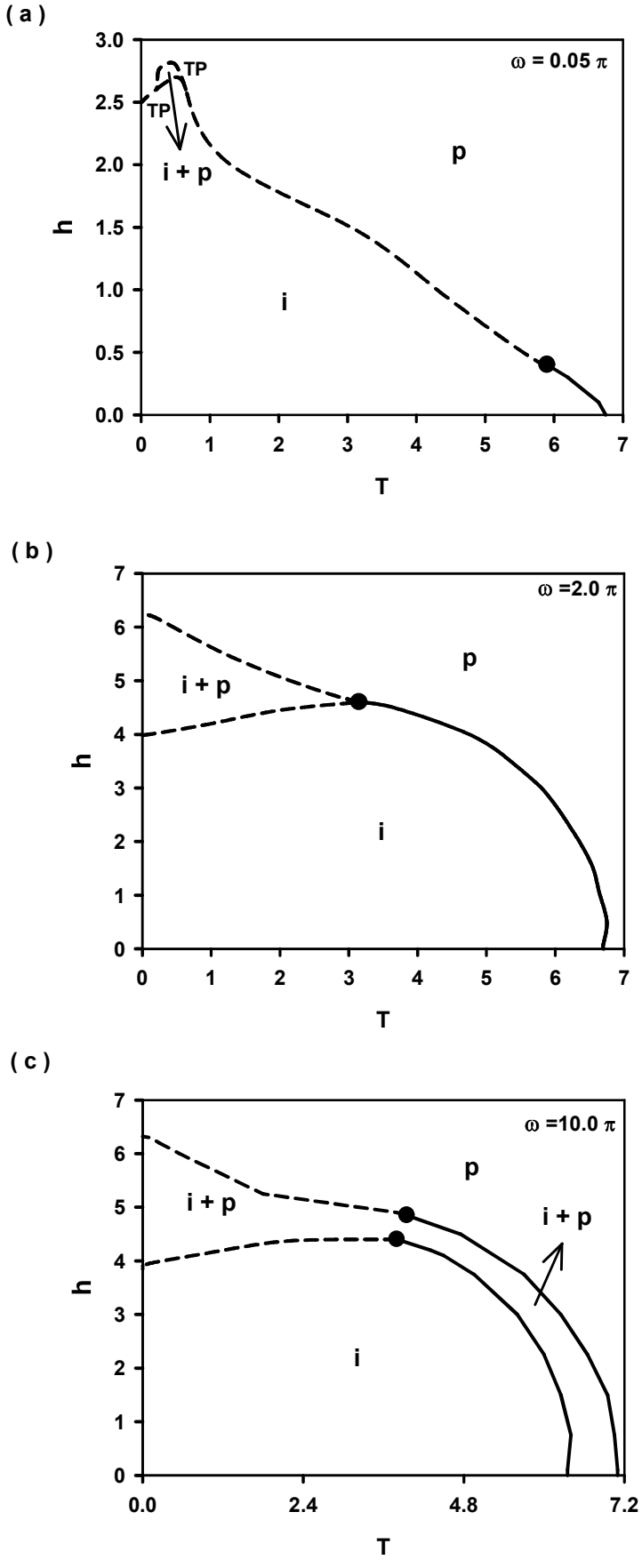


**Fig. 3**

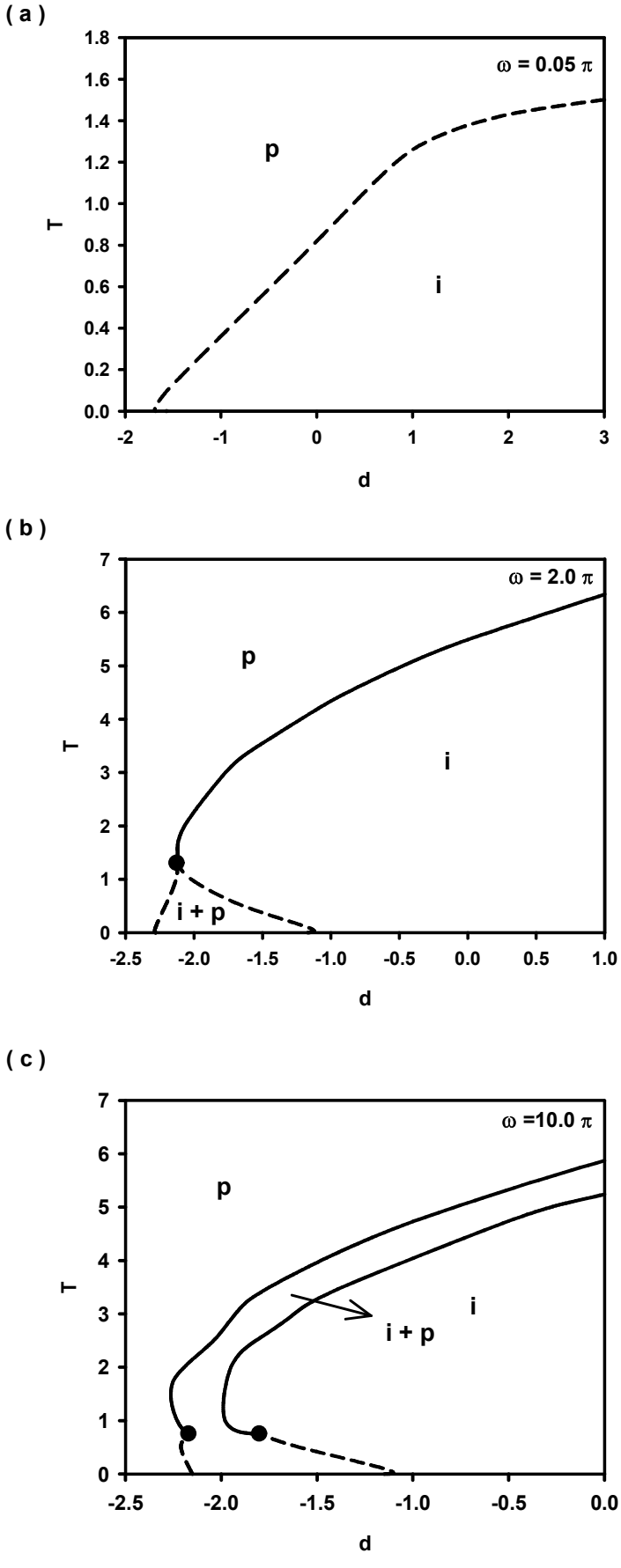


**Fig. 4**

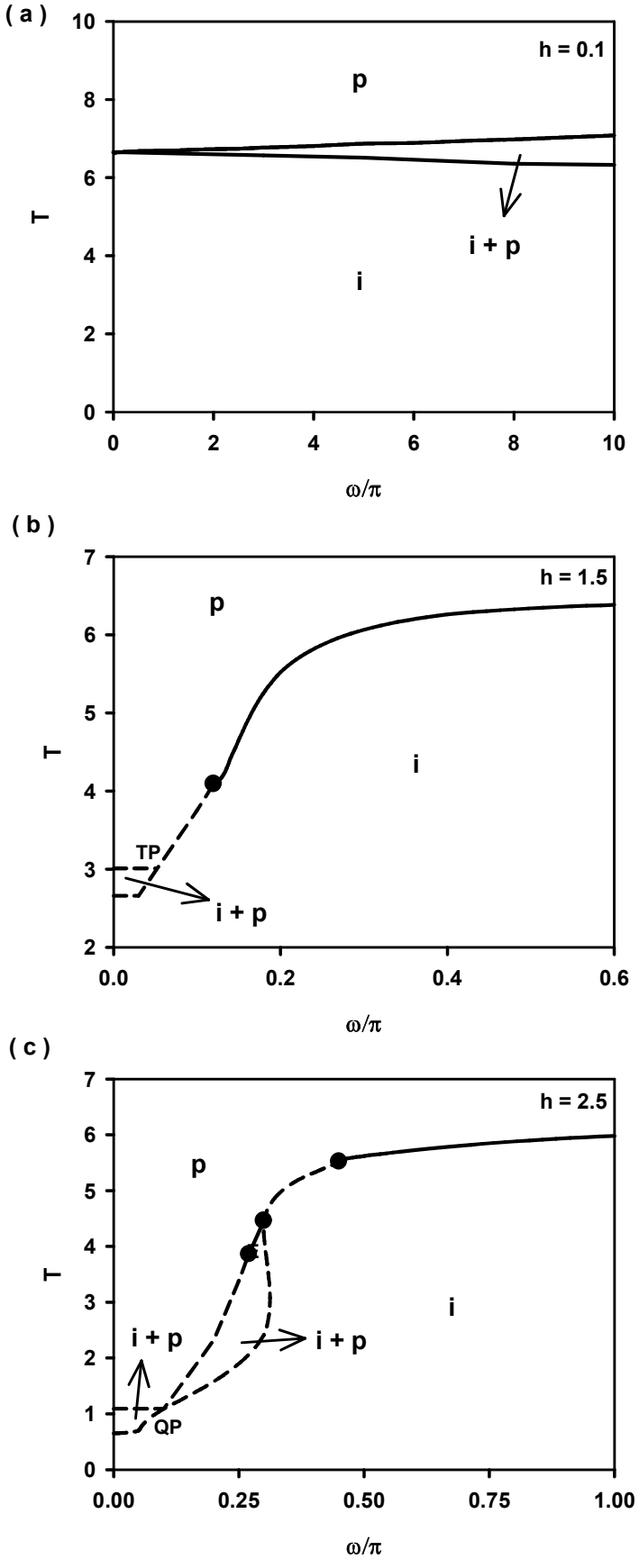


**Fig. 5**

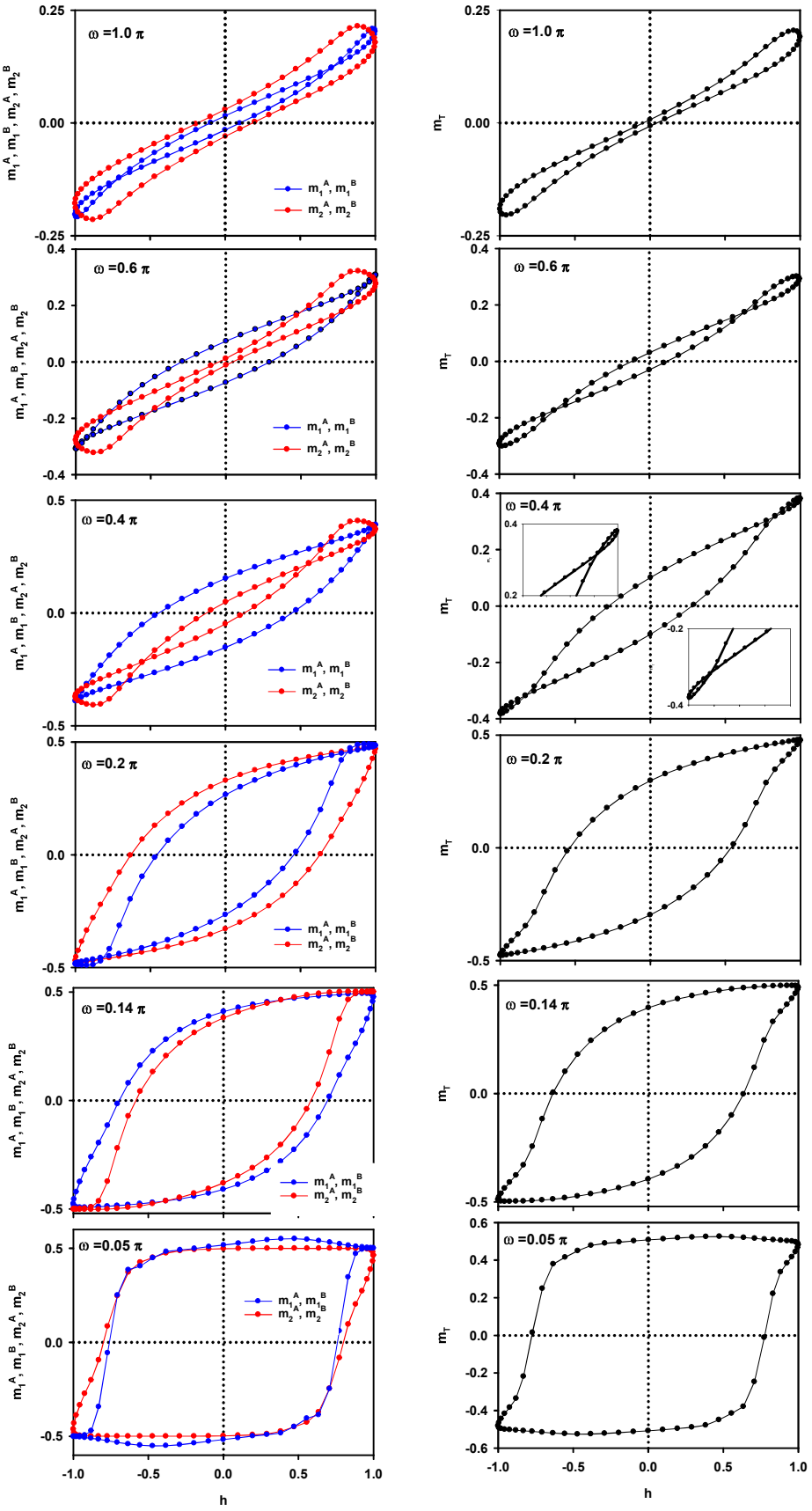


**Fig. 6**